ΕΘΝΙΚΟ ΜΕΤΣΟΒΙΟ ΠΟΛΥΤΕΧΝΕΙΟ
ΣΧΟΛΗ ΝΑΥΠΗΓΩΝ ΜΗΧΑΝΟΛΟΓΩΝ ΜΗΧΑΝΙΚΩΝ
ΤΟΜΕΑΣ ΝΑΥΤΙΚΗΣ ΜΗΧΑΝΟΛΟΓΙΑΣ

Διπλωματική Εργασία

Ανάπτυξη μοντέλου υπολογισμού των παραμορφώσεων γάστρας πλοίου, με εφαρμογή στη βέλτιστη ευθυγράμμιση του αξονικού συστήματος

Δαρδαμάνης Αναστάσιος

Εξεταστική επιτροπή:

Επιβλέπων: **Χ. Ι. Παπαδόπουλος, Αναπληρωτής Καθηγητής ΕΜΠ**
Μέλη: **Κ. Ανυφαντής, Αναπληρωτής Καθηγητής ΕΜΠ**
Λ. Καϊκτσής, Καθηγητής ΕΜΠ

Αθήνα, Ιούλιος 2022

NATIONAL TECHNICAL UNIVERSITY OF ATHENS
SCHOOL OF NAVAL ARCHITECTURE & MARINE ENGINEERING
DIVISION OF MARINE ENGINEERING

Diploma Thesis

Development of model for the calculation of ship hull deflection, with application to the optimal alignment of propulsion shafting system

Dardamanis Anastasios

Thesis Committee:

Supervisor:	**C.I. Papadopoulos, Associate Professor NTUA**
Members:	**K. Anyfantis, Associate Professor NTUA**
	L. Kaiktsis, Professor NTUA

Athens, July 2022

Acknowledgements

After an intensive period, today is the finish line. It has been an amazing journey, with a lot of hard and great times. I would like to reflect on the people who have supported and helped me so much throughout this period.

Firstly, I would like to thank my thesis advisor, Associate Professor Christos Papadopoulos. Prof. Papadopoulos was always there to answer the hard questions and steer me in the right direction whenever I needed it. With his vast knowledge over a variety of engineering fields, he helped in delivering great results and acquiring the most of everything we did.

Special Thanks goes out to George Rossopoulos for the support and relentless dedication he showed in this diploma thesis. Always to the point and with his great engineering knowledge and programming skills, he helped on developing and executing great ideas. His presence was vital for this Diploma Thesis.

At this point, I would like to thank my friends and classmates for their friendship and assistance throughout our studies at NTUA. I cannot express how grateful I am towards my fellow classmates, Orfeas Bourchas and Nikos Papanikolaou for their assistance, and advice over the university years. Also, their everyday “roasting” motivated me to finish my thesis.

Last, but surely not least, I must express my deepest gratitude to my parents, my brother and sister and to my partner in crime. This journey would not have been possible without their support.

Table of Contents

Abstract

Proper shaft alignment is vital for the safe operation and efficient performance of a vessel. Until recently, hull deflections had been rarely considered in the calculations of shaft alignment, mainly due to the time-consuming task of creating a 3d finite element representation of the vessel, and solving for many different loading condition scenaria. However, for some loading conditions, the effect of hull deformation on bearings vertical displacement and corresponding loads is quite significant. Having the ability to account for hull deflections in an early design stage will lead to increased calculations quality, will aid in preventing bearing operation at very low / very high loads and increased possibility of failure, while it will minimize dependence on the experience of shipyard personnel, which could be of particular concern when implementing alignment on new hull designs. The addition of hull deflections in the alignment design allows bearing reactions to be accurately assessed and confirmed for every vessel loading condition. Recently, Classification Society ABS released rule notations concerning the shaft alignment procedure, and noted that the 1D beam theory finite element model can provide acceptable hull deflection estimates, in comparison to deflections obtained from complex 3D finite element analyses.

In the present work, the hull deflections of a typical 10K containership are being calculated with the use of 1d beam theories. In particular, the Euler- Bernoulli and Timoshenko beam theories have been used to determine the hull deflections of the vessel. A Graphical User Interface application was developed in the course of the present thesis to calculate the sectional properties, such as neutral axis, second moment of area and shear area, for several longitudinal transverse sections of the containership and to automate the procedure of shaft alignment calculations. Several parts of the vessel must be taken into account in the calculations to properly assess the vertical bearings' offsets. After the transverse bending, shear stiffness and load distribution for several frames has been used as input, the finite element method is utilized to calculate relative hull deflections for a series of representative loading conditions of the vessel. This method not only provides a robust early approximation of the hull deflection using the broadly available information, but also requires minimum pre-processing by the user.

The aforementioned vertical offsets due to hull deflections are used in combination with the vertical offsets from hydrodynamic lubrication characteristics (oil film thickness) and elastic bearing foundation to calculate the bearings' reaction forces. The proper investigation and assessment of the bearings' offsets leads to better efficiency of the propulsion system, less wearing down of the journal bearings and increased bearing reliability. Based on the above, conclusions are drawn regarding the errors that can be produced by both the 3d and 1d modeling of the vessel and important parameters that should be considered beforehand to create a more accurate model.

Additionally, a comparative analysis of the key parameters affecting the shaft alignment procedure is conducted and a review of those key factors, including but not limited to the ship voyage and the sea swell, but also the many parameters that should be considered beforehand. Finally, suggestions for future work are discussed, that would extend the work done in this thesis and broaden our knowledge about the parameters affecting the hull deflection.

Σύνοψη

Η σωστή ευθυγράμμιση του αξονικού συστήματος ενός πλοίου είναι ζωτικής σημασίας για την ασφαλή λειτουργία και απόδοση αυτού. Μέχρι προσφάτως, οι παραμορφώσεις της γάστρας δεν λαμβάνονταν υπόψη στους υπολογισμούς της ευθυγράμμισης του άξονα λόγω της χρονοβόρας διαδικασίας δημιουργίας της τρισδιάστατης αναπαράστασης του πλοίου, παρόλο που σε πολλές καταστάσεις φόρτωσης, η επίδραση των παραμορφώσεων της γάστρας στην κατακόρυφη θέση των εδράνων είναι υψίστης σημασίας. Η δυνατότητα υπολογισμού των παραμορφώσεων της γάστρας στα πρώτα στάδια σχεδίασης του πλοίου ελαχιστοποιεί την εξάρτηση από ικανό προσωπικό με εμπειρία, και θα βοηθήσει ιδιαίτερα στην διαδικασία ευθυγράμμισης του άξονα σε νέα μοντέλα πλοίων. Η προσθήκη των παραμορφώσεων της γάστρας στους υπολογισμούς της ευθυγράμμισης επιτρέπει μια πιο ακριβή αξιολόγηση των δυνάμεων αντίδρασης των εδράνων για κάθε κατάσταση φόρτωσης. Πρόσφατα, ο αμερικανικός νηογνώμονας (ABS) εξέθεσε κανονισμούς που αφορούν την ευθυγράμμιση του άξονα, τονίζοντας ότι η εφαρμογή της μονοδιάστατης θεωρίας δοκού μπορεί να παράγει πολύ κοντινές παραμορφώσεις με αυτές του τρισδιάστατου μοντέλου πλοίου.

Στην παρούσα εργασία, η παραμορφώσεις της γάστρας για ένα τυπικό πλοίο μεταφοράς εμπορευματοκιβωτίων 10,000 TEU υπολογίζονται με τη χρήση της θεωρίας μονοδιάστατης δοκού. Η θεωρίες των Timoshenko και Euler-Bernoulli χρησιμοποιήθηκαν για τους υπολογισμούς των παραμορφώσεων. Μια εφαρμογή γραφικής διασύνδεσης χρήστη δημιουργήθηκε στα πλαίσια της παρούσας διπλωματικής για τον γρηγορότερο και πιο εύκολο υπολογισμό των ιδιοτήτων επιφανείας, όπως ο ουδέτερος άξονας, δεύτερη ροπή επιφανείας και η επιφάνεια διάτμησης, για πολλές εγκάρσιες τομές κατά το μήκος του πλοίου, καθώς και για την αυτοματοποίηση της διαδικασίας ευθυγράμμισης του άξονα. Διάφορα μέρη του πλοίου πρέπει να ληφθούν υπόψη στους υπολογισμούς, ώστε να αξιολογηθούν σωστά οι κατακόρυφες θέσεις των εδράνων. Αφού η καμπτική και διατμητική αντοχή πολλών εγκάρσιων τομών του πλοίου καθώς και η φόρτωση του πλοίου έχει υπολογιστεί για τις διάφορες καταστάσεις, η μέθοδος πεπερασμένων στοιχείων χρησιμοποιείται για τον υπολογισμό των σχετικών μετατοπίσεων της γάστρας σε σχέση με μια κατάσταση φόρτωσης αναφοράς . Οι εύκολα διαθέσιμες απαιτούμενες πληροφορίες σε συνδυασμό με τα εύκολα επεξεργάσιμα απαιτούμενα δεδομένα για αυτή την μέθοδο δίνουν μια επαρκή γρήγορη προσέγγιση των παραμορφώσεων της γάστρας.

Οι παραπάνω παραμορφώσεις χρησιμοποιούνται σε συνδυασμό με τις κατακόρυφες μετατοπίσεις των εδράνων που προκαλούνται από τα υδροδυναμικά χαρακτηριστικά λίπανσης και την ελαστική παραμόρφωση των εδράνων για τον υπολογισμό των δυνάμεων αντίδρασης των εδράνων. Η κατάλληλη αξιολόγηση των κατακόρυφων θέσεων των εδράνων οδηγεί σε μεγαλύτερη απόδοση της προωστήριας εγκατάστασης και επίσης σε μικρότερη διάβρωση των εδράνων ολίσθησης και ώσης. Με βάση τα παραπάνω, βγάζουμε συμπεράσματα για τα λάθη που μπορεί να παραχθούν και από τις δύο μεθόδους, τρισδιάστατη και μονοδιάστατη, και τις παραμέτρους που πρέπει να λάβουμε υπόψη εκ των προτέρων για να δημιουργήσουμε ένα ακριβές μοντέλο.

Επιπλέον γίνεται μια συγκριτική ανάλυση των κύριων παραμέτρων που επηρεάζουν τη διαδικασία ευθυγράμμισης του άξονα, όπως ο κυματισμός και οι απώλεια αναλωσίμων κατά τη διάρκεια του ταξιδιού, αλλά και τις πολλές παραμέτρους που πρέπει να ληφθούν υπόψη. Τέλος γίνονται προτάσεις για μελλοντική έρευνα που θα βοηθήσουν να αναπτυχθεί αυτή η δουλειά και συγχρόνως να διευρύνουμε τις γνώσεις μας σχετικά με τις παραμέτρους που επηρεάζουν τις παραμορφώσεις της γάστρας.

Nomenclature

E: Young modulus of Elasticity (GPa)

I: Second Moment of Area (m^4)

u(x): deflection of beam (m)

q: load distribution (t/m)

V: shear force (t)

M: bending moment (tm)

τ: Shear stress(N/ m^2)

As: Shear Area (m^2)

A: Section Area (m^2)

G: Shear modulus (GPa)

k: shear correction coefficient

Π : Potential Energy

Q: First Moment of Area (m^3)

TPC: Tones per Centimeter (t/cm)

MCT: Moment to Change Trim (tm)

ρ: water density (1.025 t/m^3)

LCG: longitudinal center of gravity for the vessel (m)

A_{WL}: Waterline Area (m^2)

List of Figures

List of Tables

1. Introduction

1.1 Historical – Literature review

Nowadays, the constantly increasing ship size, in the pursuit for greater ship carrying capacity, has been found to cause shaft bearing damage due to an increase in hull deformation. This increase leads to a change of bearings' vertical position (also referred as bearing offset) that supports the propulsion shafting system. Therefore, classification societies, ship-owners and shipyards are trying to find a solution by conducting analysis and verification process for proper shaft alignment, which includes hull deformation effects.

At present, the shaft alignment calculation for hull deformation typically requires a detailed 3D finite element modeling of the vessel, in particular the stern tube part, the engine room and the propeller shaft system. While the 3D analytical method provides very accurate results, it is time consuming and expensive approach and at many situations not viable, since the essential data is missing. Having the ability to measure hull deflections in an early design stage minimizes dependence on the experience of personnel and allows bearing reactions to be quite accurately assessed and confirmed for all vessel service drafts.

The current study focuses in the development of an easy and fast 1D finite differences model to determine the relative bearings' offsets. Only primary stresses are taken into account so the model can't be absolutely accurate since secondary and tertiary won't be included, but the main objective is to have an early estimation to assess the shaft alignment process. As ABS propulsion shaft alignment guidance notes state, the global deformation of hull girder modeled as a 1D beam gives accurate results to determine the bearings' offsets.

In his paper Global hydroelastic analysis of ultra large container ships by improved beam structural model (2014) , Ivo Senjanovic used a modified Timoshenko beam theory to calculate flexural vibrations for a ULCS of 20000 TEU subjected on bending and torsion and analyzed the coupled horizontal and torsional ship hull vibration with beam finite elements. Through STIFF program they acquired the longitudinal sectional geometrical properties of the vessel and compared the 1D FEM + 3D BEM hydroelastic model with the fully coupled 3D FEM + 3D BEM hydroelastic model. Although, very good agreement is achieved, especially in the high frequency range where springing influence is pronounced, some minor improvements in the low frequency domain could be done to increase the accuracy of damage calculation.

In recent guidance notes on propulsion shaft alignment by ABS (2019) concerning the shaft alignment procedure onboard large vessels, ABS states the an analytical method based on the 1D beam theory can also be used for hull deflection evaluation, if information about sectional modulus inertia and shear area are provided. The 1d model may produce high accuracy hull deflection results that match the 3D model. As mentioned in the notes, calibrations need to be made due to the abrupt change of inertia of the stern tube, so the coupling between the 1D and 3D model is necessary.

Finally, the diploma thesis Elastic Shaft Alignment of a Container Vessel by Stavros Siamantas was used as our rule of thumb. In his work, Siamantas developed a detailed finite element model of a typical 10,000 TEU container ship. The FE model was utilized to accurately calculate hull deflections for a series of representative loading conditions of the vessel. The aforementioned hull deflections are used for calculation of the additional vertical offsets of the bearings due to hull bending, and the corresponding effect on shaft equilibrium and bearing reactions. The same drawings and plans were used to acquire the input data for our thesis and the hull deformations we assessed are being compared with these calculated by the 3D finite element analysis conducted by Stavros Siamantas. In both thesis, hull deformations were calculated in still water loading conditions, where the marine diesel engine is cold and not running so deflections due to thermal expansion of the steel at the engine room area where excluded from this work.

1.2 Goals of Present Study

The main goal of this thesis is to develop a process to calculate, without much time and computing power, the bearing offsets caused by hull deformation without the need for 3D modeling. The purpose was to examine the hull deformation 1D problem and create and algorithm that will lead to close approximation of the bearing offsets for each loading condition, relative to those of a 3D Finite element analysis. The initial input in this algorithm are mainly information that every ship-owner can find in the loading manual (Shear Forces diagram, Moments diagram, Lightweight, Framespacing) and also input that requires a little bit of preprocessing from ship's drawings. Several tools were created to automate this process and make it as easy as possible even for engineers that don't have deep learning on bearing's offsets and shaft alignment process.

Secondary goals are:

1. Generation of a "relatively trustworthy" and simplified tool for non-expert engineers in order to quickly calculate the ship hull deflections at several loading conditions, without requiring much processing power.
2. Development of an application for fast calculation of transverse frame's second moment of area and shear area.
3. Determination of the least necessary data needed to solve the hull deflection problem.
4. Determination of the parts that need to be taken into consideration to achieve more precise and scientifically correct results.

2. Finite Element - Beam theory

2.1 Hull Girder Deflections

From the point of view of shaft alignment, the only hull deflections of interest are those manifested in the stern section and engine room of the ship, where the propulsion shafting is located.

The shaft bearings experience changes in their offset when the vessel's draft changes. This is caused by the varying load distribution on the vessel's hull. The measurement of bearing offset for various load conditions is crucial to minimize the possibility of shaft bearings and shaft damage.

According to ABS Guidance Notes on Propulsion Shafting Alignment an analytical method based on the 1D beam theory can be utilized for hull deflection evaluation. The structural response of the hull girder and the primary structural members under normal, shear, bending and torsional loads results in global (i. e. large area) deformations and stresses. In this case study, we will try to determine the bearing offsets due to hull girder deflections, as simple as possible and determine a simple and accurate method for their calculation. The Euler-Bernoulli and Timoshenko beam theory were used to determine hull deflections.

Before and during the evaluation, the results shall be examined for plausibility. This involves the visual presentation and checking of the deformations to see whether their magnitudes lie within the expected range and whether their distributions are meaningful with respect to the loads and boundary conditions or supports.

2.1.1 Euler Bernoulli beam

The Euler-Bernoulli beam theory is a model which provides a means of calculating the deflection of beams. It was developed around 1750 and is still the method that we most often use to analyze the behavior of bending elements.

The Bernoulli-Euler beam theory relies on a couple major assumptions:

(1) Plane sections perpendicular to the NA before deformation stay plane and perpendicular to the NA after deformation
(2) The beam is essentially prismatic (no openings or discontinuities)
(3) Other modes of response to the loads do not affect hull girder bending and may be treated separately
(4) The material is homogenous and elastic
(5) The deformations are small

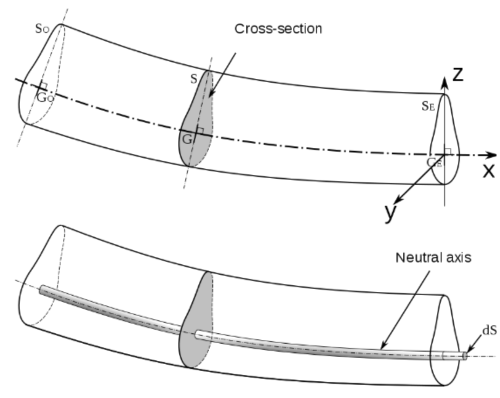

Figure 1: Euler Bernoulli beam theory

Those assumptions can be validated in a ship, as the total deformation of a ship's hull is insignificant to its principal dimensions (Breadth, Depth and Length). There is a little opening to none in a ship's hull and throughout vessel's length the material is homogenous (naval steel) and elastic.

The Euler–Bernoulli static beam equation describes the relationship between the beam's deflection and the applied load:

$$\frac{d^2}{dx^2}(EI\frac{d^2u}{dx^2}) = q$$

E: Young modulus of Elasticity (GPa)

I: Second Moment of Area (m^4)

w(x): deflection of beam at some position x

q: load distribution (t/m)

2.1.2 Timoshenko beam

The Timoshenko-Ehrenfest beam theory takes into account shear deformation and rotational bending effects. The resulting equations consist of a fourth order and second order partial derivatives. By taking into account the added shear deformation, the result is a larger deflection under a static load.

The assumptions of the formulation are:

(1) The longitudinal axis of the unloaded unreformed beam is straight.
(2) All loads applied to the beam act transverse to the longitudinal axis
(3) The total slope (x) of the centerline results from the effects of bending deformation and shears deformation and can be expressed as the sum of the rotations due to shear deformation and the rotation due to bending deformation.
(4) The material is considered linear elastic, homogeneous and isotropic. Hence, the generalized Hooke's stress-strain laws are valid.
(5) The deformations and strains are considered so small, and the strain-displacement equations of infinitesimal elasticity are used.
(6) Plane sections perpendicular to the neutral axis before deformation stay plane but not necessarily perpendicular to the neutral axis after deformation.

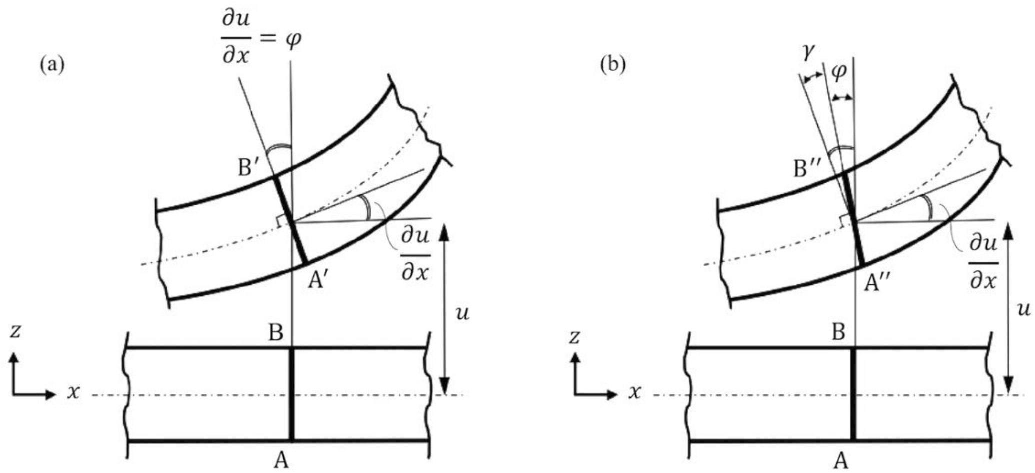

Figure 2: (a) Euler Bernoulli beam theory – (b) Timoshenko beam theory

The Timoshenko-Ehrenfest governing equations consist of a coupled system of ordinary differential equations:

$$\frac{d^2}{dx^2}(EI\frac{d\varphi}{dx}) = q$$

$$\frac{du}{dx} = \varphi - \frac{1}{G * As}\frac{d}{dx}(EI\frac{d\varphi}{dx})$$

As: Shear Area (m^2)

G: Shear modulus (GPa)

Where $\varphi = \frac{\partial u}{\partial x} - \gamma$ and $\gamma(x) = -\frac{V(x)}{GA_S(x)}$

V: shear force (N)

As mentioned at the assumptions above the Timoshenko theory assumes the deformed cross-section planes remain plane but not normal to the middle axis. The second governing equation implies this assumption and slope γ(x) is causing the warping of the section as shown on figure 2.

2.2 Loads

A ship is subjected to numerous loads, which can be divided into three major categories: (a) lightship weight, (b) deadweight and (c) buoyancy.

Lightship weight is the actual weight of a vessel when complete and ready for service but empty. It consists of: (a) hull weight, (b) superstructures weight, (c) machinery and (d) outfitting. Deadweight tonnage (DWT) is the displacement at any loaded condition minus the lightweight. Finally, buoyancy is the upward pressure applied at the hull underneath the waterline.

To acquire the ship's longitudinal load distribution in each load condition, we need firstly to obtain the shear forces for each condition from the loading manual. The rate of change of the shearing force through vessel's length is equal to the load:

$$q(x) = \frac{dV(x)}{dx}$$

V: shear force (t)

q: load distribution (t/m)

Since the data of shear forces in the loading manual contains only the frames from stern tube to front bulb (fr13 - fr378 studied vessel), forward and after frames lightweight must be added. This assumption is quite accurate, because there is no payload before the stern tube and after the front bulb and also buoyancy is little to none at those longitudinal positions. Another close approach would be to manually apply zero shear forces at the most fore and most aft length of the vessel.

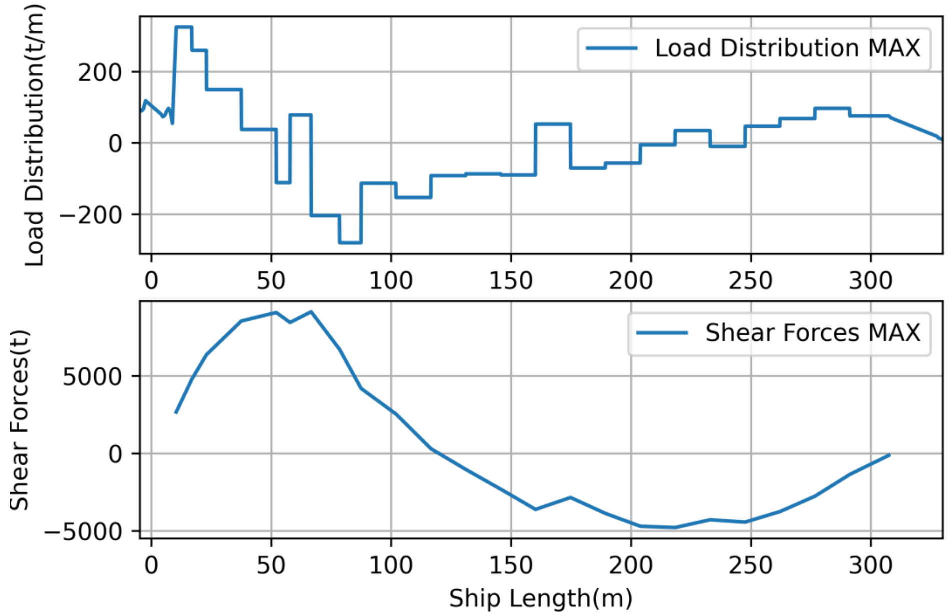

Figure 3: Shear Forces and Load Distribution at MAX condition for studied vessel

To verify the assumption, the integral of load distribution for the total length of the vessel must be equal or close to zero. It is particularly important to check the sums of the forces. For static load cases, it is to be ensured that the residual forces and moments are negligible. The error for the loading distribution of the different conditions is shown on the table below.

Load condition	DOCK1	BLD	BLA	11TDS	11TAS	MAX
Residual weight (t)	-210.45	-112.21	-280.27	-66.04	-34.25	-284.42
Displacement (t)	49604.6	78298.8	67174.0	153101.0	151443.0	150756.0
Error (%)	-0.424	-0.143	-0.417	-0.043	-0.023	-0.189

Table 2.1: Load distribution error for each load condition

$$\int_0^L q(x) = reisdual\ weight\ \cong 0$$

$$Error(\%) = \frac{Residual\ weight}{Displacement}$$

2.3 Second Moment of Area

The second moment of area, also known as the area moment of inertia is a geometric property of an area, which reflects the efficiency of a shape to resist bending caused by a load condition. Objects tend to change shape when loaded. The second moment of area is a measure of a shape's resistance to change. Therefore, the area moment of inertia, or inertia, is necessary for the calculation of deflection due to primary stresses.

The second moment of area of ship's cross section depends on how its points are distributed about an arbitrary axis, which is called the Neutral Axis (NA). The points of the Neutral Axis have no longitudinal stresses or strains. Therefore, firstly we need to calculate the Neutral Axis. The cross section of a ship, also called frame, consists of the outer shell, inner shell, girders, platforms and stiffeners. Primarily, we calculate the area and the position above bottom line of the elements above. After this, the Neutral Axis derives from the equation:

$$NA = \frac{\sum_i^n A_i * y_i}{\sum_i^n A_i}$$

n = number of same elements

A = area of each element

y = vertical distance from Bottom Line

Finally, by using the parallel axis theorem (Steiner), the second moment of area of each element is calculated from the Neutral Axis and the inertial summary of all the elements provides the frame inertia.

$$Inertia = I = \sum_i^n Ix_i + A_i {d_i}^2$$

Ix = inertia of element through its centroidal axis

A = area of element

d = perpendicular distance between element's centroidal axis and the Neutral Axis of the section

For the inertia of each element from its centroidal axis the calculations are shown below

2.3.1 Plating

The plating of the vessel contributes the most in the stiffness of the vessel. There several different shell plating throughout the vessel. Inner bottom, double bottom, side shell, bilge and deck plating are the most common, found in every vessel. Except from longitudinal, a ship has many transverse plating which contribute the web frame. All the longitudinal plating is taken into account in our thesis and an investigation is conducted to determine how the web frames contribute to the bending and shear stiffness of the vessel.

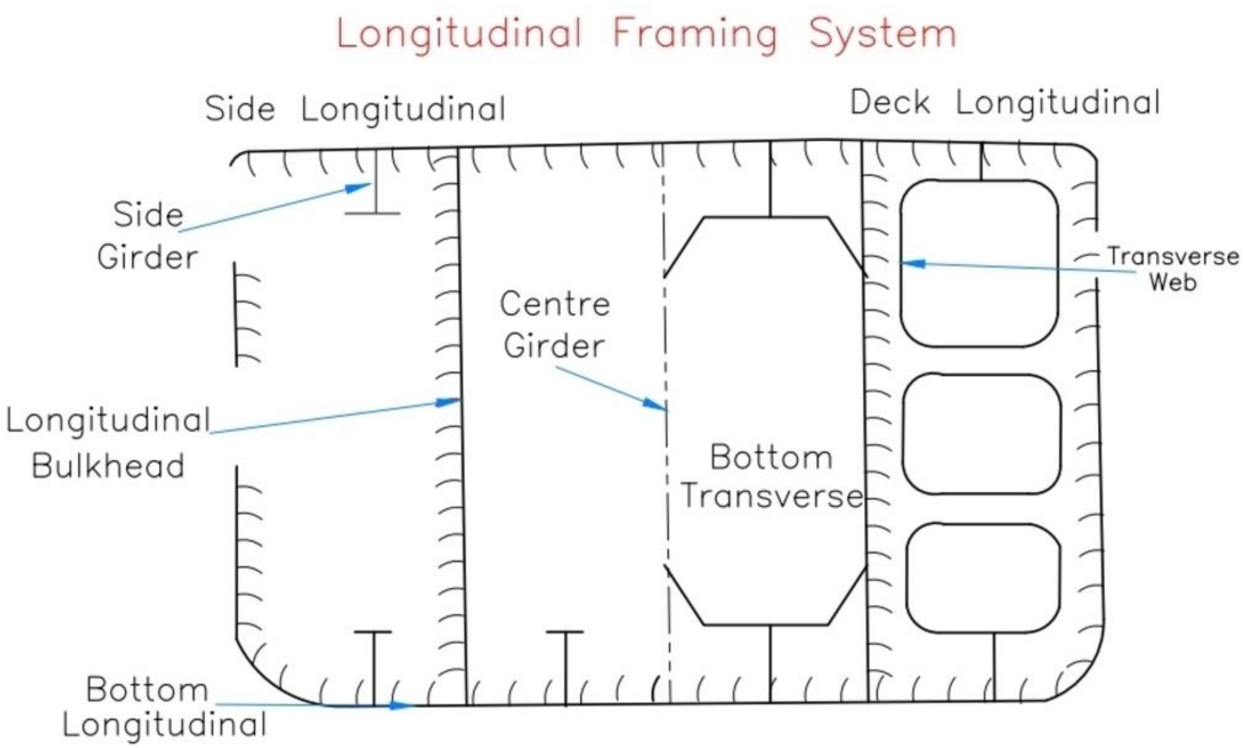

Figure 4: Transverse ship frame

$$ix = \frac{b * t^3}{12}\ , if\ element\ is\ parallel\ to\ neutral\ axis$$

$$ix = \frac{t * b^3}{12}\ , if\ element\ is\ vertical\ to\ neutral\ axis$$

$$ix = \frac{b * h^3}{12}\ , if\ plating\ is\ transverse\ (web\ frame)$$

If the plating has a different angle the inertia is derived from the equation:

$$iu = \frac{ix + iy}{2} + \frac{ix - iy}{2} * \cos 2\varphi - ixy * \sin 2\varphi$$

φ: the angle between the plating and axis parallel to NA

2.3.2 Stiffeners

Stiffeners are secondary plates or sections that are welded on plates to stiffen them against out of plane deformation. The most common types of stiffeners used on ships are flat bars, bulb flats, tee-bars and angle stiffeners.

Depending on the type of the stiffener, one must proceed with different calculations for the acquisition of the area, centroid points and inertia.

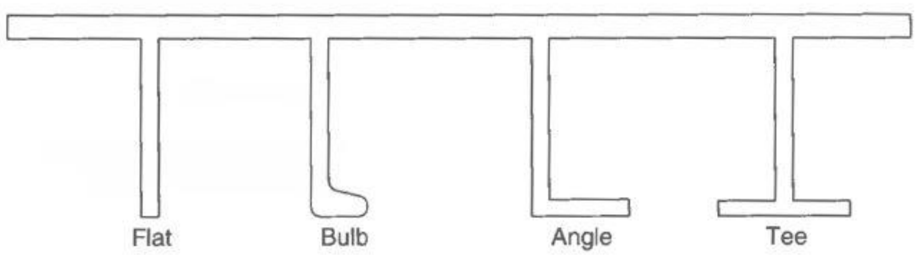

Figure 5 : Various types of beam stiffeners

2.3.2.1 Flat Bars

The moments of inertia of a flat bar with centroidal axis perpendicular to the Neutral Axis of the section can be found as this of plating:

$ix = \frac{t*h^3}{12}$, where h, t the height and thickness of the flat bar

$iy = \frac{h*t^3}{12}$

If the element is rotated by an angle φ, we apply the rotated axis as shown below. Also we apply the parallel axes theorem to its element.

2.3.2.2 Bulb flats

All the necessary data for bulb flats, dimensions and section properties (Area, Inertia, center of gravity etc.) was obtained by British steels' brochure [3].

	b	t	dx	dy	Ix	Iy	Zx	Zy	rx	ry	H	J
	mm	mm	mm	mm	cm4	cm4	cm3	cm3	cm	cm	cm^6/10^3	cm4
160x7	160	7	96.7	6.5	371.1	5.85	38.4	9	5.05	0.63	1.11	3.65
180x9	180	9	107.4	7.7	661.09	10.92	61.6	14.1	5.66	0.73	2.47	7.57
200x9	200	9	121.3	8.4	939.14	15.75	77.4	18.8	6.3	0.82	4.76	10
200x10	200	10	119.7	8.7	1010.47	17.18	84.4	19.8	6.28	0.82	4.83	11.78

Table 2.2: Bulb flat data from British Steels

If the element is rotated by an angle φ, we apply the rotated axis as shown below. Also, we apply the parallel axes theorem to its element.

2.3.2.3 Angle bar

The moments of inertia of an angle can be found, if the total area is divided into three, smaller ones, A, B, C, as shown in figure below. The final area may be considered as the additive combination of A+B+C. However, the calculation is more straightforward if the combination (A+C) + (B+C) - C is adopted. Then, the moment of inertia I_{x0} of the angle, relative to axis x0 is determined like this:

$$I_{x0} = I_{x0}^{A+C} + I_{x0}^{B+C} - I_{x0}^{C}$$

$$I_{x0} = \frac{bt^3}{3} + \frac{th^3}{3} - \frac{t^4}{3}$$

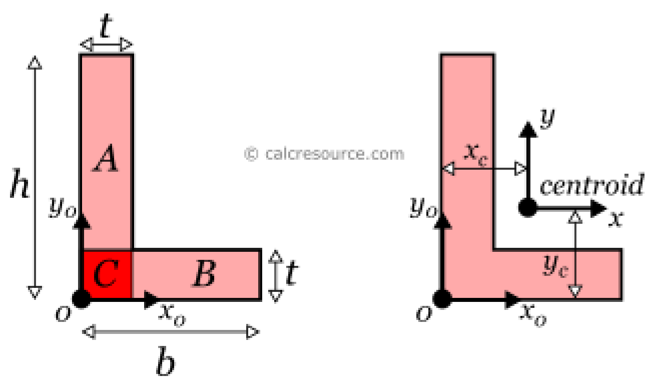

Figure 6: Angle bar

Following the same procedure, the moment of inertia of the angle, relative to axis y0 is:

$$I_{y0} = \frac{ht^3}{3} + \frac{tb^3}{3} - \frac{t^4}{3}$$

Finally, the product of inertia of the angle, relative to axes x0,y0 is found:

$$I_{xy0} = \frac{t^2h^2}{4} + \frac{t^2b^2}{4} - \frac{t^4}{4}$$

The moments of inertia relative to centroidal axes x,y, can be found by application of the Parallel Axes Theorem, as shown below. The centroid position can be found by the equation below:

$$x_c = \frac{ht^2 + tb^2 - t^3}{2A}$$

$$y_c = \frac{bt^2 + th^2 - t^3}{2A}$$

Where A is the area of the shape

<u>Tee bar:</u> Tee bar calculations are similar as those of angle bar.

2.3.3 Rotated axis

For the transformation of the moments of inertia from one system of axes x,y to another one u,v, rotated by an angle φ, the following equations are used:

$$iu = \frac{ix + iy}{2} + \frac{ix - iy}{2} * \cos 2\varphi - ixy * \sin 2\varphi$$

$$iv = \frac{ix + iy}{2} - \frac{ix - iy}{2} * \cos 2\varphi + ixy * \sin 2\varphi$$

$$iuv = \frac{ix - iy}{2} - \frac{ix - iy}{2} * \cos 2\varphi + ixy * \sin 2\varphi$$

Where ix, iy the moments of inertia about the initial axes and ixy the product of inertia. iu, iv and iuv are the respective quantities for the rotated axes u,v. The product of inertia ixy for symmetrical elements is equal to zero and for non-symmetrical must be calculated from the equation below:

$$ixy = \iint y * x \, dxdy$$

2.3.4 Parallel Axes Theorem

The second moment of area of any shape, in respect to an arbitrary, non centroidal axis, can be found if its moment of inertia in respect to a centroidal axis, parallel to the first one, is known. The Parallel Axes Theorem (Steiner) is given by the following equation:

$$I_{NA} = I + A * {y_{NA}}^2$$

where I_{NA} is the moment of inertia in respect to transverse section's Neutral Axis, I the moment of inertia in respect to element's centroidal axis, parallel to the first one, y_{NA} the distance between the two parallel axes and A the area of the element.

For the product of inertia Ixy, the parallel axes theorem takes a similar form:

$$Ixy_{NA} = Ixy + A * y_{NA} * x_{NA}$$

Where Ixy_{NA} is the product of inertia, relative to centroidal axes x, y, and Ixy is the product of inertia, relative to axes that are parallel to element's centroidal x,y ones, having offsets from them y_{NA} and x_{NA} respectively.

2.4 Section Properties Calculator app

For the calculations of the ships' longitudinal inertia (second moment of area), a Graphic User Interface (GUI) application was developed in Python programming language with the use of Tkinter library. In a simple and efficient interface, a ship's frame can be imported over a canvas widget. After calibrating (scaling) the image to turn pixels into lengths, one can add up all the elements consisting the frame, like outer and inner shell plating, girders and platforms, and longitudinal stiffeners. By clicking the points of those elements, the application stores their position. As soon as the necessary section data (plate thickness, stiffener's height and type, etc.) is applied, the app calculates the Neutral Axis, Second moment of area and Shear Area and generates an excel file with all the data for possible future changes.

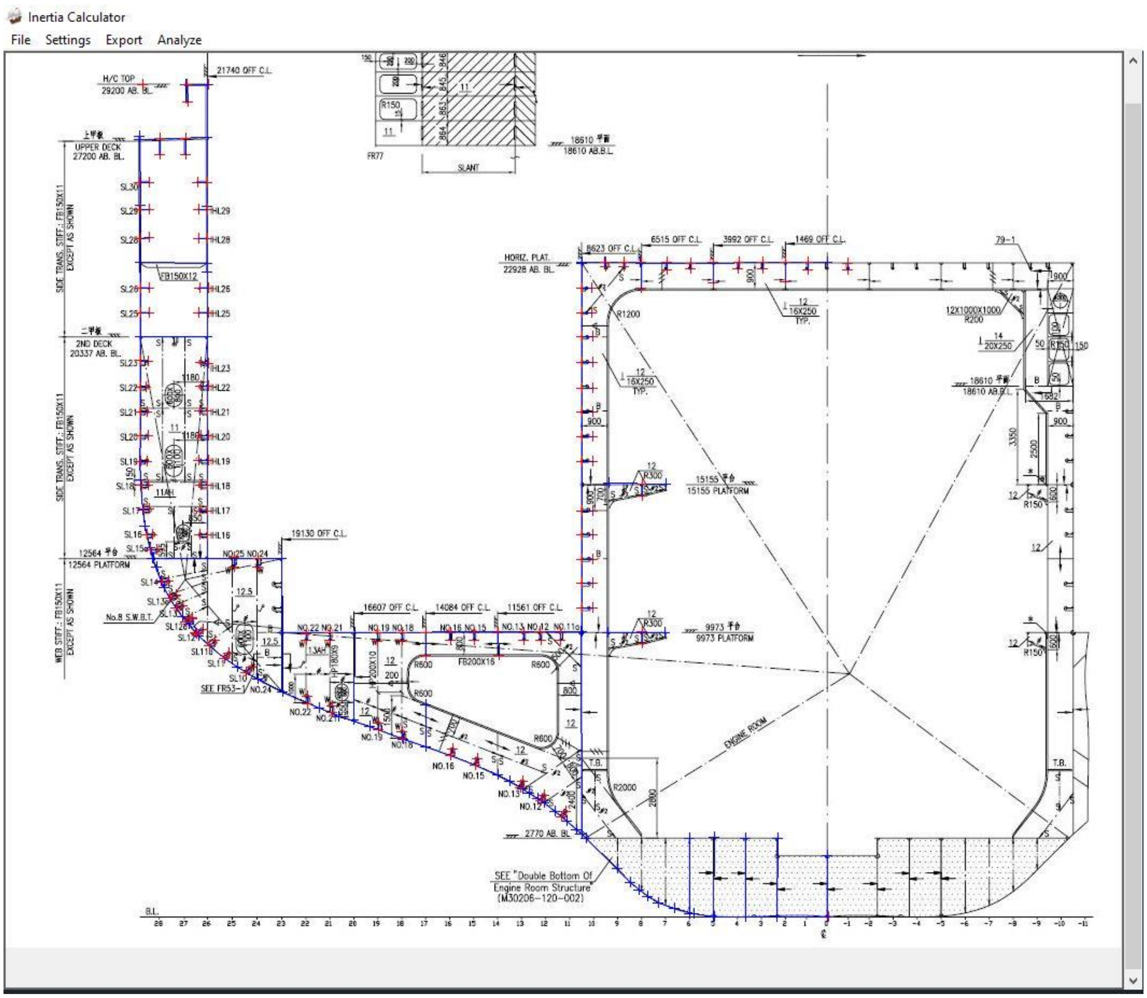

Figure 7: Inertia Calculator application environment

2.5 Compartmentation

The construction drawings are divided into four major sections; shell expansion, decks, buttocks and frames. Only elements that run through the ship's length were included. Transverse plates and stiffeners were excluded from the calculations since they do not contribute in the hull girder strength (primary stresses). The total steel structure of a containership contains several vital substructures, some of which are mentioned in the next paragraphs.

2.5.1 Stern Tube

The stern tube (Figure 2.) is a hollow tube which accommodates the bearings and the propeller shaft. It is located at the lower aft part of the ship and is usually equipped with two journal bearings which support the weight of the shaft passing through the tube and that of the propeller. This part is of high importance for the hull girder deflection due to its high stiffness. The stern tube consists of thick plates to support the weight of the shaft and the propeller. Except from the longitudinal plating, the stern tube consists of many web frames, more dense than the rest of the ship, leading to a higher stiffness capacity of the stern tube area. In his work Siamantas modeled the stern frame (faded part on the drawing) with a solid part which increases abruptly the sectional properties of the stern tube frames, as it will be discussed later.0

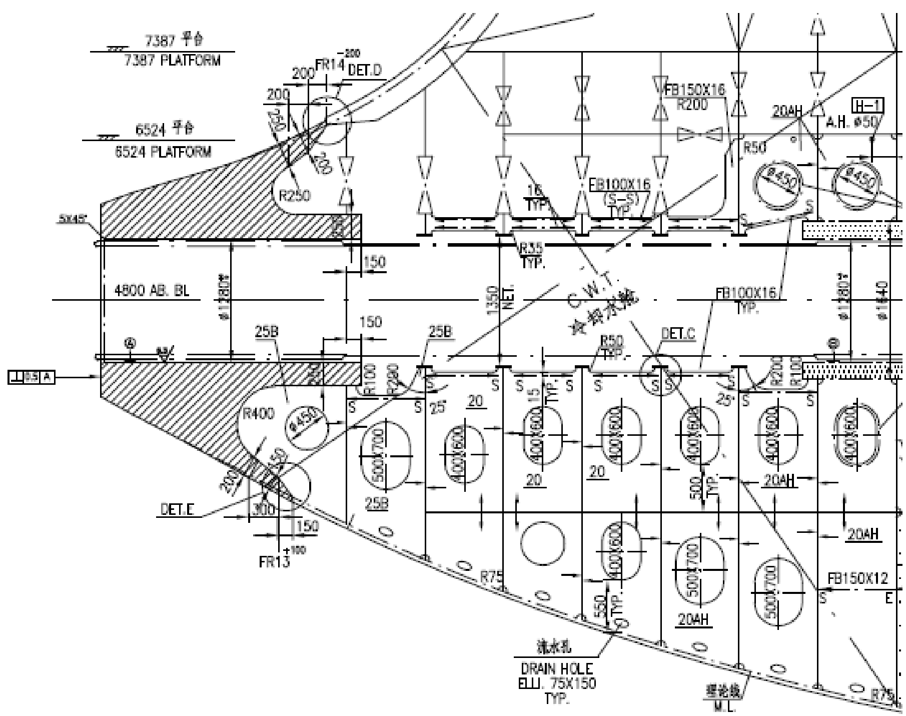

Figure 8: Stern tube of a vessel

2.5.2 Deck house

The deckhouse consists of the parts of the ship that project above the main deck. Deckhouse contains spaces available for accommodation of the crew and passengers. According to studies, since the length and breadth of the superstructure is small in proportion to those of the ship, the bending stiffness of the deckhouse does not contribute in the hull girder stiffness, thus it can be excluded. Although stiffness is not included the weight of the superstructure must be in the calculations of the load.

Figure 9: Deckhouse

2.5.3 Hatch Covers

Hatch covers are the vertical surfaces on a ship that close the hatch openings. In containerships, hatch covers aren't yielded on the deck, but they are hinged in many longitudinal points across the vessel. During loading and unloading the covers are rolling on and off the deck to add containers in the hatch. Generally, the hatch covers do not contribute in the hull bending and shear stiffness but since in the 3D FEA model they were included, we included them in the model as well. The hatch covers, consist of 30mm plating and 14 T-shaped longitudinal stiffeners. The exclusion of the hatch covers would lead to more actual results and would lower significantly the second moment of area and produce different hull deformations.

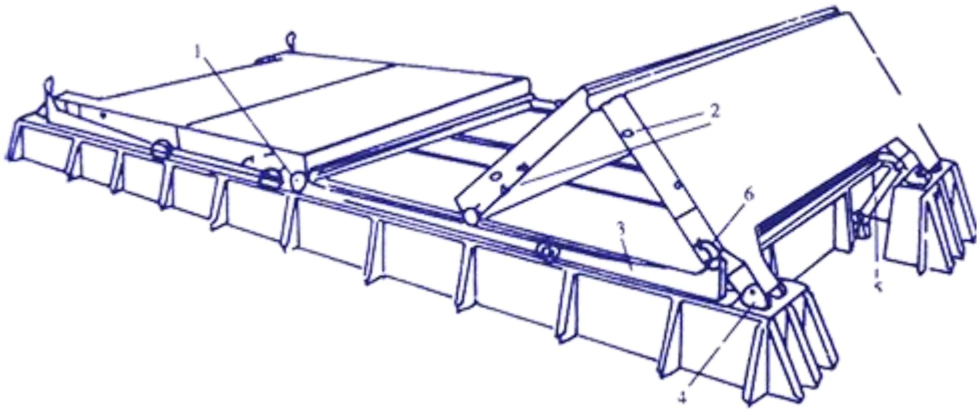

Figure 10: Containership hatch covers

As it is known, container ships are highly subjected to torsional moments because of their large hatch openings. This leads to even higher warping stresses at the corners of the openings due to lack of torsional rigidity. The upper part of the double hull in such ships is fitted with torsion box to deliver those stresses avoiding failure of the structure.

Therefore, while designing ships with large openings (like container ships) it must ensured that proper FEM analysis and model testing procedures are carried out. Proper strength analysis of the hull and deck plating should be done.

2.5.4 Web frames

In a typical vessel, except from the longitudinal elements there are also transverse elements supporting the structure. In ships they are called web frames and they are deep-section built-up frames which provide additional strength to the structure. After, testing the total deflection of the ship without the web frames we came to the conclusion that they must be inserted in order to achieve better results. In the figure 2.11 we can see a web frame of a containership midship section. For the distribution of web frame's stiffness in the rest of the vessel we assumed triangular distribution, where the whole stiffness of the web frame is divided triangularly in different nodes around the web frame (effective nodes).

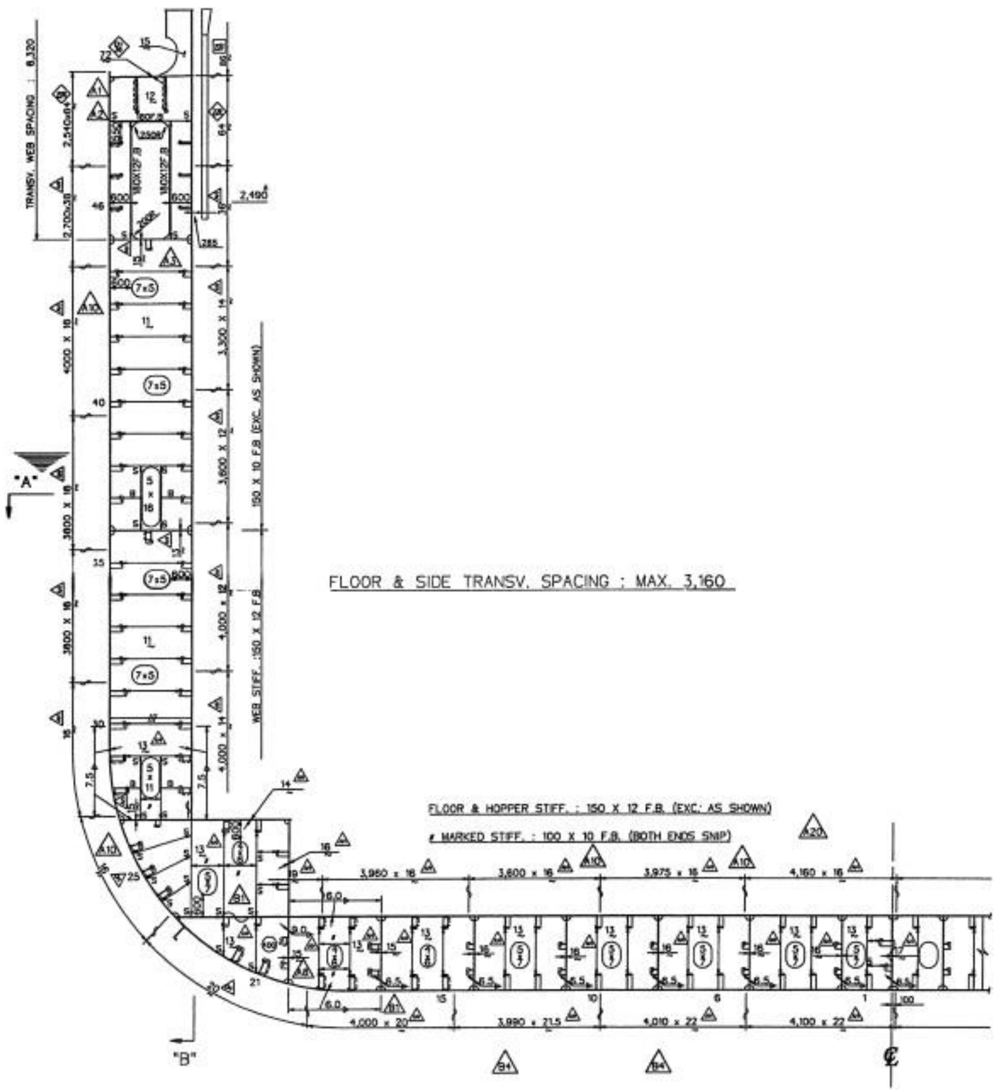

Figure 11: Containership Midship Web Frame

3 Finite Element Analysis

3.1 Euler Bernoulli Beam FDM Analysis

As mentioned before, in order to measure the hull deflection, we firstly used the Euler-Bernoulli beam theory, due its simplicity. In a ship, the flexural rigidity varies throughout its length, which means that the term EI is not constant. The equation needed to calculate the deflection can be found by applying the Leibniz product rule in the EB beam equation. Young's elastic modulus (E) was considered constant and equal to 207GPa, as there is no way to determine the exact value for each steel section. This assumption is right, as the steel types used in studied vesse; are A grade naval steel (A, AH36).

$$Leibniz\ product\ rule: \frac{d^2}{dx^2}(fg) = f''g + 2f'g' + fg''$$

$$\frac{d^2}{dx^2}\left(EI(x)\frac{d^2u(x)}{dx^2}\right) = E * \left(I''(x) * \frac{d^2u(x)}{dx^2} + 2 * I'(x) * \frac{d^3u(x)}{dx^3} + I(x) * \frac{d^4u(x)}{dx^4}\right) = q(x)$$

To measure u(x) from the equation we need to construct the global matrix A and B, and solve the linear equation:

$$A * u = B$$

A: global stiffness matrix

B: Load matrix

Firstly, the Second moment of Area was measured by the inertia calculator app. Several transverse sections were calculated to determine the inertia distribution through ship's length. After that, we interpolated the inertia data with a continuous, piecewise linear function throughout the length, with small step size (10cm), to construct the mesh. With a step size of 10cm and total length of studied vessel equal to 334.75m, our mesh is divided in 3347 nodes for simply supported beam and 975 nodes for cantilever beam analysis. The first and second derivatives of inertia can be obtained with numpy.grad command in Python.

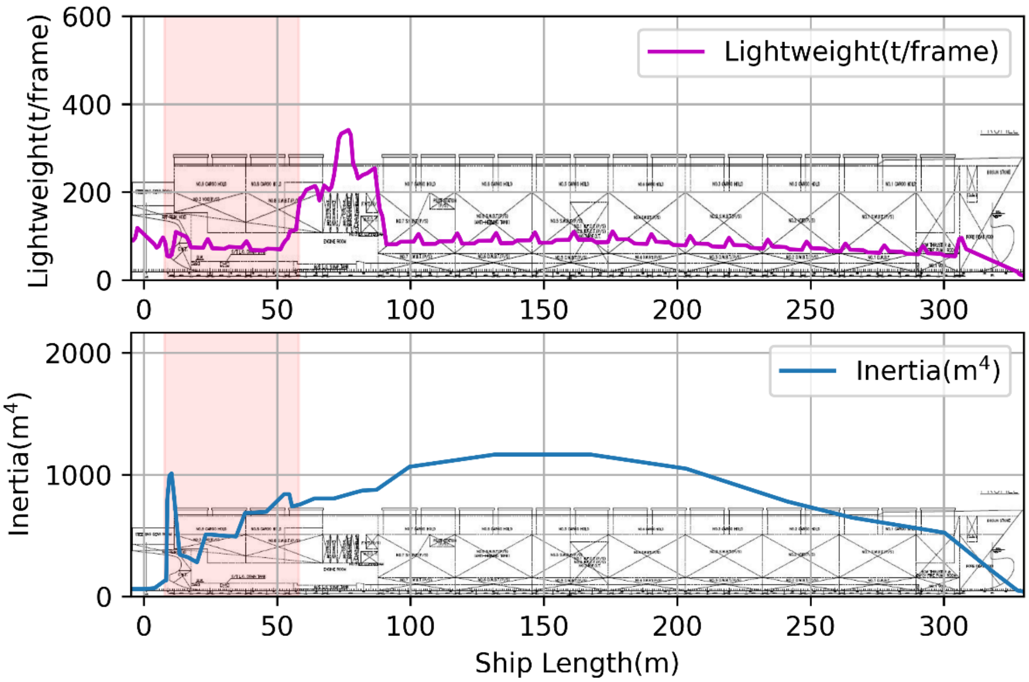

Figure 12: Lightweight and Inertia distribution of studied vessel without Deckhouse

As can be noticed from Inertia distribution on the figure above, the stern area has a high inertia due to thick plating and solid parts of the stern tube. After this at the stern tube frames (fr13-fr17), we notice a second spike of inertia due to high stiffness of the stern tube area. Lastly, the third increase can be identified in the engine room frames below deckhouse (fr.83-107).

Central difference formula for the internal nodes, forward difference for the first 2 nodes and backward difference for the last 2 nodes, were used to develop the second, third and fourth derivative of u(x) and approximate the deflection. From Taylor series expansion for central differentiation:

$$\frac{d^2u(x)}{dx^2} = \frac{u(x-\Delta x) - 2u(x) + u(x+\Delta x)}{\Delta x^2}$$

$$\frac{d^3u(x)}{dx^2} = \frac{-\frac{1}{2}u(x-2\Delta x) + u(x-\Delta x) - u(x+\Delta x) + \frac{1}{2}u(x+2\Delta x)}{\Delta x^3}$$

$$\frac{d^4u(x)}{dx^2} = \frac{u(x-2\Delta x) - 4u(x-\Delta x) + 6u(x) - 4u(x+\Delta x) + u(x+2\Delta x)}{\Delta x^2}$$

From Taylor series expansion for forward differentiation:

$$\frac{d^2u(x)}{dx^2} = \frac{2u(x) - 5u(x+\Delta x) + 4u(x+2\Delta x) - u(x+3\Delta x)}{\Delta x^2}$$

$$\frac{d^3u(x)}{dx^2} = \frac{-5u(x) + 18u(x+\Delta x) - 24u(x+2\Delta x) + 14u(x+3\Delta x) - 3u(x+4\Delta x)}{\Delta x^3}$$

$$\frac{d^4u(x)}{dx^2} = \frac{3u(x) - 14u(x+\Delta x) + 26u(x+2\Delta x) - 24u(x+3\Delta x) + 11u(x+4\Delta x) - 2u(x+5\Delta x)}{\Delta x^4}$$

From Taylor series expansion for backward differentiation:

$$\frac{d^2u(x)}{dx^2} = \frac{2u(x) - 5u(x-\Delta x) + 4u(x-2\Delta x) - u(x+3\Delta x)}{\Delta x^2}$$

$$\frac{d^3u(x)}{dx^2} = \frac{-5u(x) + 18u(x-\Delta x) - 24u(x-2\Delta x) + 14u(x-3\Delta x) - 3u(x-4\Delta x)}{\Delta x^3}$$

$$\frac{d^4u(x)}{dx^2} = \frac{3u(x) - 14u(x-\Delta x) + 26u(x-2\Delta x) - 24u(x-3\Delta x) + 11u(x-4\Delta x) - 2u(x-5\Delta x)}{\Delta x^4}$$

The resulting stiffness matrix A is a pentadiagonal matrix with 6 and 7 elements on first and last 2 rows, due to forward differentiation and backward differentiation.

$$
\begin{bmatrix}
a_1 & b_1 & c_1 & d_1 & e_1 & f_1 & 0 & \cdots & 0 & 0 \\
a_2 & b_2 & c_2 & d_2 & e_2 & f_2 & g_2 & 0 & \cdots & 0 \\
a_3 & b_3 & c_3 & d_3 & e_3 & 0 & \cdots & \cdots & \cdots & 0 \\
0 & a_4 & b_4 & c_4 & d_4 & e_4 & 0 & \cdots & \cdots & 0 \\
\vdots & \ddots & \ddots & \ddots & \ddots & \ddots & \ddots & \ddots & \ddots & \vdots \\
0 & \cdots & \cdots & 0 & a_{i-3} & b_{i-3} & c_{i-3} & d_{i-3} & e_{i-3} & 0 \\
0 & \cdots & \cdots & \cdots & 0 & a_{i-2} & b_{i-2} & c_{i-2} & d_{i-2} & e_{i-2} \\
0 & \cdots & \cdots & 0 & a_{i-1} & b_{i-1} & c_{i-1} & d_{i-1} & e_{i-1} & f_{i-1} \\
0 & \cdots & 0 & a_i & b_i & c_i & d_i & e_i & f_i & g_i
\end{bmatrix}
*
\begin{bmatrix}
u_1 \\ u_2 \\ u_3 \\ u_4 \\ u_5 \\ \vdots \\ \vdots \\ \vdots \\ u_i
\end{bmatrix}
=
\begin{bmatrix}
q_1 \\ q_2 \\ q_3 \\ q_4 \\ q_5 \\ \vdots \\ \vdots \\ \vdots \\ q_i
\end{bmatrix}
$$

3.2 Finite Element Method

3.2.1 Euler Bernoulli FEM

Except from Finite differences method, Finite Element Method (FEM) was used to test the results and apply boundary conditions. The Finite differences method was mainly used for validation of the model and the results of this thesis were produced by the Finite Element Method. The element stiffness matrix and force vector can be produced via the method mention on the Timoshenko Analysis chapter below.A reasonable assumption for the interpolation field would be at least a third order polynomial expression:

$$u(x) = a_0 + a_1 x + a_2 x^2 + a_3 x^3$$

$$\Theta(x) = a_1 + 2a_2 x + 3a_3 x^2$$

$$\{u(x)\} = [1 \quad x \quad x^2 \quad x^3]\begin{Bmatrix} a_0 \\ a_1 \\ a_2 \\ a_3 \end{Bmatrix}$$

The above relation must hold for the arbitrary displacements at the nodal points of each element. Meaning at nodal boundaries: $u(0)=u_i$, $u(L)=u_{i+1}$, $\theta(0)=\theta_i$, $\theta(L)=\theta_{i+1}$

$$\begin{Bmatrix} u(0) = u_i \\ \theta(0) = \theta_i \\ u(L) = u_{i+1} \\ \theta(L) = \theta_{i+1} \end{Bmatrix} = \begin{bmatrix} 1 & 0 & 0 & 0 \\ 0 & 1 & 0 & 0 \\ 1 & l & l^2 & l^3 \\ 0 & 1 & 2l & 3l^2 \end{bmatrix}\begin{Bmatrix} a_0 \\ a_1 \\ a_2 \\ a_3 \end{Bmatrix}$$

Therefore, by solving with reference to the polynomial coefficients:

$$\begin{Bmatrix} u(0) = u_i \\ \theta(0) = \theta_i \\ u(L) = u_{i+1} \\ \theta(L) = \theta_{i+1} \end{Bmatrix} = \begin{bmatrix} 1 & 0 & 0 & 0 \\ 0 & 1 & 0 & 0 \\ -\frac{3}{l^2} & -\frac{2}{l} & \frac{3}{l^2} & -\frac{1}{l} \\ \frac{2}{l^3} & \frac{1}{l^2} & -\frac{2}{l^3} & \frac{1}{l^2} \end{bmatrix}\begin{Bmatrix} v_1 \\ \theta_1 \\ v_2 \\ \theta_2 \end{Bmatrix}$$

Now we can derive the 2-dimensional Euler/Bernoulli finite element interpolation scheme (i.e. a relation between the continuous displacement field and the beam nodal values):

$$\{u(x)\} = [1 \quad x \quad x^2 \quad x^3]\begin{bmatrix} 1 & 0 & 0 & 0 \\ 0 & 1 & 0 & 0 \\ -\frac{3}{l^2} & -\frac{2}{l} & \frac{3}{l^2} & -\frac{1}{l} \\ \frac{2}{l^3} & \frac{1}{l^2} & -\frac{2}{l^3} & \frac{1}{l^2} \end{bmatrix}\begin{Bmatrix} u_i \\ \theta_i \\ u_{i+1} \\ \theta_{i+1} \end{Bmatrix} = [N][d]$$

Where $N1 = 1 - \frac{3x^2}{l^2} + \frac{2x^3}{l^3}$, $N2 = x - \frac{2x^2}{l} + \frac{x^3}{l^2}$, $N3 = \frac{3x^2}{l^2} - \frac{2x^3}{l^3}$, $N4 = -\frac{x^2}{l} + \frac{x^3}{l^2}$

The beam element stiffness matrix is readily derived as:

$$k^e = \int_x (B^T[EI(x)]B)dx$$

$$k^e = \frac{EI(x)}{l^3}\begin{bmatrix} 12 & 6l & -12 & 6l \\ 6l & 4l^2 & -6l & 2l^2 \\ -12 & -6l & 12 & -6l \\ 6l & 2l^2 & -6l & 4l^2 \end{bmatrix}$$

Before proceeding further let's consider the format for the element force vector for transverse loading. So for uniform distributed load q_i:

$$\vec{f_e} = \frac{q_e * l}{2}\begin{bmatrix} 1 \\ \frac{l}{6} \\ 1 \\ -\frac{l}{6} \end{bmatrix}$$

3.2.2 Timoshenko FEM

Except from Euler-Bernoulli beam analysis, the hull girder was investigated as a Timoshenko beam. The Timoshenko beam has two main differences from EB method, which is:

(a) Shear deformation is taken into account,

(b) Plane sections perpendicular to the neutral axis before deformation stay plane but not necessarily perpendicular to the neutral axis after deformation.

The transverse deformation of a beam with a shear and bending strains may be separated into a portion related to shear deformation and a portion related to bending deformation:

$$u(x) = u_b(x) + u_s(x)$$

$$u''_b(x) = \frac{M(x)}{EI(x)}$$

$$u'_s(x) = \frac{V(x)}{GA_S(x)}$$

An infinite Shear Area implies negligible effect of transverse shear deformation and the model degenerates to the classical theory of Euler-Bernoulli Beam. From the deflection equation above it is obvious that the precise calculation of bending and shear stiffness is of high importance. Overestimating or underestimating one of the above will lead to the other having a significantly higher or lower contribution to the total deflection of the vessel.

To acquire the shear deformations, one must find the longitudinal shear area of the vessel. The simplest estimate of the shear area is based on the assumption that the shear stress varies proportional to cosθ, where θ is the angle between the tangent to the thin walled members and the y-axis. So the shear area As is defined as:

$$As = \int_A cos^2\theta dA$$

The method above overestimates the area of the section contributing in the shear stiffness. Rather than using this extremely simple approach, several authors have argued for a more consistent method, in which the shear stress distribution τ = τ (z) due to a unit shear force is used. The reduction of the cross-sectional area results from different distribution of the material law and the cross-section equilibrium, which leads to a contradiction. This contradiction is due to the hypothesis that the cross-sections remain the same, although the cross-section would actually be subjected to warping when the shear force effect occurs. Therefore, the shear area is introduced into the strength of the materials. The derivation of this shear area is described below:

$$\int_A \frac{\tau^2(z)}{2G} dA = \int_A \frac{{\tau_m}^2(z)}{2G} dA_s = \frac{V^2}{2GA_s}$$

$$\frac{1}{2G}\int_A \left(\frac{VQ(z)}{It(z)}\right)^2 dA = \frac{V^2}{2GA_s}$$

$$dA = t(z)dz$$

$$A_s = \frac{I^2}{\int_{z0}^{zu} \frac{Q^2(z)}{t(z)} dz}$$

The above although it consists of difficult area calculations creates more accurate results close to the ones generated by a 3d model. On APPENDIX B there is a calculation of shear area for a simple section to help engineers understand better the procedure.

The total potential energy of the beam considers both bending and shear contribution:

$$\Pi\big(u(x), \theta(x)\big) = \frac{1}{2}\int_V \sigma_x \varepsilon_x dV + \frac{1}{2}\int_V \tau_{xy}\gamma_{xy} dV - \int_{x_i}^{x_j} qu(x)dx$$

Where the normal stress is obtained by the Hooke's law as:

$$\sigma_x = E\varepsilon_x$$

While the transverse shear stress is obtained as

$$\tau_{xy} = kG\gamma_{xy}$$

Where G the shear modulus and k the shear correction factor. This factor is dependent on the cross-section. Considering dV = dAdx and integrating through the thickness, we obtain the potential energy in terms of the generalized displacements.

$$\Pi\big(u(x), \theta(x)\big) = \frac{1}{2}\int_x EI(x)(\theta'(x))^2 + \frac{1}{2}\int_x GA_s(x)(\frac{\partial u}{\partial x} - \theta(x))^2 dx - \int_{x_i}^{x_j} qu(x)dx$$

To turn in a more convenient form:

$$e = \begin{bmatrix} \theta'(x) \\ -\theta(x) + u'(x) \end{bmatrix}$$

$$\Pi = \frac{1}{2}\int_x \left(e^T \begin{bmatrix} EI(x) & 0 \\ 0 & GAs(x) \end{bmatrix} e\right) dx - \int_{x_i}^{x_j} qu(x)dx$$

The deflection w(x) and slope θ(x) of the hull girder can be expressed through third order polynomial shape functions as shown below:

$$\begin{Bmatrix} u(x) \\ \theta(x) \end{Bmatrix} = \begin{bmatrix} N1 & 0 & N2 & 0 \\ 0 & N3 & 0 & N4 \end{bmatrix} \begin{Bmatrix} v_i \\ \theta_i \\ v_{i+1} \\ \theta_{i+1} \end{Bmatrix}$$

$$\begin{Bmatrix} u(x) \\ \theta(x) \end{Bmatrix} = \begin{bmatrix} 1 - \frac{3x^2}{l^2} + \frac{2x^3}{l^3} & 0 & x - \frac{2x^2}{l} + \frac{x^3}{l^2} & 0 \\ 0 & \frac{3x^2}{l^2} - \frac{2x^3}{l^3} & 0 & -\frac{x^2}{l} + \frac{x^3}{l^2} \end{bmatrix} \begin{Bmatrix} v_i \\ \theta_i \\ v_{i+1} \\ \theta_{i+1} \end{Bmatrix} = Nd$$

$$e = \begin{bmatrix} \theta'(x) \\ -\theta(x) + w'(x) \end{bmatrix} = \begin{bmatrix} 0 & N1' & 0 & N2' \\ N1' & -N1 & N2' & -N2 \end{bmatrix} \begin{Bmatrix} v_i \\ \theta_i \\ v_{i+1} \\ \theta_{i+1} \end{Bmatrix} = Bd$$

$$\Pi = \frac{1}{2} \int_x \left(d^T B^T \begin{bmatrix} EI(x) & 0 \\ 0 & GAs(x) \end{bmatrix} Bd \right) dx - \int_{x_i}^{x_j} qu(x) dx$$

Minimize the total potential energy with respect to the unknown nodal quantities:

$$\int_x \left(B^T \begin{bmatrix} EI(x) & 0 \\ 0 & GAs(x) \end{bmatrix} B \right) dx\, d - \int_{x_i}^{x_j} qu(x) dx \ = 0$$

By solving the above for each different element we can produce the global stiffness matrix and the global force vector. For the hull girder, since the mesh is divided in many elements, we can assume that for each element the load distribution, second moment of area and shear area can be described by different uniform distributed functions. So for each element those values are fixed values.

For each element we acquire the below:

$$\{f\} = [k]\,\{u\}$$

$$\begin{Bmatrix} f_{y1} \\ m_1 \\ f_{y2} \\ m_2 \end{Bmatrix} = \begin{bmatrix} k_{11} & k_{12} & k_{13} & k_{14} \\ k_{21} & k_{22} & k_{23} & k_{24} \\ k_{31} & k_{32} & k_{33} & k_{34} \\ k_{41} & k_{42} & k_{43} & k_{44} \end{bmatrix} \begin{Bmatrix} v_1 \\ \theta_1 \\ v_2 \\ \theta_2 \end{Bmatrix}$$

$$k^e = \frac{EI(x)}{l^3(1+\Phi)} \begin{bmatrix} 12 & 6l & -12 & 6l \\ 6l & (4+\Phi)l^2 & -6l & (2-\Phi)l^2 \\ -12 & -6l & 12 & -6l \\ 6l & (2-\Phi)l^2 & -6l & (4+\Phi)l^2 \end{bmatrix}$$

Where $\Phi = \frac{12EI(x)}{(GA_S(x)l^2)}$

Before proceeding further let's consider the format for the element force vector for transverse loading. So for uniform distributed load q_i:

$$\vec{f_e} = \frac{q_e * l}{2}\begin{bmatrix} 1 \\ \frac{l}{6} \\ 1 \\ -\frac{l}{6} \end{bmatrix}$$

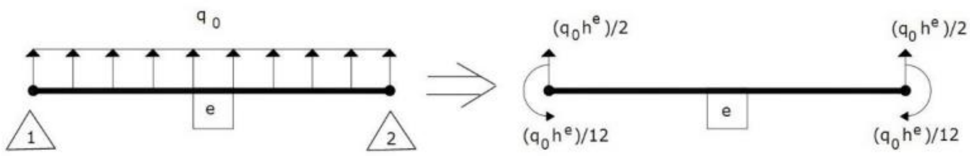

Figure 13: Element load to force vector

On closer inspection of the results for the above two cases, one can see that the applied distributed load is in essence replaced with a statically equivalent set of nodal forces acting at the ends of the element.

From continuity the displacement and slope at the common node of two elements must be the same. So when we assemble the global stiffness matrix the terms in the element stiffness matrices corresponding to each node should be summed for each degree of freedom. The resulting global matrix is diagonal and symmetric. In the same way, the force vector can be produced. By solving the problem {F} = [K]*{U}, we acquire the displacement and slope of the hull girder.

K: Global Stiffness Matrix

U: Nodal displacements and slopes

F: Nodal forces

3.3 Boundary Conditions

The proper selection of boundary conditions is the most serious task when using finite element analysis. Incorrect boundary conditions can lead to considerable errors by suppressing or raising the deformation modes of the cross sections. Many different conditions were checked to define the most proper and realistic solution.

The modeling of the aft end structure, as in Siamantas thesis, can be expressed by a cantilever beam as shown in Figure below. The aft most end of the ship is a free edge (as shearing force and bending moment is zero, and displacement and slope are non-zero), therefore no boundary condition should be introduced. On the other hand, the foremost end of the engine room does not allow the section to translate vertically nor rotate in the vertical plane, thus shearing force and bending moments are non-zero.

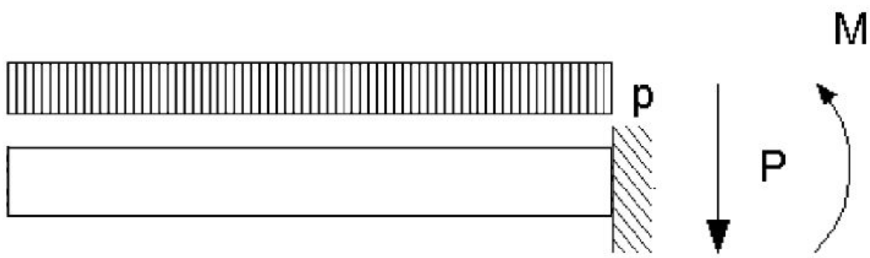

Figure 14: Beam representing the loading condition and boundary conditions

When modeling the whole ship as hull girder, in order to predict the primary displacements of hull girder the boundary conditions should be such as to induce nodal forces and moments that, when summed, correspond to the hull girder shearing forces and bending moments. According to Indian Register of Shipping (IRS) guidelines on Structural Assessment of Ships based on Finite Element Method (2020), when simulating the full ship finite element model in static structural analysis the applied boundary conditions must prevent the rigid body motions without over-constraining the model. Location of boundary condition is to be far away from the area of interest. Generally, boundary conditions are typically applied at two locations, one in the aft and the other in the fore. The chosen aft position is the engine room front bulkhead and the fore is the collision bulkhead as shown in Figure 14 below. In our 1D model the aft support is pin and fore is roller.

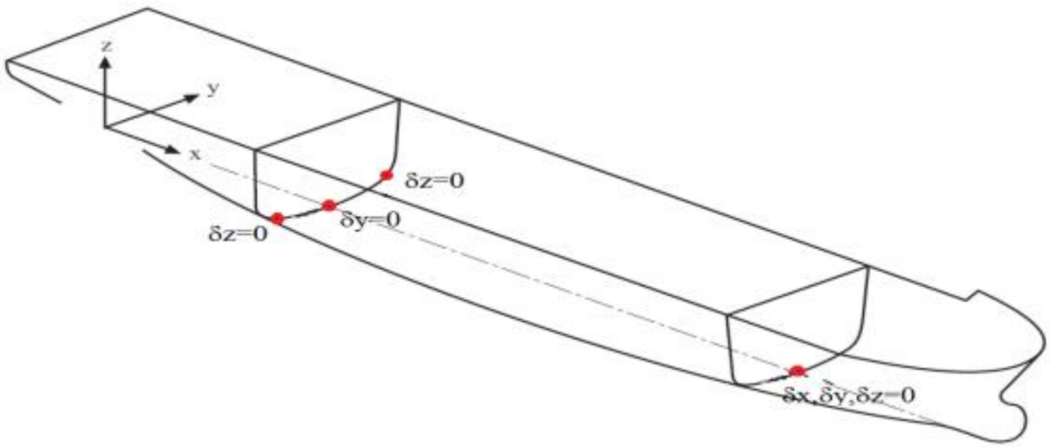

Figure 15: Full FE ship model boundary conditions

The results on both boundary conditions, simply supported and cantilever were quite same so the results shown are for cantilever beam, since our area of interest is the shaft area.

4. Shaft Alignment

4.1. Definition

The ship propulsion system is usually composed of a two-stroke diesel engine and a shaft system, which transmits power from the engine to the propeller. If a four-stroke diesel engine is installed on the ship, a reduction gear is necessary to achieve the most efficient rotational speed for the shafting system. The shaft comprises three individual parts: (a) the crankshaft, (b) the intermediate shaft and (c) the propeller shaft. Each one of these parts is supported by different (amount and type) journal bearings according to the loads to be supported. (Propeller, flanges, pistons, flywheel, flanges etc.).

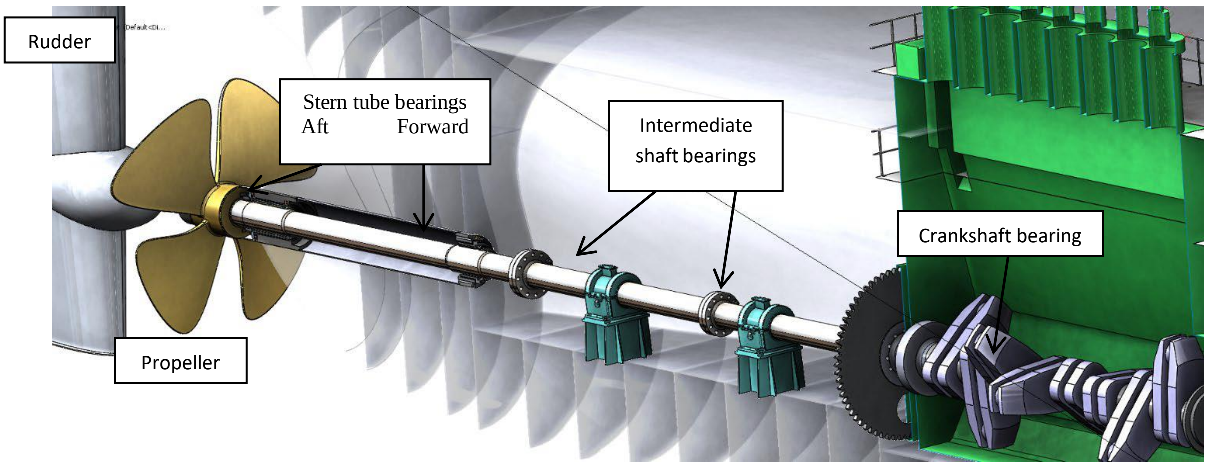

Figure 16: Marine Propulsion system components

Firstly, the crankshaft of the marine engine is supported and connected to the connecting rod via the crankshaft bearings whose main goal is to transmit the load without any contact between the rod and the crankshaft. The number of crankshaft bearings is equal to the number of cylinders of the main engine increased by one or two (one when the crankshaft comes as a single piece, and two if the crankshaft is divided into parts, usually on large engines). Next, the intermediate shaft is supported by at least one intermediate bearing. Vessels with lengthy shafting systems, like large containerships, are obliged to have more bearings, in order to endure the shaft weight. Finally the shaft in the stern tube is supported by two stern tube bearings (aft and fore stern tube bearing).

The propulsion shafting alignment is a process for the calculation, selection and proper arrangement of the bearings throughout the shaft, to achieve optimal operating conditions for the all the different service conditions of the vessel.

According to ABS Guidance notes on propulsion shafting alignment (2019) shaft alignment calculations and a shaft alignment procedure are to be submitted for the following alignment-sensitive type of installations:

a) Propulsion shafting of diameter larger than 400 mm,

b) Propulsion shafting with reduction gears where the bull gear is driven by two or more ahead pinions,
c) Propulsion shafting with power takeoff or with booster power arrangements, and
d) Propulsion shafting for which the tail shaft bearings are to be bored sloped.

Propulsion shafting alignment is carried out so that:

- Bearing loads are within the acceptable limits specified by the bearing manufacturer under all vessel loading conditions
- Bearing reactions are always positive
- The number of bending points of the shaft is the minimum
- The operation of the propulsion system is the optimum for hot and cold main engine condition, in each different load condition and weather scenario.

4.1.2 Importance of Proper Alignment

The misalignment of the shaft may damage several parts (crankshaft, bearings, shaft etc.) and lead to an unplanned machine downtime. This failure not only causes costly delays in maintenance, but also increases the chance of personnel injury, change of bearings and even total failure of propulsion shafting system. Failing to carry a proper alignment also cause:

- Uneven loaded bearings; some bearings will have to support extra loads,
- Decrease of shafting system efficiency, due to extreme friction on the bearings,
- Excessive wear of bearings and shaft,
- Massive amplitudes of torsional and lateral vibration leading to imminent shaft and bearings failure,
- Fatigue failure, caused by over the limit bending stresses.

After the malfunction of the propulsion shafting system, the vessel must be immobilized to avoid further damage and a series of costly events must be initialized for the repair of the propulsion system.

4.2 Shaft Alignment plan implementation

4.2.1. Design - Calculations

The process of shaft system design, due to hull deflection, consists of specific steps. Firstly, one must choose the necessary number and longitudinal position of support points. After, we assure that propulsion shafting bearing; the engine and gearbox are on the required vertical position (zero vertical offsets) and calculate the reaction forces of each bearing, shaft deflections. At this point, the influence coefficients of the system are also calculated. Taking everything into consideration, we determine the vertical offsets of each bearing. This is an iterative process to optimize everything mentioned above. Lastly, we calculate SAG – GAP values for all shafts in decoupled state.

4.2.2 Installation process

After the design process, the next stage is the installation of the shafting system. As soon as, stern structure is in place the shaft alignment procedure should start.

At start, a reference line is established between the flywheel and the aft end of the stern tube (figure). The procedure is called bore sighting and can be achieved by three different methods: (a) Piano wire, (b) Optical telescope, (c) Laser. The proper definition of the reference line is of high importance, since the vertical offsets will be conducted by this reference line. So, the measurement of the vertical offsets of this reference condition must be accurate.

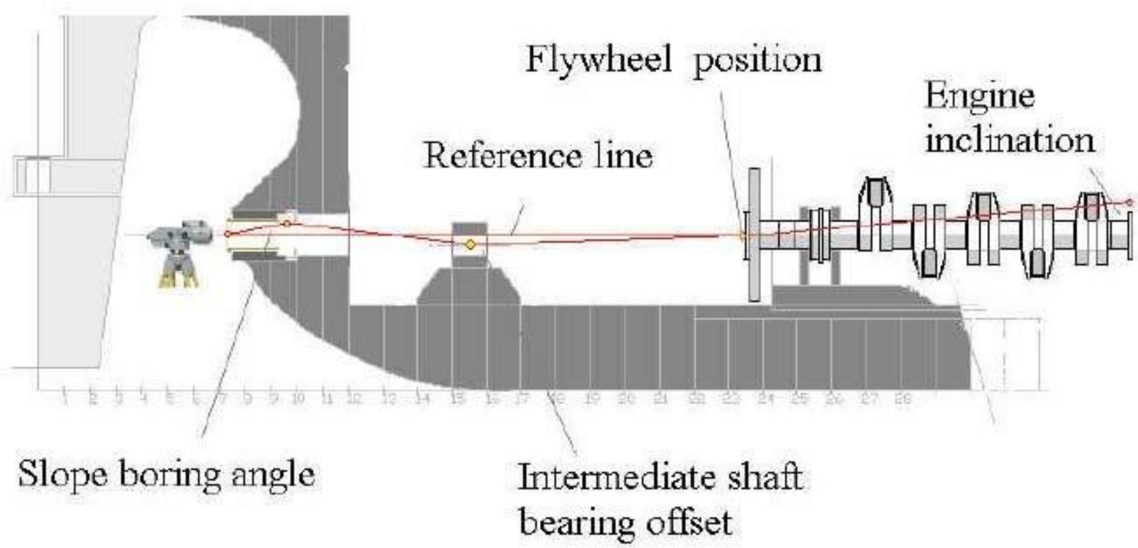

Figure 17: Shaft alignment procedure, definition of reference line.

4.2.2.1 The piano wire method

A thin steel wire (0.5-0.7mm diameter) is used to represent the reference line. The wire extends from the aft stern tube end to the flywheel or a temporary support that represents the M/E future location, if the engine has not been installed yet. This wire is threaded through centering spiders or a pulley positioned at the stern tube and is pre-tensioned with a known force using a weight.

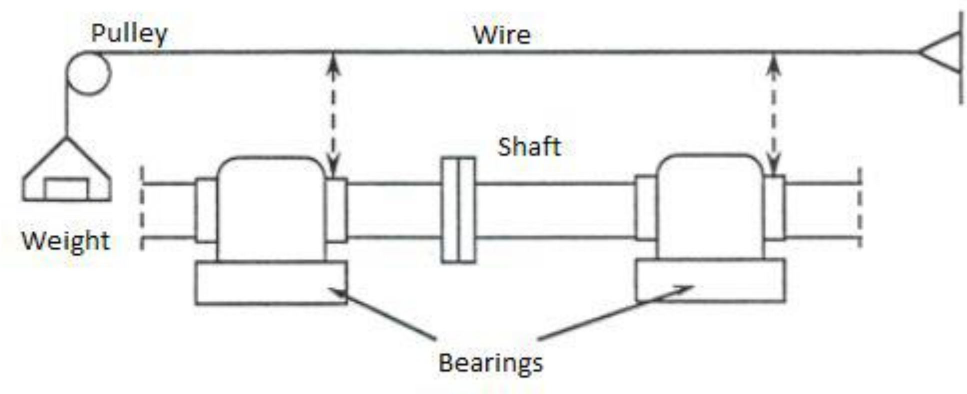

Figure 18: Piano wire method

Although this method is dependable, low-cost, and easy to understand, special attention should be given by the worker conducting this procedure. Several problems may occur through this method, like wire vibration, surface irregularities or measurement errors if an analog micrometer is used and the deflections of the wire.

4.2.2.2 Optical Methods

This method employs the use of a precision telescope that projects an optical reference line (figure). The telescope is positioned on a base so that its vertical and lateral position is the same as that of a reference target, which is utilized to establish a reference line. Transparent targets, usually glass disks, are set at several longitudinal positions and with the exact vertical position of each support bearing center. The deviation of each target center is recorded relative to the reference line.

Although the optical methods are more expensive, they are extremely accurate and dependable. Nowadays, industry utilizes laser systems to facilitate the alignment procedure.

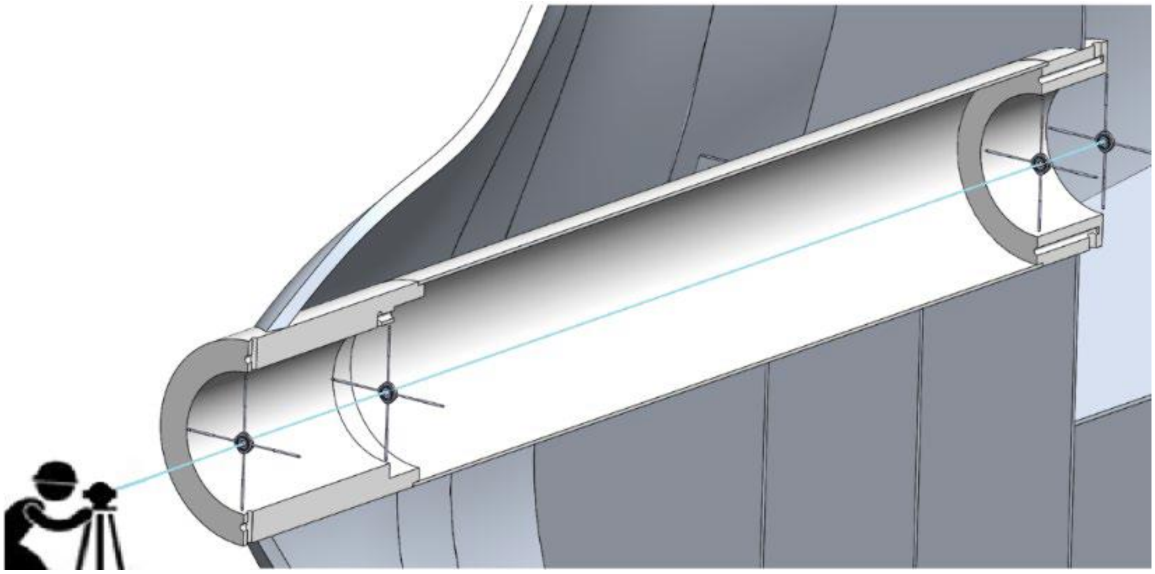

Figure 19: Optical methods

4.2.2.3 Laser

The laser instrument sighting is quite like the optical method mentioned above. The Laser instrument is positioned at one end (either M/E, either aft stern tube) and two reference targets are defined. Those targets are located inside the bearing in the specified by the shaft alignment calculations position and a reference reading is taken. Then the receiver is relocated to the next measuring point along the reference line and additional readings are taken. The results are digitally recorded. Although the laser method is the most expensive, the results are highly accurate (tolerance = 0.005 mm).

5. Case Study

5.1 General particular of the vessel

5.1.1 General Particular and Dimensions

In the present study, a typical 10,000 TEU containership is considered. The vessel under consideration, whose main particulars are listed in table 5.1, is shaft alignment sensitive taking into consideration the following facts:

- Shafting system length: Over 50 meters
- Number of intermediate bearings: Three (3)
- Power output: 51,000 kW x 84 RPM
- Propeller shaft diameter: 990 mm

TYPE	10,000 TEU CONTAINERSHIP
LENGTH BETW. PERP.	320.00 M
BREADTH	48.20 M
DEPTH	27.20 M
DESIGN DRAFT	13.00 M
SCANTLING DRAFT	15.20 M
SERVICE SPEED	23.80 KN
MAIN ENGINE	MAN B&W 10S90ME-C9.2-TII
POWER OUTPUT	51,000 kW x 84 RPM
KEEL LAID	2013

Table 5.1: Ship main particulars

5.1.2 Shafting System Particulars

Figure 5.19 illustrates the shafting system model of the studied containership. The shafting system model comprises the propeller shaft, the intermediate shaft and part of the crankshaft. Two stern tube bearings support the propeller shaft, while the intermediate shaft is supported by three bearings. In our study, only the first six crankshaft bearings are taken into consideration. Bearing characteristics are presented below:

Aft Stern Tube Bearing (ASB)

- Outer shaft diameter 988 mm
- Effective bearing length 2174 mm
- Length over diameter 2.20
- Radial clearance 0.75 mm
- Max permissible load 0.8 MPa / 1718 kN
- Foundation stiffness 3.5E+10 N/m

Forward Stern Tube Bearings (FSB)

- Outer shaft diameter 990 mm
- Effective bearing length 990 mm
- Length over diameter 1.00
- Radial clearance 0.75 mm
- Max permissible load 0.8 MPa / 784 kN
- Foundation stiffness 2.0E+10 N/m

Intermediate Shaft Bearing (ISB)

- Outer shaft diameter 830 mm
- Effective bearing length 850 mm
- Length over diameter 1.02
- Radial clearance 0.40 mm
- Max permissible load 1.0 MPa / 705 kN
- Foundation stiffness 5.0E+10 N/m

General Considerations

- Shaft density 7850 kg/m 3
- Young’s modulus 2.1x10 11 N/m 2
- Lubricant dynamic viscosity 0.1 Pa S

The shaft consists of 78 beam elements and a total of 79 nodes. The geometry characteristics and various loads of each beam are presented in **APPENDIX A**

On the figure below the exact shaft for the studied vessel is shown developed in National Technical University of Athens (NTUA) shaft alignment tool.

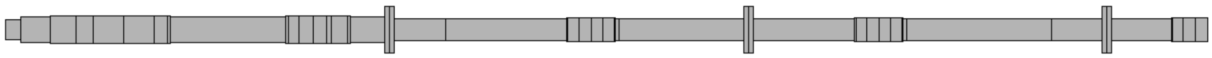

Figure 20: Shaft of studied vessel

5.2. Finite Element Analysis of the Vessel

5.2.1. FEM Generation

The process for the 1D beam theory approach followed to determine the relative bearings' offsets due to hull deflection is shown below:

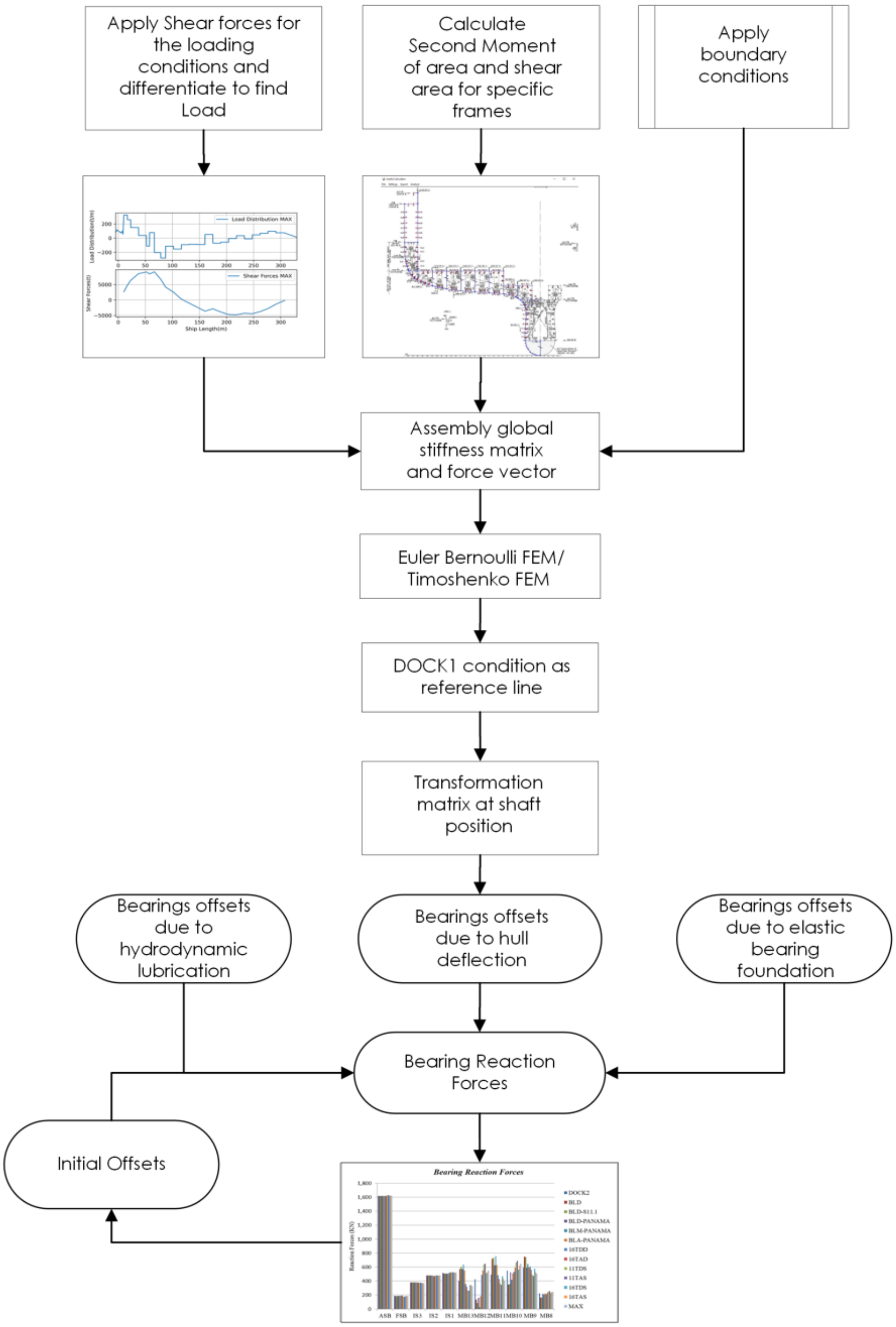

Figure 21: 1D beam theory process

5.2.2. FEM Validation

In our analysis, the best way to ensure the validity of the process and the results is to test every single parameter used in the finite element modeling. Firstly, the reaction forces calculated on each node were acquired through the loading manual of the vessel. The longitudinal load distribution for each condition was calculated by differentiating the Shear Forces from the loading manual. The validity of the coding of 1d Timoshenko and Euler-Bernoulli was tested with simple beam problems that can be calculated on paper. Lastly, the sectional properties deprived from the graphic user interface application that was developed in this thesis were calculated by hand and also were compared with sectional properties of containerships from other published papers, like 'an advanced theory of thin-walled girders with application to ship vibrations', by I. Senjanovic et al [], where ship vibrations coupling of 3d FEA and 1d beam theory for an 11400 TEU VLCS (Very Large Container Ship) was deducted. The sectional properties in the paper above were calculated on NASTRAN program.

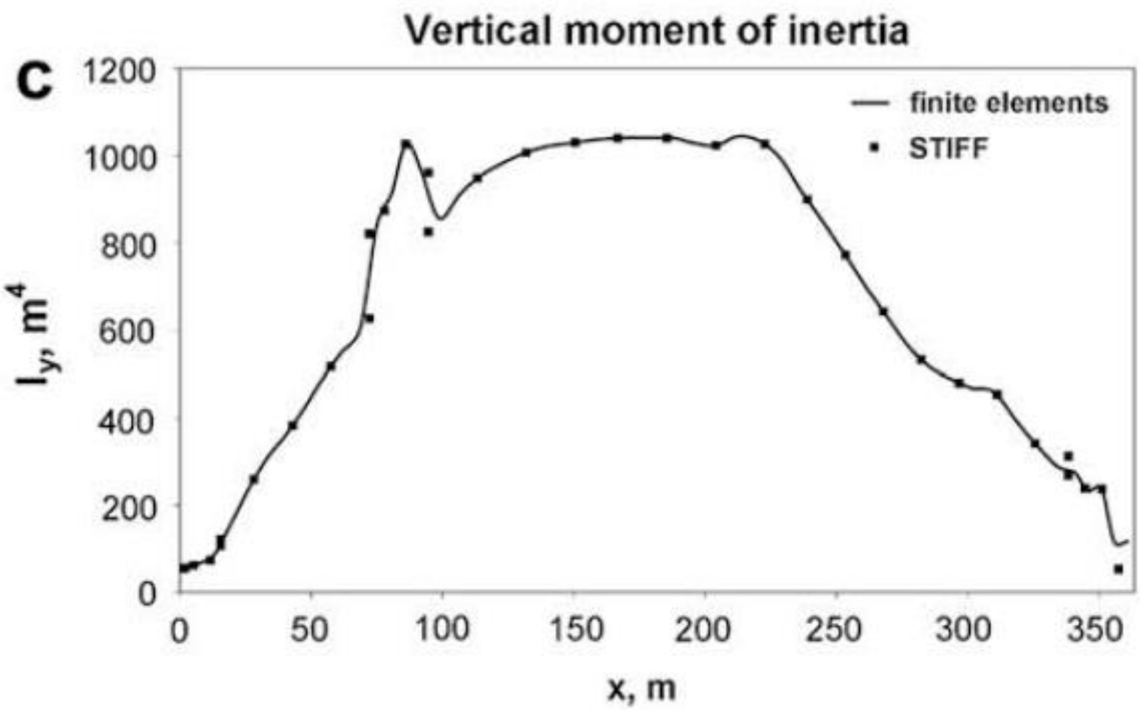

Figure 22: Second moment of area for an 11400 TEU VLCS

5.3. Shaft Alignment Calculations - Parameters

5.3.1 Operating Conditions

Firstly, the considerations made in this study must be analyzed extensively to achieve precise results. For our static analysis of each condition, the main engine is cold and not running, so additional vertical offsets due to thermal expansion of the M/E have been neglected. Furthermore, the deflection of the hull girder occurred from static still water condition, since the results are been compared with the thesis of Stavros Siamantas [ ]. Additional considerations should be taken to calculate the offsets done by sea swell. Considering sea waves would lead to closer to reality results. The change of the waterline causes a change in the buoyancy, and so changes the longitudinal load distribution.

#	Case	Description	Draft Aft	Draft Fore
1	DOCK1	NORMAL DOCKING	6157	6168
2	DOCK2	DOCKING WITH 12000t CARGO(12T x 1000)	6610	6576
3	BLD	BALLAST DEP.	10854	6951
4	BLD-S11.1	BALLAST DEP.-(URS11.1)	11186	5575
5	BLD-PANAMA	BALLAST DEP. - PANAMA	9915	8649
6	BLM-PANAMA	BALLAST MID. - PANAMA	9450	8104
7	BLA-PANAMA	BALLAST ARR. - PANAMA	9054	7669
8	16TDD	16T/TEU DEP. AT DESIGN DRAFT (16T x 4676)	13326	12595
9	16TAD	16T/TEU ARR. AT DESIGN DRAFT (16T x 4676)	12803	11454
10	11TDS	11T/TEU DEP. AT SCANTLING DRAFT(11Tx 8984)	15431	14886
11	11TAS	11T/TEU ARR. AT SCANTLING DRAFT(11Tx8984)	15495	14511
12	16TDS	16T/TEU DEP. AT SCANTLING DRAFT(16Tx 6474)	15409	14916
13	16TAS	16T/TEU ARR. AT SCANTLING DRAFT(16Tx6474)	15122	14185
14	MAX	HOMO. AT 15.2m DRAFT FOR CLASS(14Tx7390)	15203	15194

Table 5.1: Loading Conditions of studied vessel

5.3.2 Compartments

The proper choice of frames is really important for the generation of credible set of data with the least possible amount and effort. Later on, we test different sets of data to investigate which is the least set of data for a precise result. The most important ship block where the data must be dense to achieve valid results is the stern tube. The stern tube consists of high thickness steel plates and stiffeners in order to receive the oscillations and forces created by the propeller. Except from high thickness plating, the stern tube consists of a thick solid part which has a high contribution in the shear and bending stiffness.

5.3.3 Static shaft alignment plan – Reference condition

The line running through the center of the stern tube and the bearings at a docking condition is the reference line. The reference condition is DOCK1, while the vessel is afloat and deckhouse weight is included. The initial offsets were taken by the calculation of shaft alignment for cold and not running engine. In Table, initial vertical offsets of the bearings relative to the reference line, based on the shaft alignment plan of the vessel.

No.	Bearing	Bearing Foundation Stiffness(N/m)	L/D	Offsets(mm)
1	ASB	3.50E+09	0.988	0.75
2	FSB	3.50E+09	0.99	0.75
3	ISB3	2.00E+09	0.83	-2
4	ISB2	2.00E+09	0.83	-3
5	ISB1	2.00E+09	0.83	-4
6	MB13	5.00E+09	1.18	-5.59
7	MB12	5.00E+09	1.18	-5.59
8	MB11	5.00E+09	0.602	-5.59
9	MB10	5.00E+09	0.602	-5.59
10	MB9	5.00E+09	0.602	-5.59
11	MB8	5.00E+09	0.602	-5.59

Table 5.2: Initial shaft alignment plan - Reference condition

The absolute bearings offsets are calculated by adding the initial offsets with the deformations due to relative hull deflections, bearings' elastic foundation and hydrodynamic lubrications. The last two were acquired from previous diploma thesis conducted by the division of marine engineering. The relative hull deflections for each condition are calculated by the hull deflections of each loading condition minus the hull deflections of reference condition (DOCK1). After calculating the relative hull deformations we use a transformation matrix. This approach is presently applied in large shipyards and recognized by the classification societies due to the fact that such a coordinate transformation method is useful not only for calculating the shaft alignment but also for understanding the analysis results. Relative and rotated hull deflection at each bearings' position can be acquired by the equation below:

$$\begin{Bmatrix} x' \\ y' \end{Bmatrix} = \begin{bmatrix} cosa & sina \\ -sina & cosa \end{bmatrix} \begin{Bmatrix} x - x_0 \\ y - y_0 \end{Bmatrix}$$

$\begin{Bmatrix} x \\ y \end{Bmatrix}$ is the point coordinate system before conversion

$\begin{Bmatrix} x' \\ y' \end{Bmatrix}$ is the point coordinate system converted by compensating with the original coordinate

$\begin{Bmatrix} x_0 \\ y_0 \end{Bmatrix}$ so that the axis become 0 after the coordinate transformation

a, the angle between After Stern Bearing (ASB) and Fore Stern Bearing (FSB)

$$Relative\ hull\ deflection_i = \begin{Bmatrix} y_1 \\ y_2 \\ \vdots \end{Bmatrix}_{condition\ i} - \begin{Bmatrix} y_1 \\ y_2 \\ \vdots \end{Bmatrix}_{Reference}$$

$$Absolute\ hull\ deflection_i\ = \begin{bmatrix} cosa & sina \\ -sina & cosa \end{bmatrix} * Relative\ hull\ deflection_i + Initial\ Offsets$$

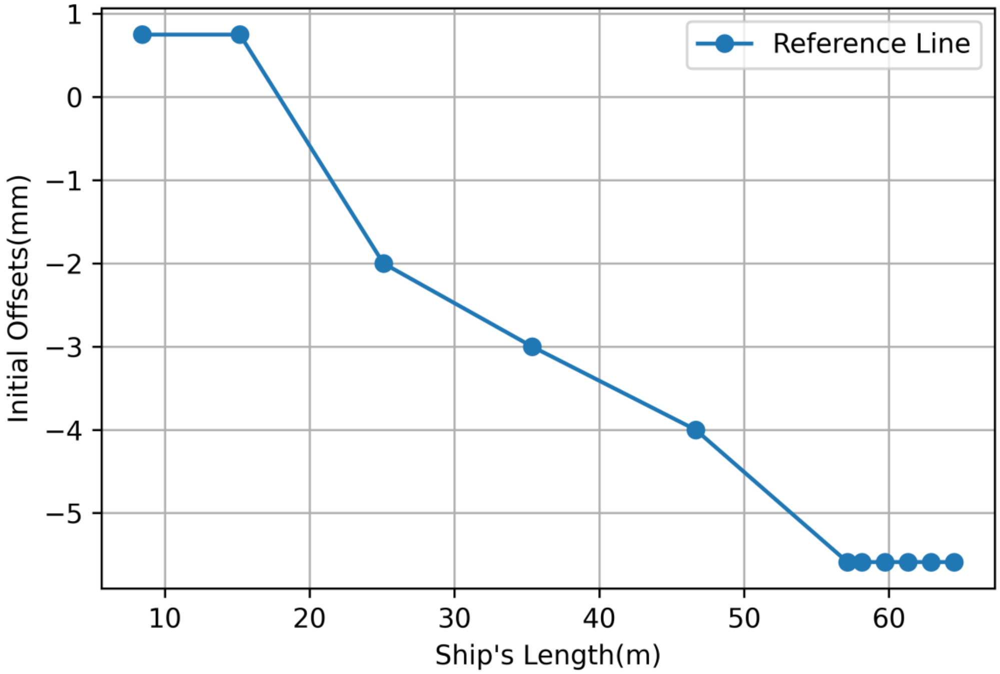

Figure 23: Initial Offsets

5.3.4 Comparison of 1d beam theory and 3d analysis

On this chapter, a comparison will be conducted between 1d and 3d model to comprehend the differences between the two methods and what can be achieved with each one of them. Additionally, notes will be given considering the parts that contribute on the stiffness of the vessel.

The plots generated on this chapter used the inertia calculated from the longitudinal plates and stiffeners with the GUI application. The web frames and deckhouse stiffness contribution is not taken into account. The **figure 5.23** shows the max condition for each different model.

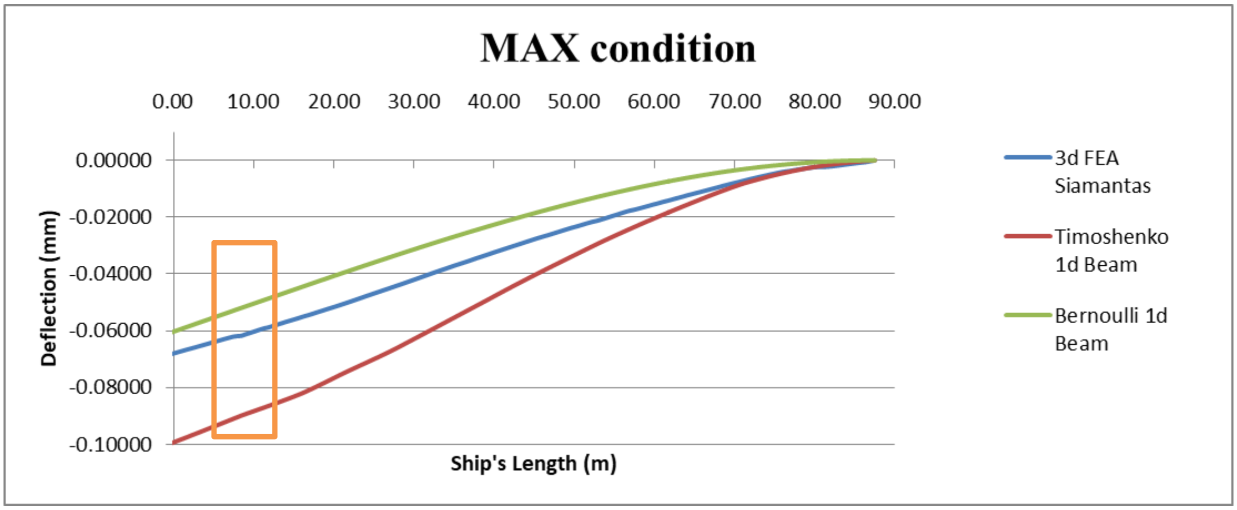

Figure 24: Comparison of different FE models

The investigation of the models was conducted per region of interest and the results are shown below:

- Boundary region: All the models used clamped boundary condition in the engine room front bulkhead. In **figure 5.24** we notice the steep start of the deflection in the 3d finite element model, due to the high weight distribution of the deckhouse in this region. This cannot be achieved by any beam theory unless we force those points to achieve this slope. After the steep slope, the 3d model follows almost the same slope as the Timoshenko 1d beam. The Euler-Bernoulli neglects the shear deflections so it is impossible to create big differences between the elements' slopes. So when trying to calculate actual deflection Euler-Bernoulli will produce false results.
- Region 79-81 m: In **figure 5.24** inside the rectangle area, there can be noticed a zero slope of the deflection of the 3d model. At this longitudinal position is the fore end of the engine. The possible explanation for the slope is:
    1. The shear area of the shear is underestimated in the engine room sections.
    2. At this length there's a high thickness plate (80mm), where maybe the deformation travelling to this point cannot change the form of this plate.
- After the region discussed above we notice the Timoshenko descending faster than the 3d model, due to lower stiffness. That leads to the conclusion that the web frames must somehow be taken into consideration to achieve more accurate results. Accounting only for the longitudinal plates and stiffeners produces high shear deflections that don't correspond to the 3d model.

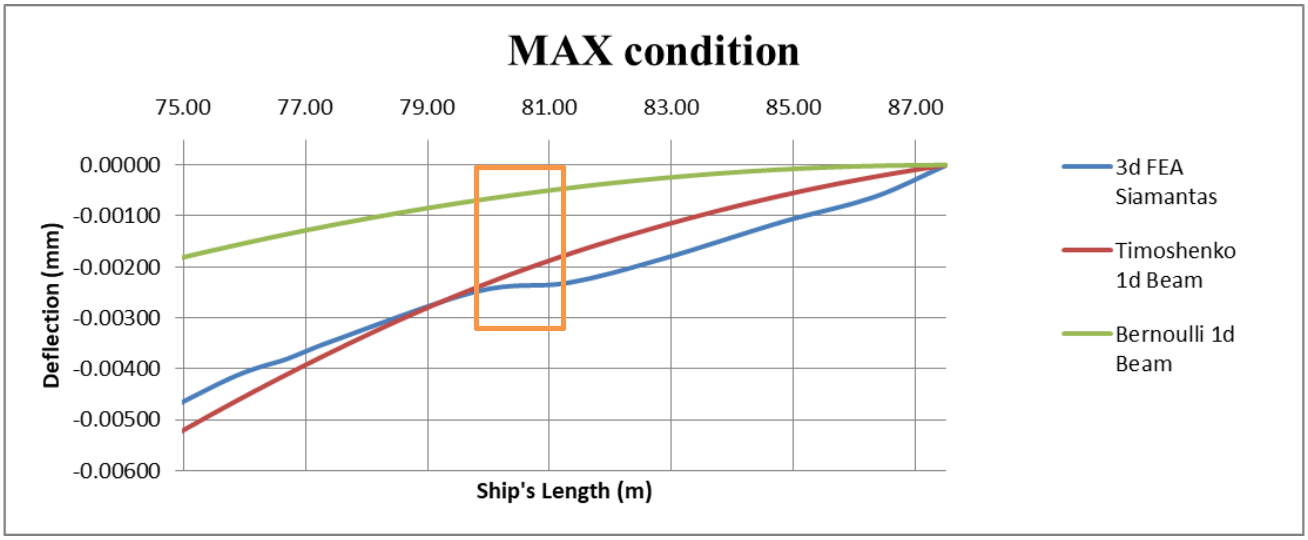

Figure 25: Fore engine region

- The previous assumption can be verified by **figure 5.25,** where the slopes of Bernoulli 1d beam and 3d FE model are quite similar and the Timoshenko deviates by having higher slope by the other two.
- Last but not least, on the marked area on **figure 5.23** we notice the same behavior as in region 79-81m. The slope is almost reaching zero due to the high stiffness of the stern tube (zero deformation and the solid part from frame 11 to frame 14 (2.4m). Unfortunately the beam theories cannot achieve a zero slope so a calibration may be needed to achieve more accurate results.

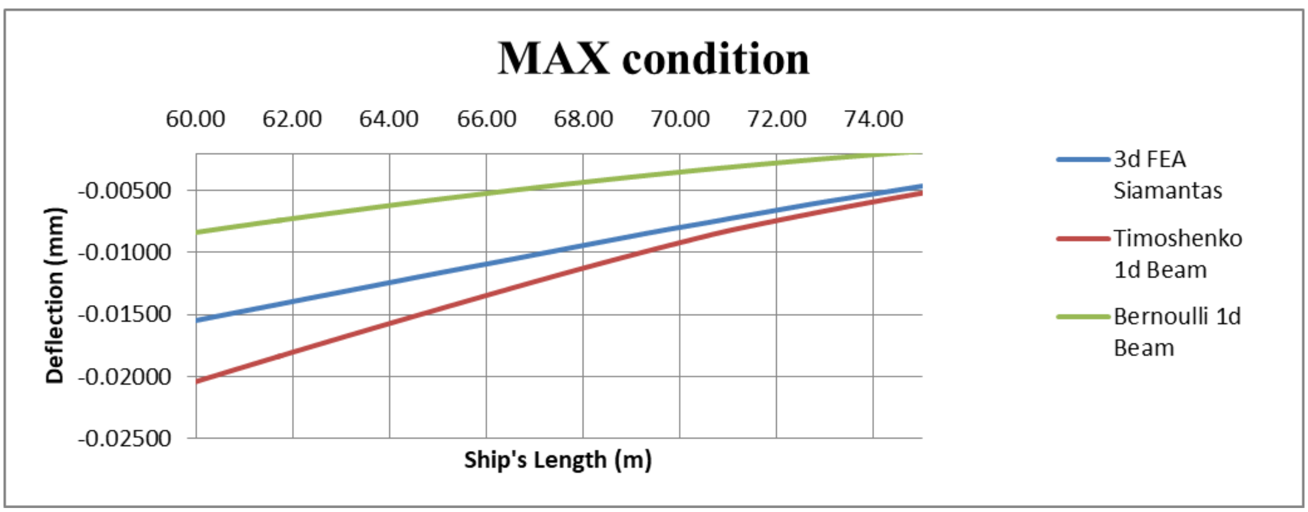

Figure 26: Aft engine region to flywheel

5.4 Shaft alignment 1D model results

5. 4.1 Loading condition "DOCK2"

Dock2 is a docking condition with 12000t cargo (12t x 1000) with displacement 53831.4 t, trim equal to -0.033 m and draft 6.593 m. On the figures below are the loads and shear force distribution (figure…), the global deflection (figure…) and the absolute bearing offsets for both Euler-Bernoulli beam and Timoshenko beam assumption of hull girder and 3d finite element analysis (figure…).

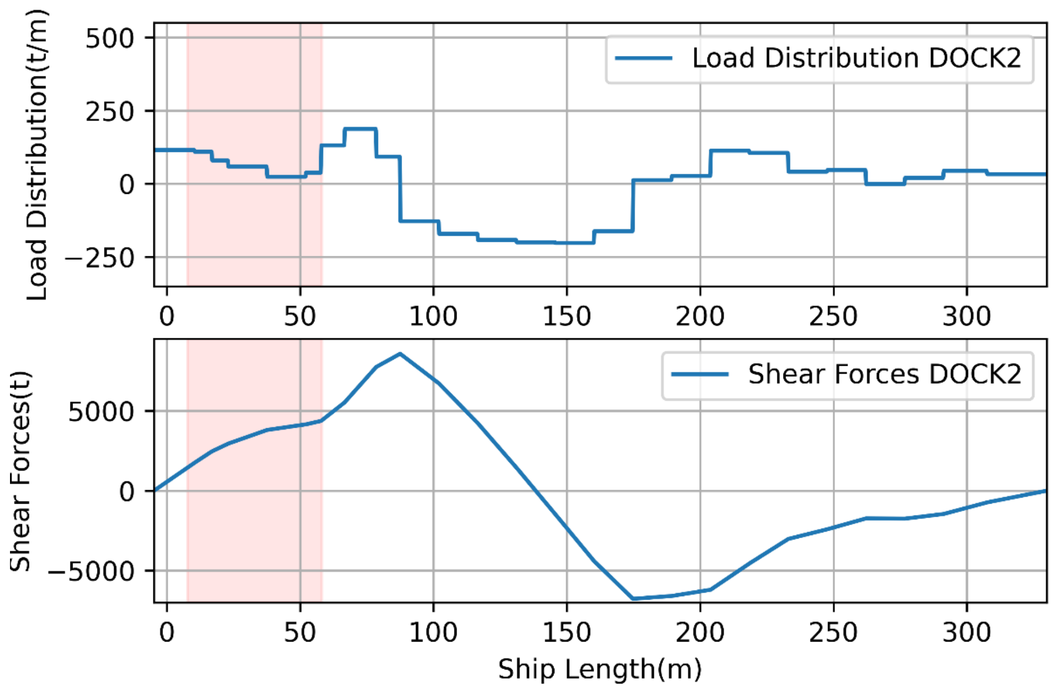

Figure 27: Dock2 load and shear force diagrams

The results on all the conditions tested below followed the assumptions:

1. Hatch covers are included in the calculations of the bending and shear stiffness
2. Web frames contribute in the strength of the vessel via a triangular distribution of their total strength in effective nodes.
3. Load distribution consists of constant functions deriving from differentiation of linearly interpolated shear forces from loading manual. (the actual load distribution).
4. The stern frame consists of a solid part which raises abruptly the second moment of area and shear area of the aft stern tube frames.

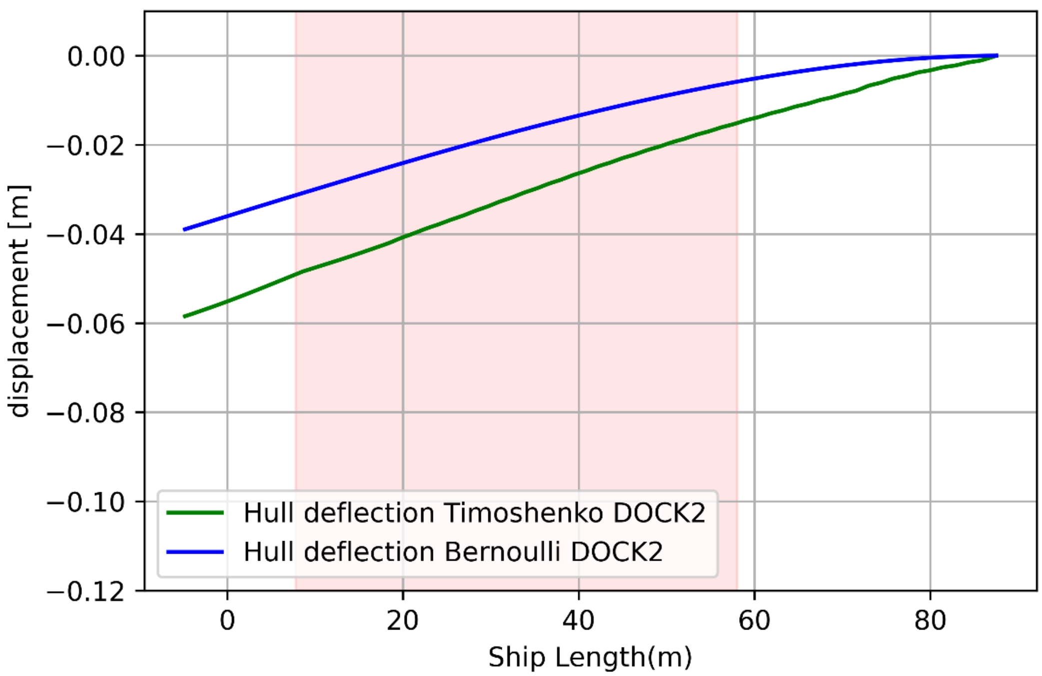

Figure 28: Hull Deflection DOCK2

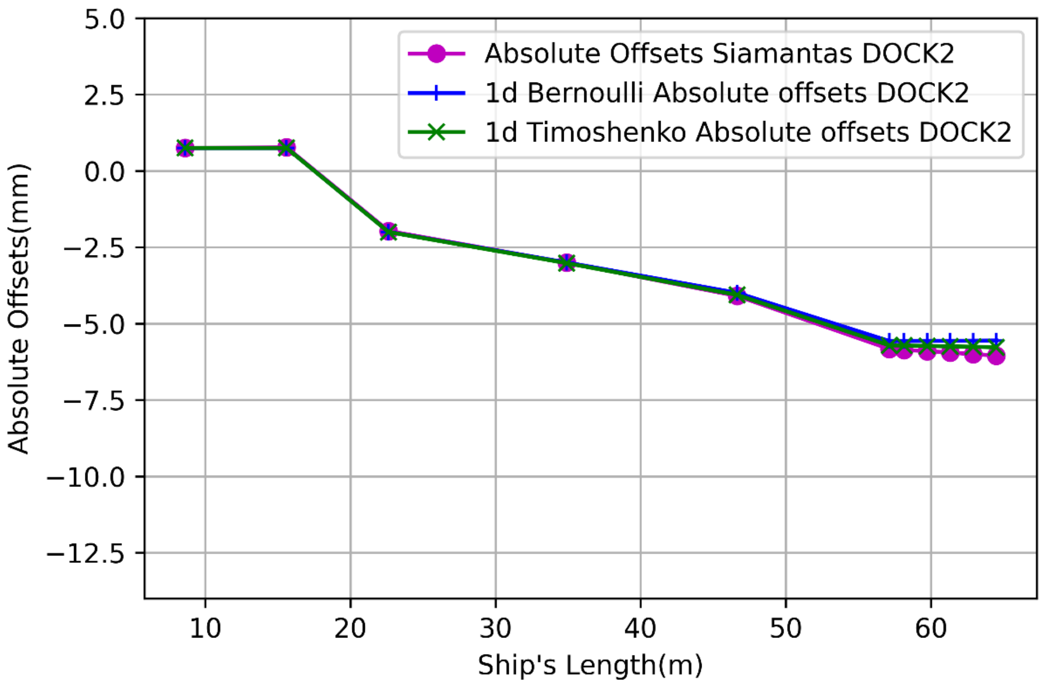

Figure 29: Absolute Offsets Dock2

DOCK2 loading condition is quite similar with DOCK1, with the difference that DOCK2 has cargo instead of ballast.

Bearing	Reaction(kN)	Mean Pressure(Pa)	Total Offsets(m)	Initial Offsets(m)	Hull Deform. (m)	Support Elastic Deformation (m)	Minimum Film Thickness(m)
ASB	1617.99	0.75329	5.86E-04	7.50E-04	0.00E+00	-4.41E-04	2.77E-04
FSB	188.921	0.08778	9.12E-04	7.50E-04	0.00E+00	-7.05E-05	2.32E-04
IS3	378.178	0.53604	-2.06E-03	-2.00E-03	-2.74E-06	-1.84E-04	1.27E-04
IS2	478.531	0.67829	-3.14E-03	-3.00E-03	-2.01E-05	-2.42E-04	1.19E-04
IS1	515.562	0.73078	-4.19E-03	-4.00E-03	-5.98E-05	-2.54E-04	1.19E-04
MB13	402.189	0.79534	-5.73E-03	-5.59E-03	-1.21E-04	-9.18E-05	7.42E-05
MB12	427.69	0.84577	-5.71E-03	-5.59E-03	-1.29E-04	-7.40E-05	8.14E-05
MB11	493	0.97492	-5.74E-03	-5.59E-03	-1.42E-04	-9.87E-05	8.65E-05
MB10	549.11	1.08588	-5.78E-03	-5.59E-03	-1.57E-04	-1.13E-04	8.34E-05
MB9	590.537	1.16781	-5.79E-03	-5.59E-03	-1.69E-04	-1.14E-04	8.30E-05
MB8	222.444	0.43989	-5.73E-03	-5.59E-03	-1.88E-04	-4.55E-05	9.05E-05

Table 5.3: Reaction Forces DOCK2

5.4.2 Loading condition “BLD”

BLD is a ballast departure condition with full fuel and water tanks, displacement 78298.8 t, trim equal to -3.903 m and draft 8.903 m. On the figures below are the loads and shear force distribution (figure…), the global deflection (figure…) and the absolute bearing offsets for both Euler-Bernoulli beam and Timoshenko beam assumption of hull girder and 3d finite element analysis (figure…).

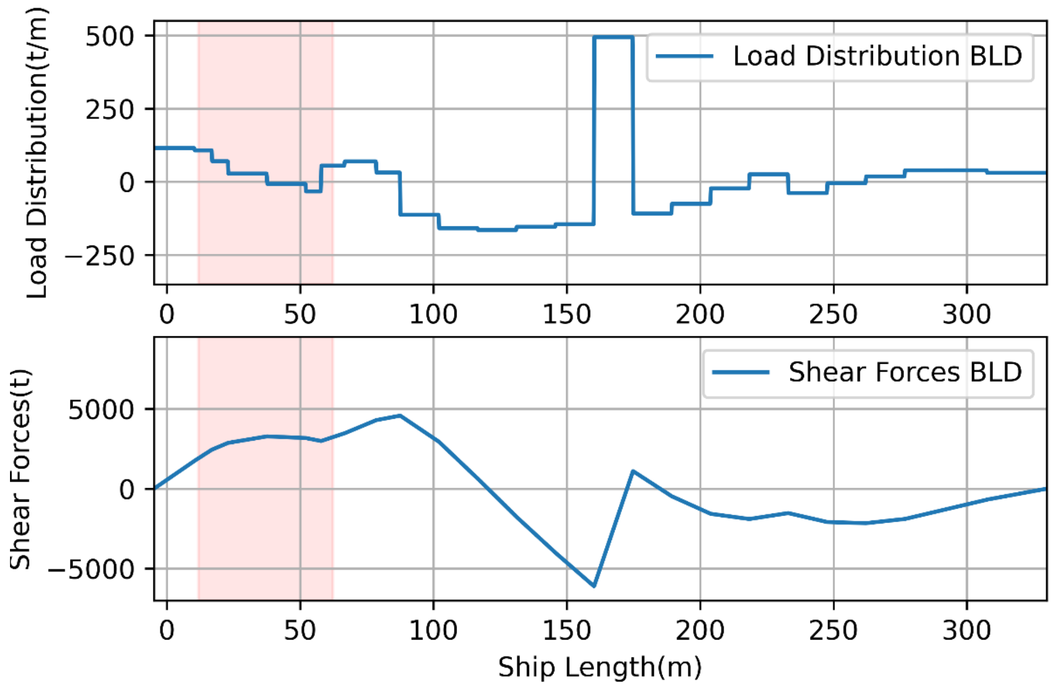

Figure 30: BLD load and shear force diagrams

The ballast condition has a high difference between the 1d and 3d modeling. From the hull deflection offsets acquired from the shaft alignment calculations of the shipyard we can notice that on the 3d FEM the values are a little bit overvalued. Also, assuming that the shipyard doesn’t account the hatch covers in the calculations of stiffness then we approach even more the results of the shipyard as seen in **figure 70.** The difference between 3d and 1d may resulted from differences in the loading of the vessel from the loading manual and the resulting load distribution created on the 3d FEM.

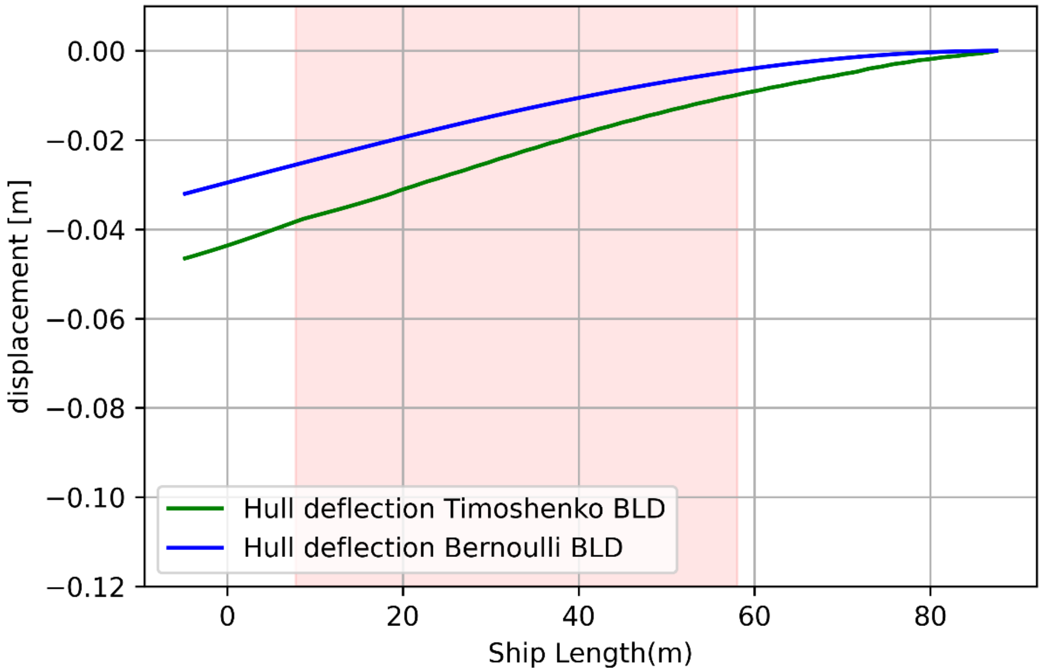

Figure 31: Hull Deflection BLD

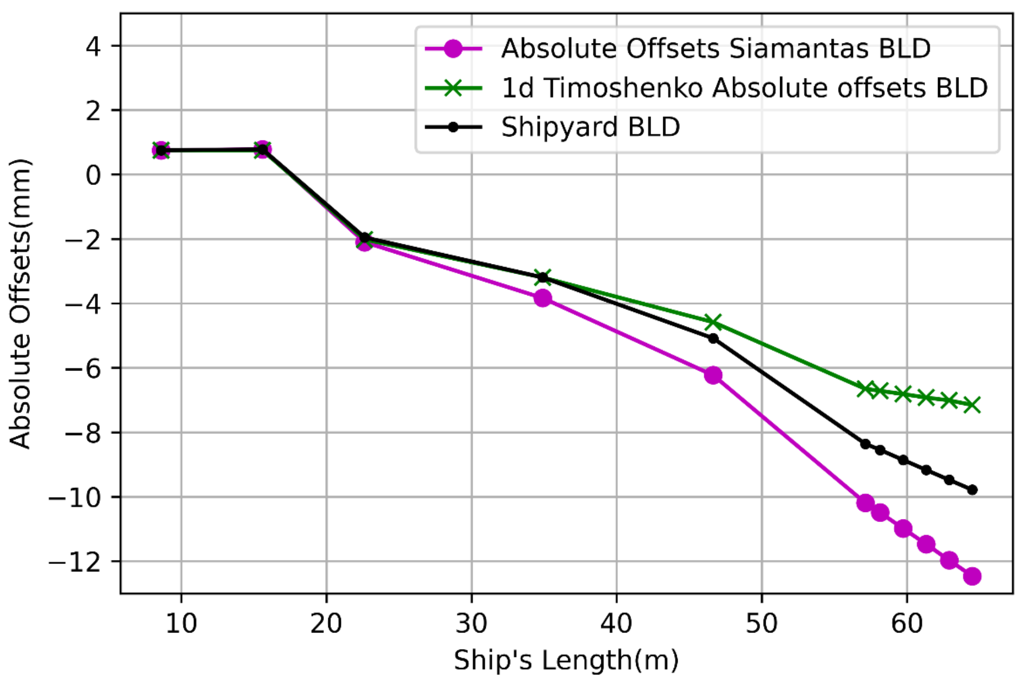

Figure 32: Absolute Offsets BLD

Bearing	Reaction(kN)	Mean Pressure(Pa)	Total Offsets(m)	Initial Offsets(m)	Hull Deform. (m)	Support Elastic Deformation (m)	Minimum Film Thickness(m)
ASB	1619.09	0.7538	6.07E-04	7.50E-04	0.00E+00	-4.27E-04	2.84E-04
FSB	186.023	0.08643	9.11E-04	7.50E-04	0.00E+00	-7.22E-05	2.33E-04
IS3	380.266	0.539	-2.07E-03	-2.00E-03	-1.82E-05	-1.85E-04	1.31E-04
IS2	479.502	0.67966	-3.32E-03	-3.00E-03	-1.98E-04	-2.43E-04	1.23E-04
IS1	509.022	0.72151	-4.70E-03	-4.00E-03	-5.84E-04	-2.47E-04	1.30E-04
MB13	571.971	1.13109	-6.66E-03	-5.59E-03	-1.06E-03	-9.39E-05	8.73E-05
MB12	136.584	0.2701	-6.71E-03	-5.59E-03	-1.12E-03	-9.75E-05	9.32E-05
MB11	717.719	1.41931	-6.79E-03	-5.59E-03	-1.22E-03	-7.75E-05	1.02E-04
MB10	348.909	0.68998	-6.94E-03	-5.59E-03	-1.33E-03	-1.18E-04	1.02E-04
MB9	749.087	1.48135	-7.01E-03	-5.59E-03	-1.42E-03	-1.01E-04	9.86E-05
MB8	165.976	0.32822	-7.11E-03	-5.59E-03	-1.56E-03	-5.25E-05	9.21E-05

Table 5.4: Reaction Forces BLD

5.4.3 Loading condition "BLD-S11.1"

BLD-S11.1 is a ballast departure (URS 11.1) condition with full fuel and water tanks, displacement 67174.0 t, trim equal to -5.611 m and draft 8.381 m. On the figures below are the loads and shear force distribution (figure…), the global deflection (figure…) and the absolute bearing offsets for both Euler-Bernoulli beam and Timoshenko beam assumption of hull girder and 3d finite element analysis (figure…).

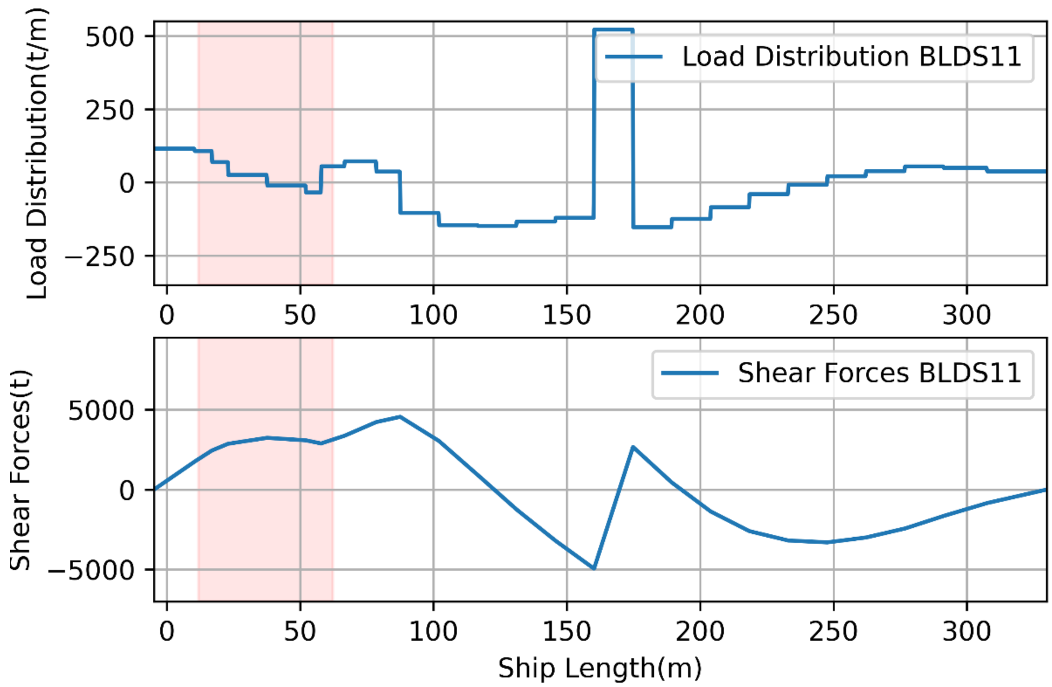

Figure 33: BLD-S11.1 load and shear force diagrams

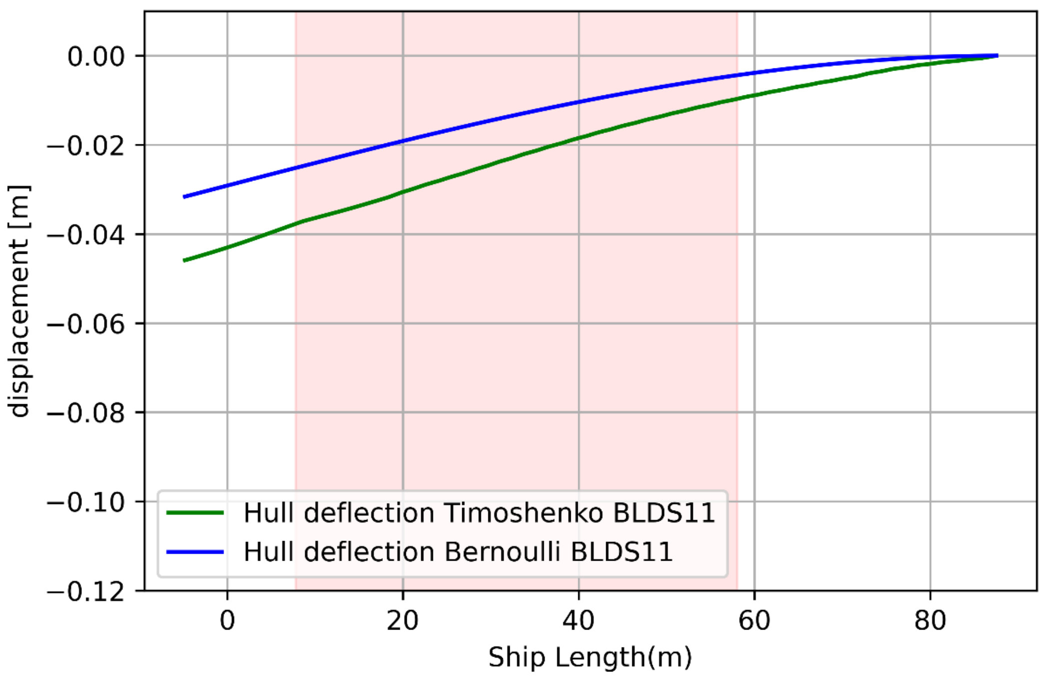

Figure 34: Hull Deflection BLD-S11.1

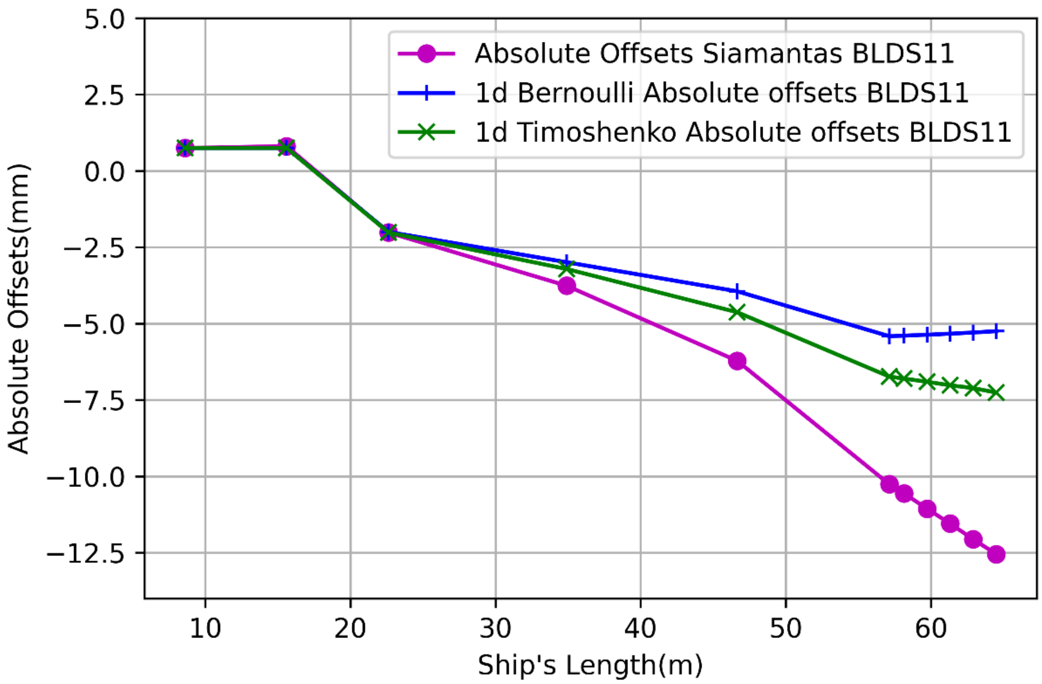

Figure 35: Absolute offsets BLD-S11.1

Bearing	Reaction(kN)	Mean Pressure(Pa)	Total Offsets(m)	Initial Offsets(m)	Hull Deform. (m)	Support Elastic Deformation (m)	Minimum Film Thickness(m)
ASB	1619.08	0.75379	6.06E-04	7.50E-04	0.00E+00	-4.27E-04	2.83E-04
FSB	186.021	0.08643	9.11E-04	7.50E-04	0.00E+00	-7.21E-05	2.33E-04
IS3	380.149	0.53884	-2.07E-03	-2.00E-03	-1.93E-05	-1.85E-04	1.31E-04
IS2	479.977	0.68034	-3.33E-03	-3.00E-03	-2.12E-04	-2.43E-04	1.23E-04
IS1	507.455	0.71928	-4.74E-03	-4.00E-03	-6.28E-04	-2.47E-04	1.31E-04
MB13	607.145	1.20065	-6.74E-03	-5.59E-03	-1.14E-03	-9.27E-05	8.76E-05
MB12	85.6075	0.16929	-6.80E-03	-5.59E-03	-1.21E-03	-9.50E-05	9.50E-05
MB11	732.367	1.44828	-6.88E-03	-5.59E-03	-1.32E-03	-8.58E-05	1.16E-04
MB10	356.678	0.70534	-7.03E-03	-5.59E-03	-1.43E-03	-1.11E-04	1.00E-04
MB9	742.793	1.4689	-7.11E-03	-5.59E-03	-1.52E-03	-1.03E-04	9.98E-05
MB8	166.881	0.33001	-7.22E-03	-5.59E-03	-1.67E-03	-5.26E-05	9.25E-05

Table 5.5: Reaction Forces BLD-S11.1

5.4.4 Loading condition “BLD-PANAMA”

BLD-PANAMA is a ballast departure panama condition with full fuel and water tanks, displacement 81833.9 t, trim equal to -1.266 m and draft 9.282 m. On the figures below are the load and shear force distribution (figure…), the global deflection (figure…) and the absolute bearing offsets for both Euler-Bernoulli beam and Timoshenko beam assumption of hull girder and 3d finite element analysis (figure…).

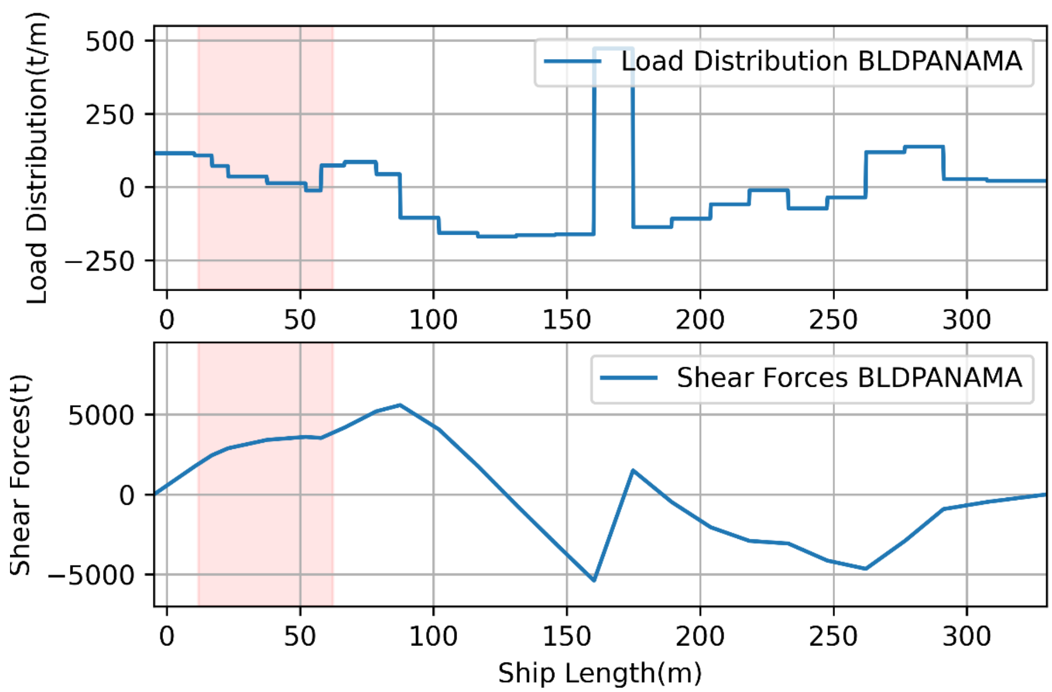

Figure 36: BLD-PANAMA load and shear force diagrams

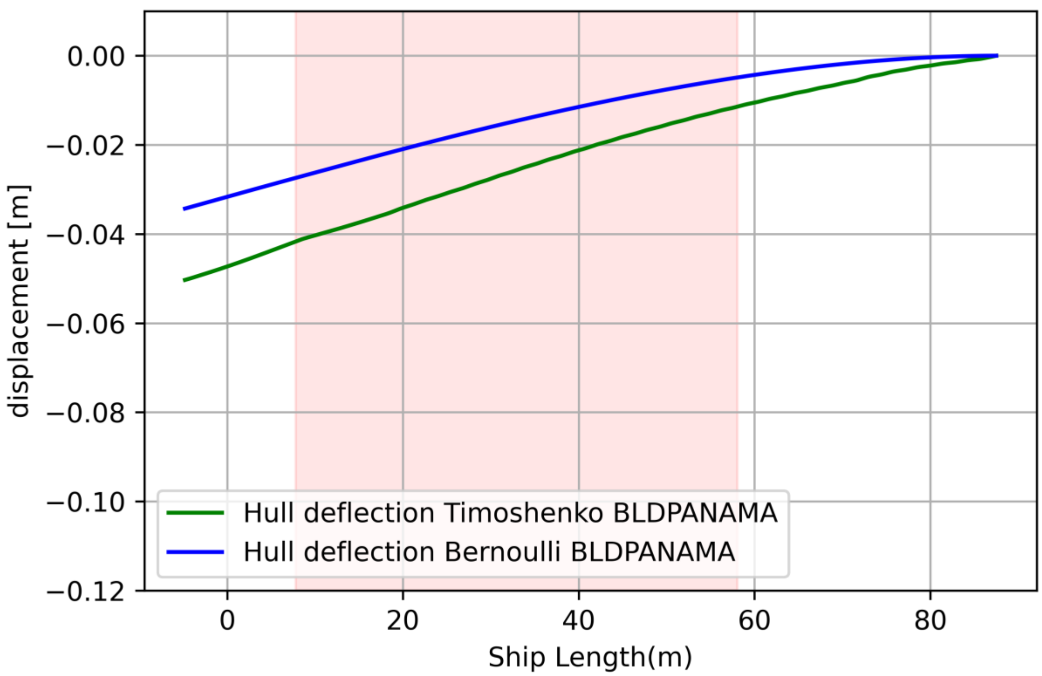

Figure 37: Hull Deflection BLDPANAMA

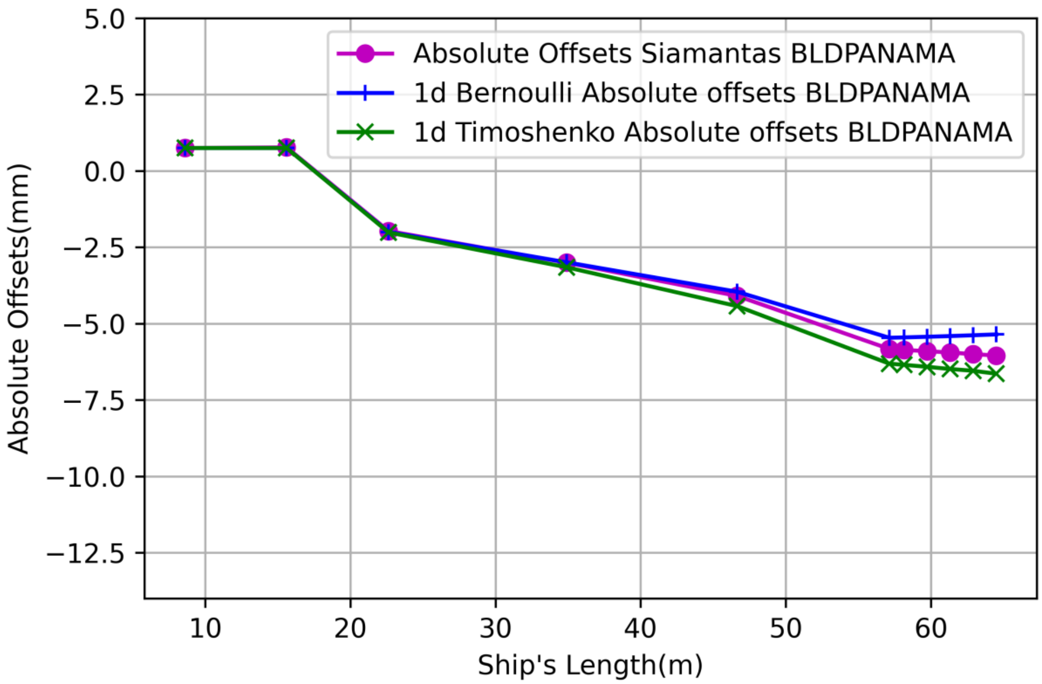

Figure 38: Absolute offsets BLDPANAMA

Bearing	Reaction(kN)	Mean Pressure(Pa)	Total Offsets(m)	Initial Offsets(m)	Hull Deform. (m)	Support Elastic Deformati on (m)	Minimum Film Thickness(m)
ASB	1618.94	0.75373	6.07E-04	7.50E-04	0.00E+00	-4.27E-04	2.84E-04
FSB	186.519	0.08666	9.11E-04	7.50E-04	0.00E+00	-7.19E-05	2.33E-04
IS3	379.87	0.53844	-2.07E-03	-2.00E-03	-1.52E-05	-1.85E-04	1.30E-04
IS2	479.821	0.68011	-3.28E-03	-3.00E-03	-1.55E-04	-2.42E-04	1.22E-04
IS1	508.261	0.72043	-4.55E-03	-4.00E-03	-4.28E-04	-2.50E-04	1.27E-04
MB13	572.732	1.1326	-6.32E-03	-5.59E-03	-7.21E-04	-9.13E-05	8.53E-05
MB12	156.432	0.30935	-6.35E-03	-5.59E-03	-7.60E-04	-9.14E-05	9.05E-05
MB11	624.955	1.23587	-6.39E-03	-5.59E-03	-8.25E-04	-9.49E-05	1.16E-04
MB10	527.287	1.04273	-6.48E-03	-5.59E-03	-8.97E-04	-9.87E-05	1.02E-04
MB9	590.212	1.16717	-6.57E-03	-5.59E-03	-9.55E-04	-1.14E-04	9.19E-05
MB8	219.123	0.43332	-6.60E-03	-5.59E-03	-1.05E-03	-4.86E-05	9.04E-05

Table 5.6: Reaction Forces BLD-PANAMA

5.4.5 Loading condition "BLM-PANAMA"

BLM-PANAMA is a ballast mid condition with half-filled fuel and water tanks, displacement 76405.9t, trim equal to -1.346m and draft 8.777m. On the figures below are the load and shear force distribution (figure…), the global deflection (figure…) and the absolute bearing offsets for both Euler-Bernoulli beam and Timoshenko beam assumption of hull girder and 3d finite element analysis (figure…).

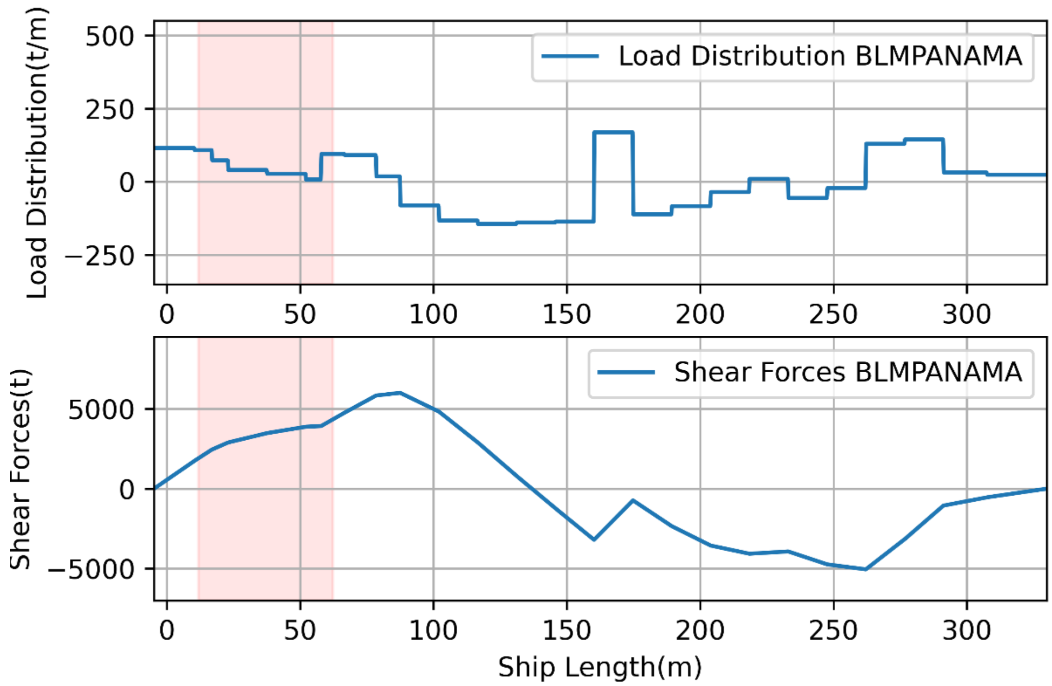

Figure 39: BLM-PANAMA load and shear force diagrams

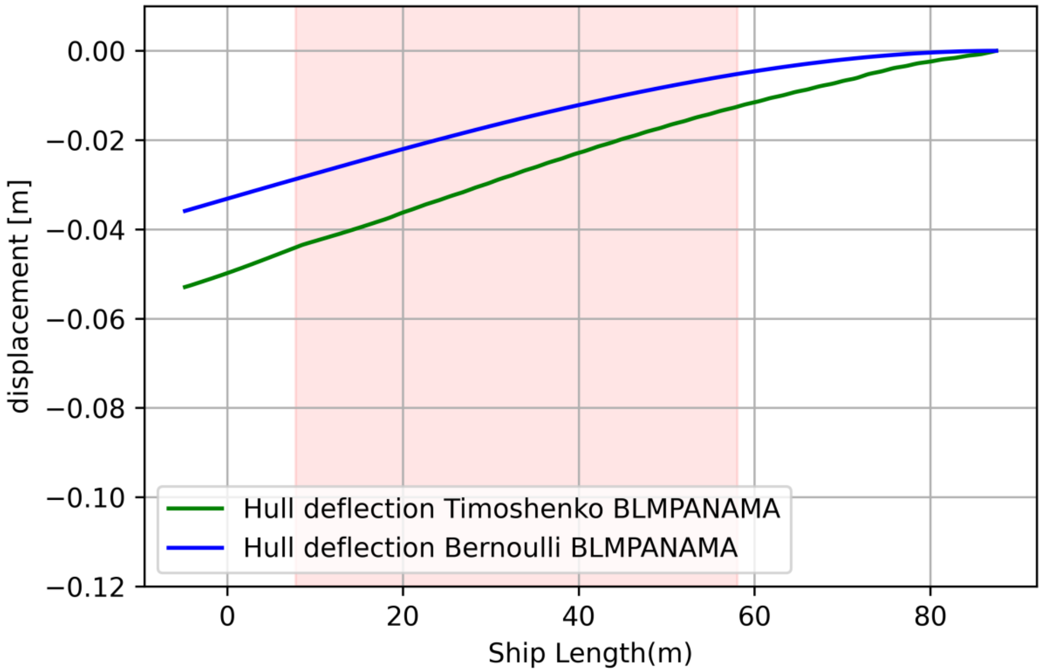

Figure 40: Hull Deflection BLMPANAMA

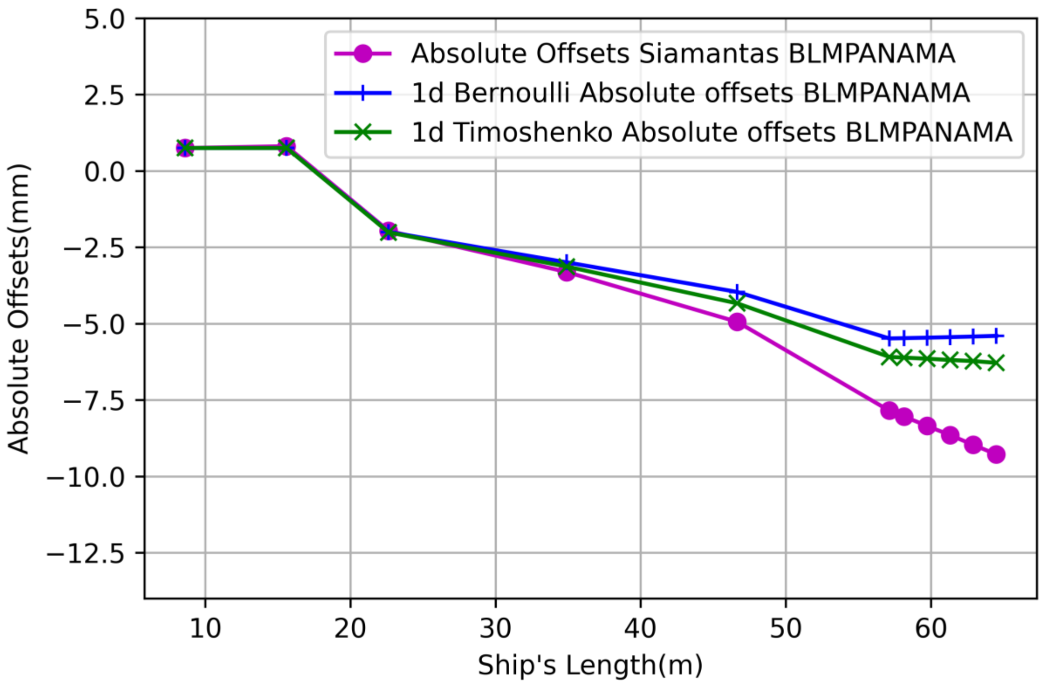

Figure 41: Absolute offsets BLMPANAMA

Bearing	Reaction(kN)	Mean Pressure(Pa)	Total Offsets(m)	Initial Offsets(m)	Hull Deform. (m)	Support Elastic Deformation (m)	Minimum Film Thickness(m)
ASB	1618.73	0.75363	6.05E-04	7.50E-04	0.00E+00	-4.28E-04	2.83E-04
FSB	187.128	0.08694	9.11E-04	7.50E-04	0.00E+00	-7.21E-05	2.33E-04
IS3	379.159	0.53743	-2.07E-03	-2.00E-03	-1.33E-05	-1.85E-04	1.28E-04
IS2	480.773	0.68146	-3.25E-03	-3.00E-03	-1.32E-04	-2.42E-04	1.21E-04
IS1	506.306	0.71766	-4.46E-03	-4.00E-03	-3.37E-04	-2.50E-04	1.25E-04
MB13	635.239	1.25621	-6.10E-03	-5.59E-03	-5.01E-04	-9.23E-05	8.01E-05
MB12	28.6708	0.0567	-6.12E-03	-5.59E-03	-5.23E-04	-9.12E-05	8.81E-05
MB11	756.312	1.49563	-6.12E-03	-5.59E-03	-5.60E-04	-8.60E-05	1.16E-04
MB10	418.804	0.8282	-6.21E-03	-5.59E-03	-6.02E-04	-1.09E-04	9.53E-05
MB9	645.18	1.27587	-6.25E-03	-5.59E-03	-6.37E-04	-1.14E-04	8.91E-05
MB8	207.855	0.41104	-6.24E-03	-5.59E-03	-6.95E-04	-4.68E-05	8.95E-05

Table 5.7: Reaction Forces BLM-PANAMA

5.4.6 Loading condition "BLA-PANAMA"

BLA-PANAMA is a ballast arrival panama condition with 10% filled fuel and water tanks, displacement 72002.8 t, trim equal to -1.385 m and draft 8.362 m. On the figures below are the loads and shear forces distribution (figure…), the global deflection (figure…) and the absolute bearing offsets for both Euler-Bernoulli beam and Timoshenko beam assumption of hull girder and 3d finite element analysis (figure…).

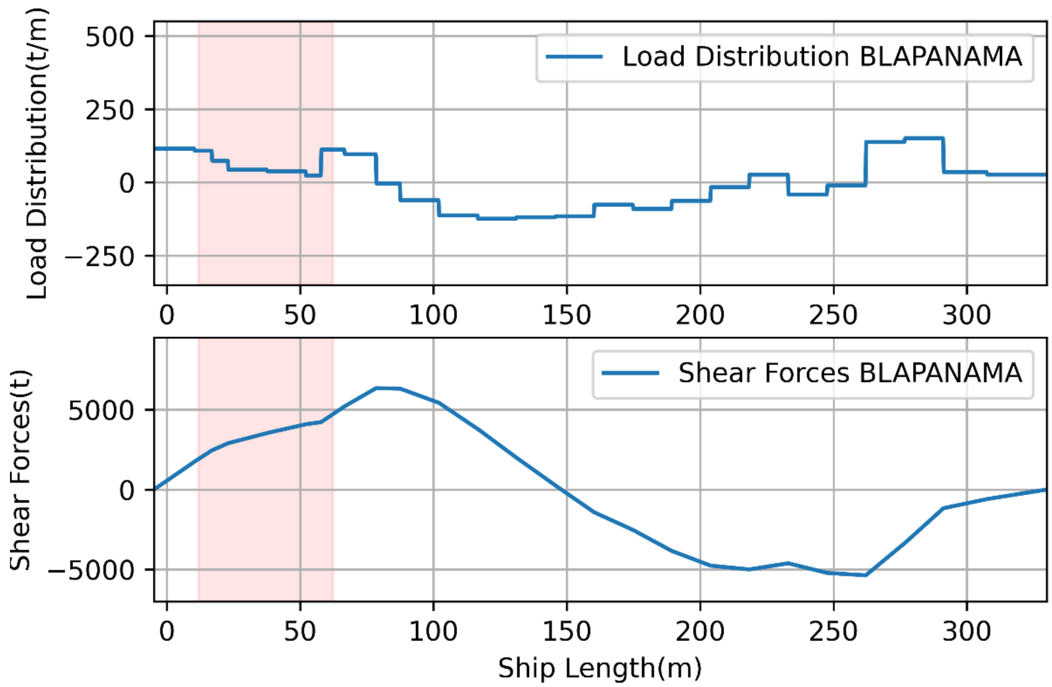

Figure 42: BLA-PANAMA load and shear force diagrams

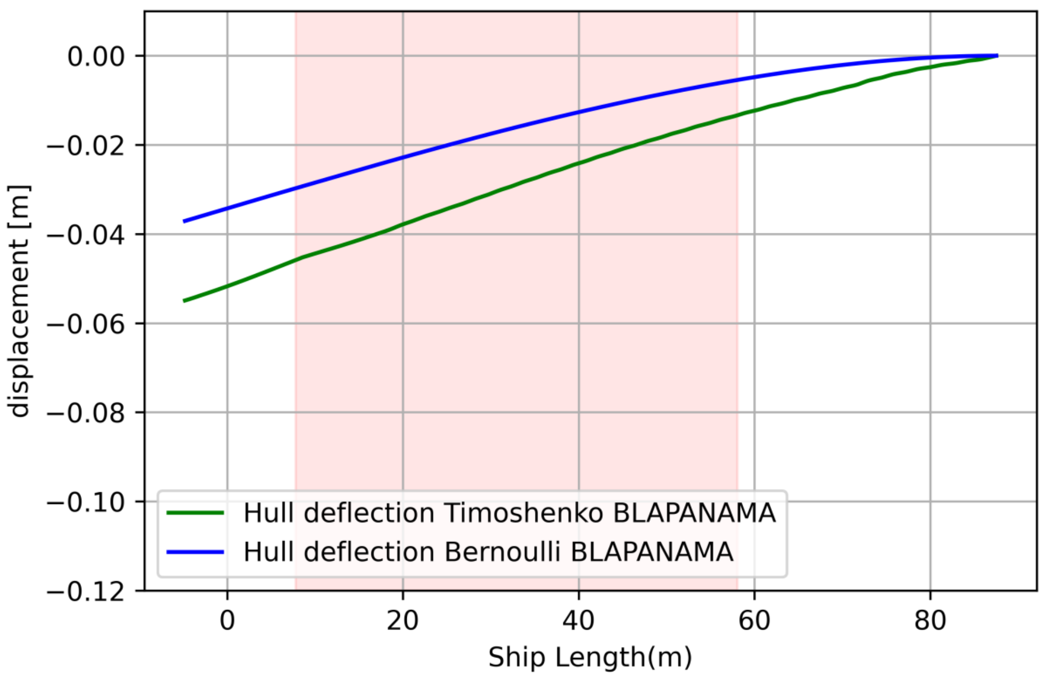

Figure 43: Hull Deflection BLAPANAMA

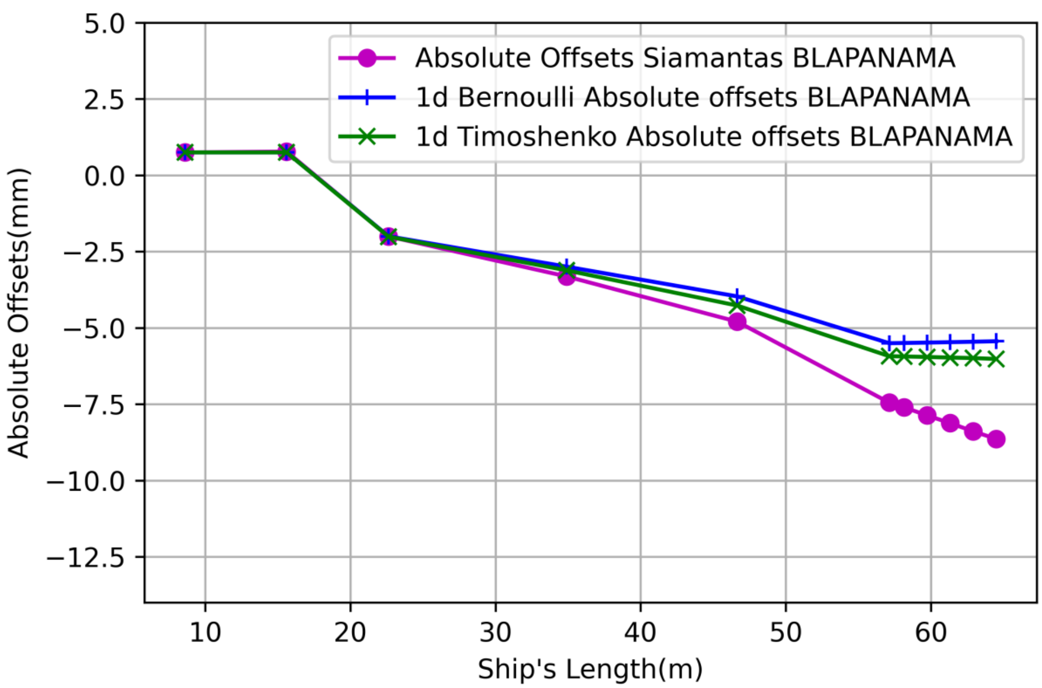

Figure 44: Absolute offsets BLAPANAMA

Bearing	Reaction(kN)	Mean Pressure(Pa)	Total Offsets(m)	Initial Offsets(m)	Hull Deform. (m)	Support Elastic Deformation (m)	Minimum Film Thickness (m)
ASB	1618.63	0.75358	6.02E-04	7.50E-04	0.00E+00	-4.30E-04	2.82E-04
FSB	187.305	0.08703	9.11E-04	7.50E-04	0.00E+00	-7.17E-05	2.33E-04
IS3	379.303	0.53764	-2.07E-03	-2.00E-03	-1.23E-05	-1.85E-04	1.29E-04
IS2	480.2	0.68065	-3.24E-03	-3.00E-03	-1.15E-04	-2.41E-04	1.21E-04
IS1	508.336	0.72053	-4.40E-03	-4.00E-03	-2.69E-04	-2.51E-04	1.23E-04
MB13	553.785	1.09513	-5.94E-03	-5.59E-03	-3.38E-04	-9.11E-05	7.73E-05
MB12	180.71	0.35736	-5.94E-03	-5.59E-03	-3.48E-04	-9.05E-05	8.68E-05
MB11	628.786	1.24345	-5.94E-03	-5.59E-03	-3.64E-04	-8.54E-05	9.75E-05
MB10	511.7	1.0119	-5.99E-03	-5.59E-03	-3.84E-04	-1.11E-04	9.09E-05
MB9	593.356	1.17338	-6.02E-03	-5.59E-03	-3.99E-04	-1.15E-04	8.73E-05
MB8	222.039	0.43909	-5.98E-03	-5.59E-03	-4.29E-04	-4.61E-05	8.92E-05

Table 5.8: Reaction Forces BLA-PANAMA

5.4.7 Loading condition "TDD16"

TDD16 is a 16T/TEU departure condition at design draft (16T x 4676), displacement 124331.0t, trim equal to -0.731m and draft 12.96m. On the figures below are the load and shear force distribution (figure…), the global deflection (figure…) and the absolute bearing offsets for both Euler-Bernoulli beam and Timoshenko beam assumption of hull girder and 3d finite element analysis (figure…).

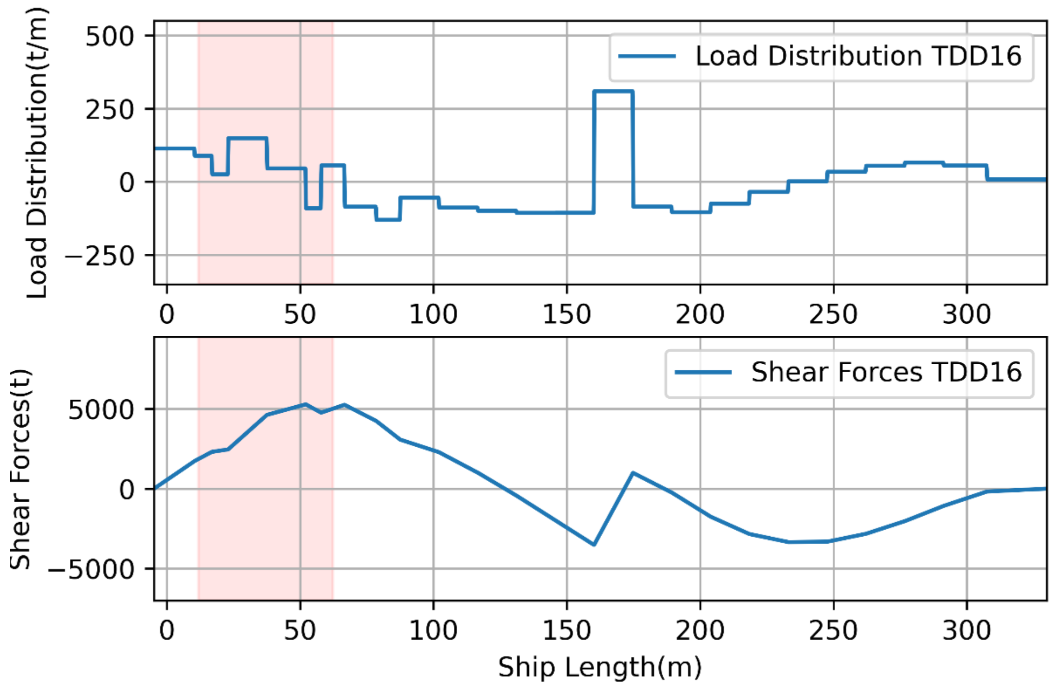

Figure 45: TDD16 load and shear force diagrams

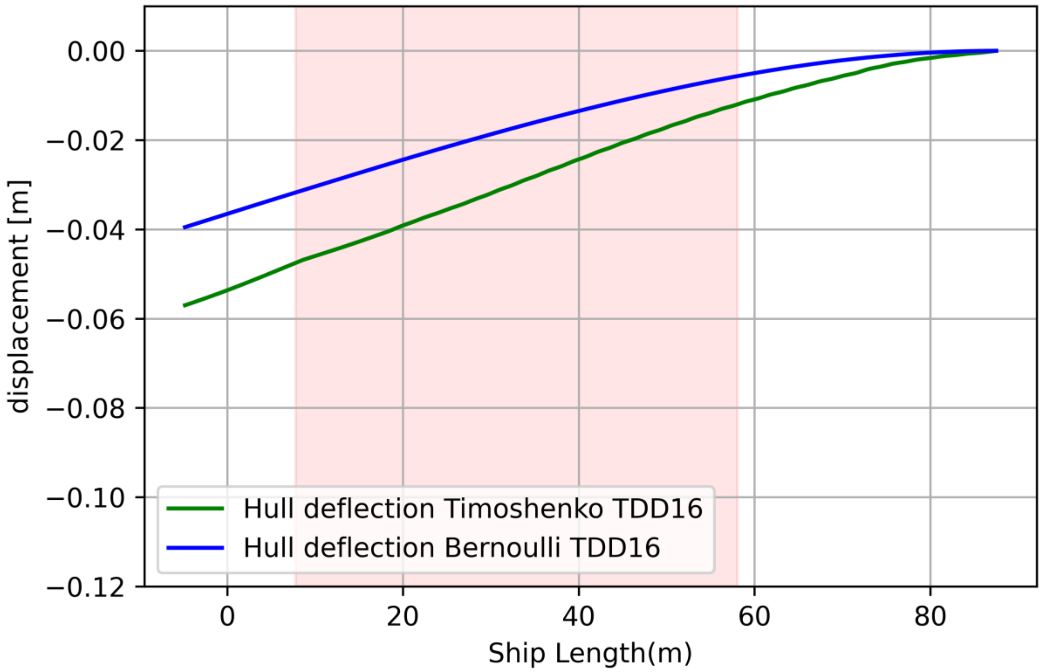

Figure 46: Hull Deflection TDD16

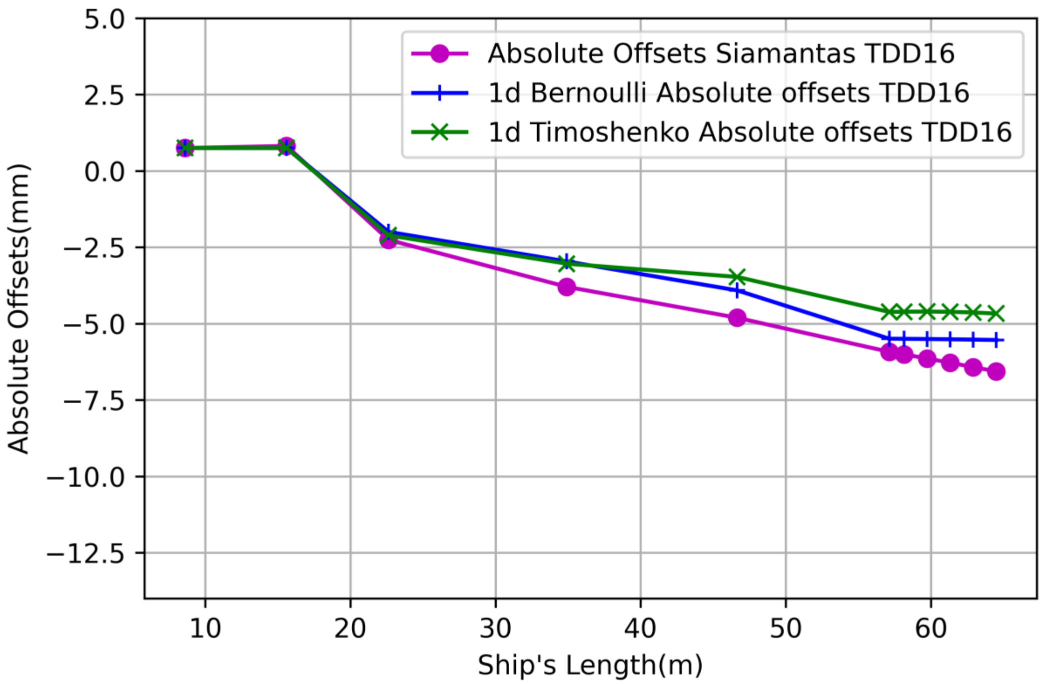

Figure 47: Absolute offsets TDD16

Bearin g	Reaction(kN)	Mean Pressure(Pa)	Total Offsets(m)	Initial Offsets(m)	Hull Deform. (m)	Support Elastic Deformation (m)	Minimum Film Thickness (m)
ASB	1616.58	0.75263	6.14E-04	7.50E-04	0.00E+00	-4.26E-04	2.90E-04
FSB	191.896	0.08916	9.10E-04	7.50E-04	0.00E+00	-7.46E-05	2.35E-04
IS3	379.142	0.53741	-2.16E-03	-2.00E-03	-1.10E-04	-1.83E-04	1.32E-04
IS2	471.863	0.66883	-3.16E-03	-3.00E-03	-3.79E-05	-2.42E-04	1.22E-04
IS1	521.161	0.73871	-3.59E-03	-4.00E-03	5.29E-04	-2.42E-04	1.21E-04
MB13	358.669	0.70928	-4.66E-03	-5.59E-03	9.70E-04	-1.13E-04	7.50E-05
MB12	487.47	0.96399	-4.60E-03	-5.59E-03	9.80E-04	-6.71E-05	7.41E-05
MB11	482.793	0.95474	-4.60E-03	-5.59E-03	9.84E-04	-8.86E-05	9.21E-05
MB10	533.493	1.055	-4.64E-03	-5.59E-03	9.74E-04	-1.13E-04	8.86E-05
MB9	607.867	1.20208	-4.66E-03	-5.59E-03	9.56E-04	-1.15E-04	8.75E-05
MB8	213.217	0.42164	-4.63E-03	-5.59E-03	9.18E-04	-4.51E-05	8.75E-05

Table 5.9: Reaction Forces TDD16

5.4.8 Loading condition "TAD16"

TAD16 is a 16T/TEU arrival condition at design draft (16T x 4676), displacement 114500.0 t, trim equal to -1.349 m and draft 12.129 m. On the figures below are the loads and shear force distribution (figure…), the global deflection (figure…) and the relative bearing offsets for both Euler-Bernoulli beam and Timoshenko beam assumption of hull girder (figure…).

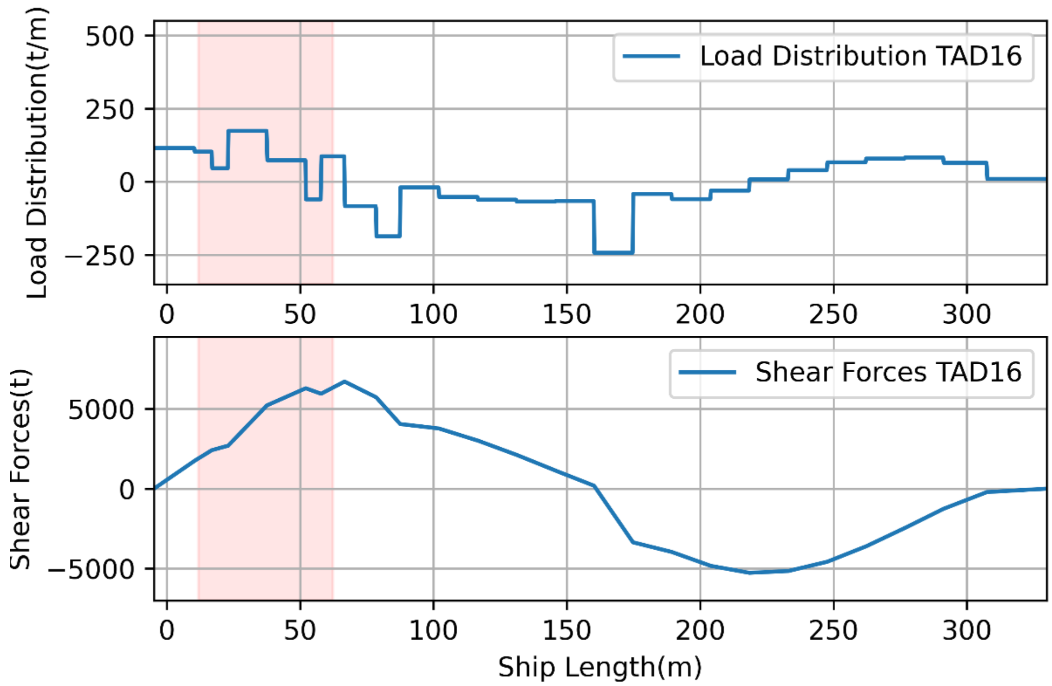

Figure 48: TAD16 load and shear force diagrams

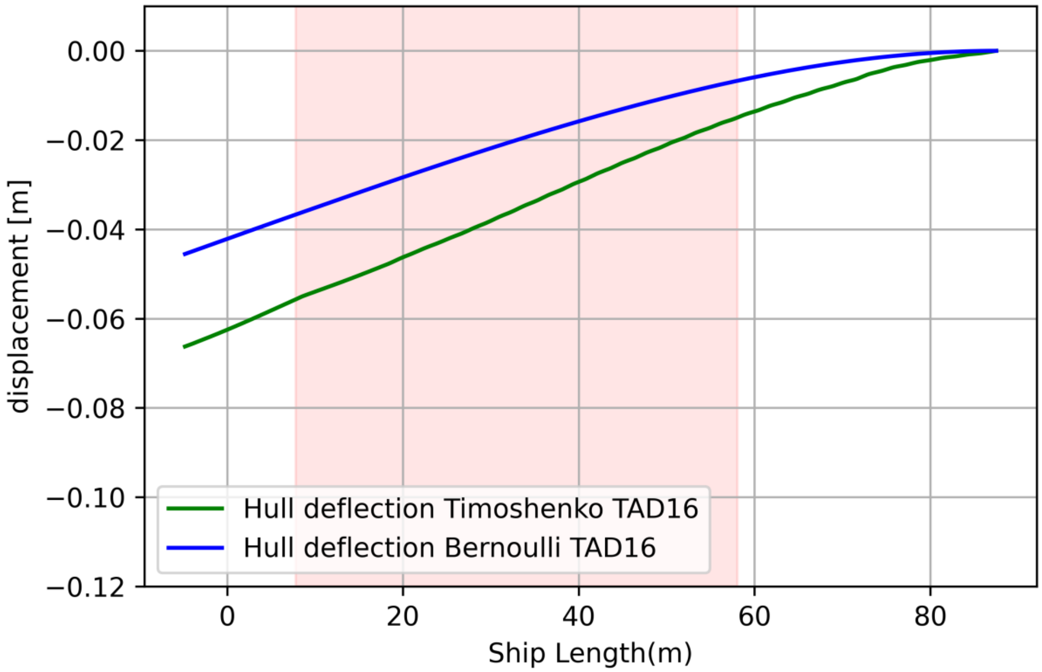

Figure 49: Hull Deflection TAD16

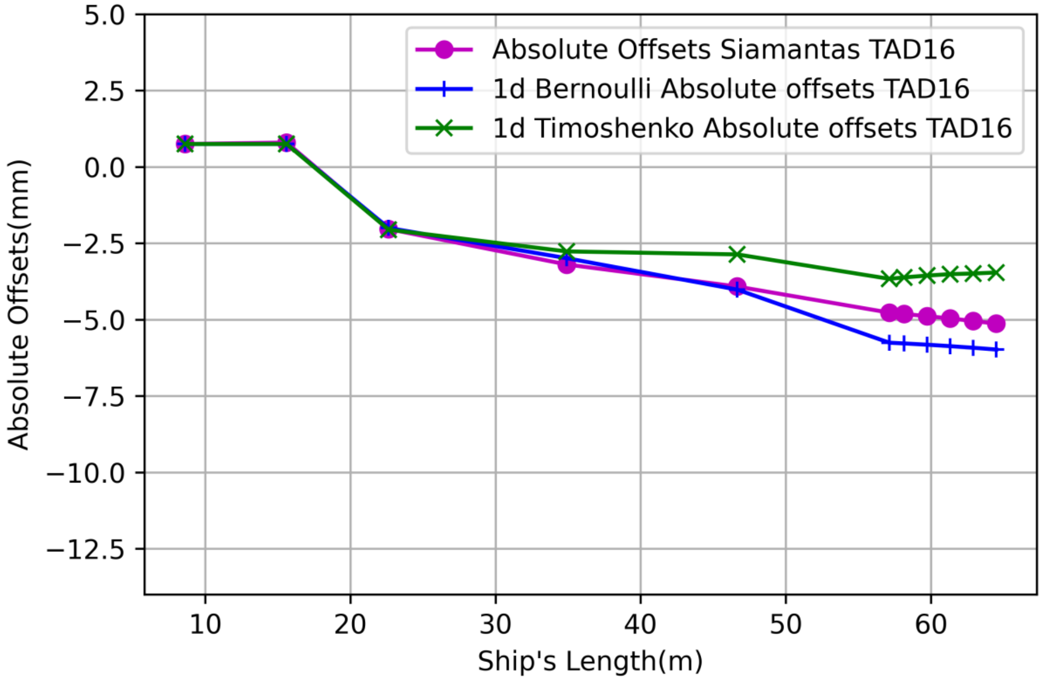

Figure 50: Absolute offsets TAD16

Bearin g	Reaction(kN)	Mean Pressure(Pa)	Total Offsets(m)	Initial Offsets(m)	Hull Deform. (m)	Support Elastic Deformation (m)	Minimum Film Thickness (m)
ASB	1616.71	0.75269	6.11E-04	7.50E-04	0.00E+00	-4.28E-04	2.89E-04
FSB	192.669	0.08952	9.12E-04	7.50E-04	-9.99E-19	-7.23E-05	2.34E-04
IS3	377.627	0.53526	-2.11E-03	-2.00E-03	-5.42E-05	-1.85E-04	1.28E-04
IS2	471.906	0.6689	-2.89E-03	-3.00E-03	2.33E-04	-2.43E-04	1.21E-04
IS1	523.145	0.74152	-2.98E-03	-4.00E-03	1.14E-03	-2.43E-04	1.21E-04
MB13	320.08	0.63297	-3.71E-03	-5.59E-03	1.92E-03	-1.12E-04	7.51E-05
MB12	551.43	1.09047	-3.61E-03	-5.59E-03	1.97E-03	-6.50E-05	7.35E-05
MB11	429.883	0.85011	-3.56E-03	-5.59E-03	2.03E-03	-9.08E-05	9.04E-05
MB10	591.986	1.17067	-3.54E-03	-5.59E-03	2.08E-03	-1.13E-04	8.73E-05
MB9	558.255	1.10397	-3.52E-03	-5.59E-03	2.10E-03	-1.15E-04	8.66E-05
MB8	230.452	0.45573	-3.42E-03	-5.59E-03	2.13E-03	-4.48E-05	8.80E-05

Table 5.10: Reaction Forces TAD16

5.4.9 Loading condition "TDS11"

TDS11 is an 11T/TEU departure condition at scantling draft (11T x 8984), displacement 153101.0t, trim equal to -0.545m and draft 15.158m. On the figures below are the loads and shear force distribution (figure…), the global deflection (figure…) and the relative bearing offsets for both Euler-Bernoulli beam and Timoshenko beam assumption of hull girder (figure…).

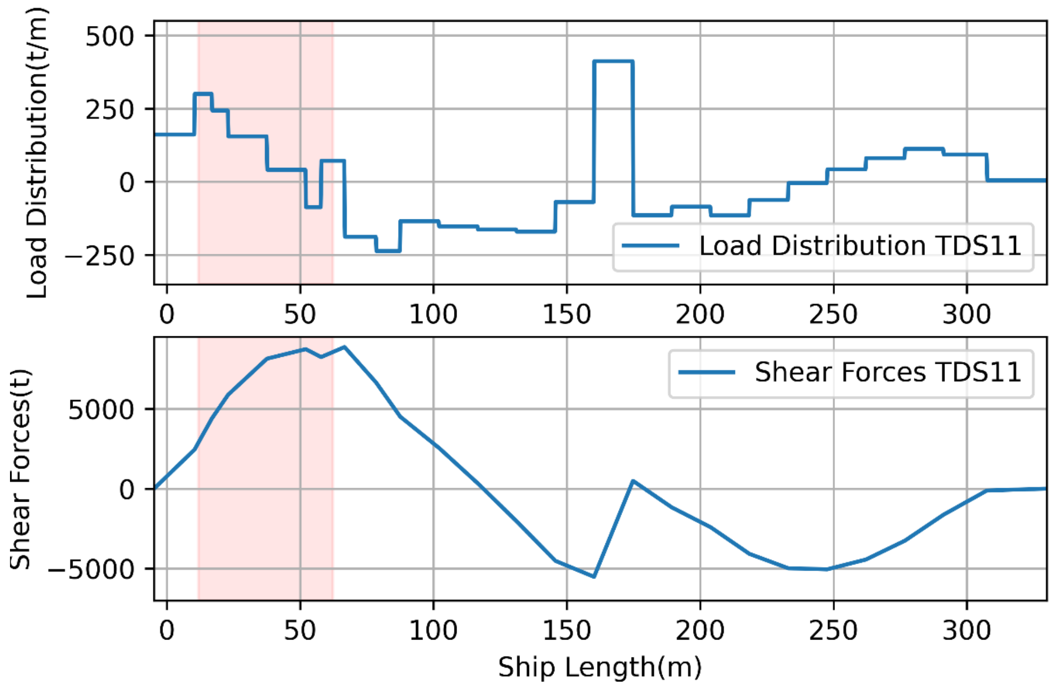

Figure 51: TDS11 load and shear force diagrams

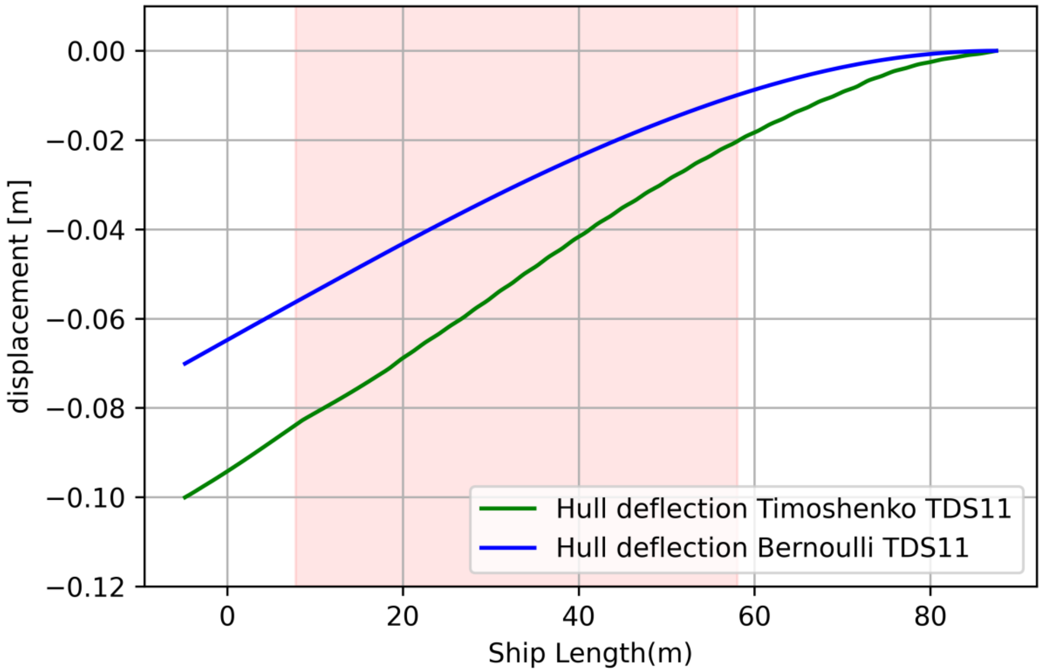

Figure 52: Hull Deflection TDS11

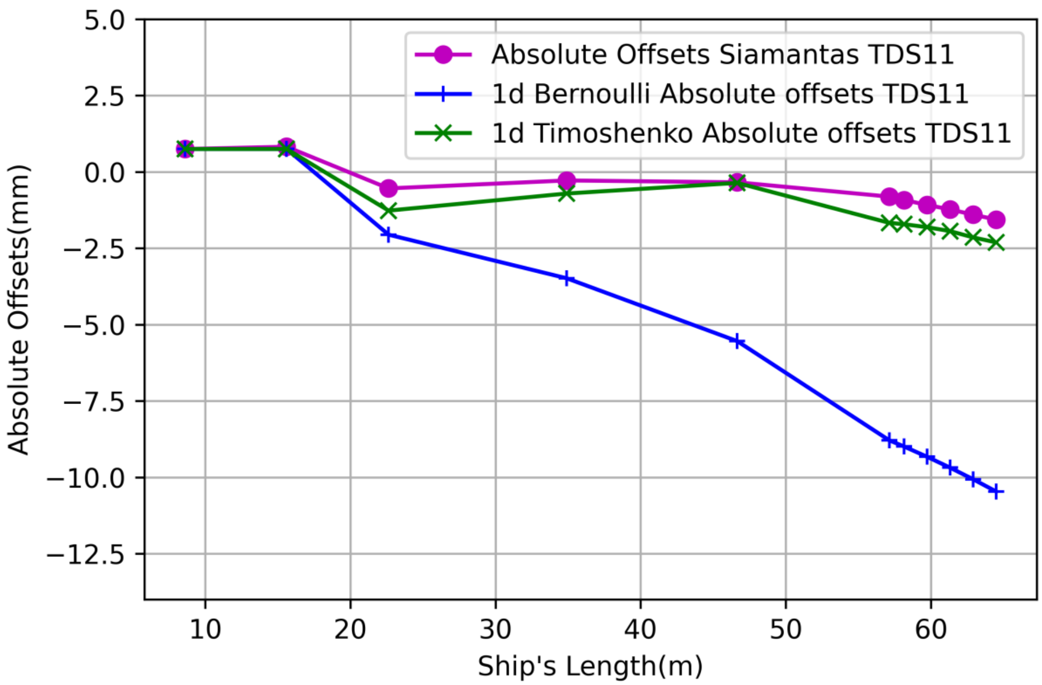

Figure 53: Absolute offset TDS11

Bearing	Reaction(kN)	Mean Pressure(Pa)	Total Offsets(m)	Initial Offsets(m)	Hull Deform. (m)	Support Elastic Deformation (m)	Minimum Film Thickness(m)
ASB	1629.02	0.75842	6.06E-04	7.50E-04	0.00E+00	-4.36E-04	2.92E-04
FSB	174.599	0.08112	9.24E-04	7.50E-04	0.00E+00	-5.72E-05	2.31E-04
IS3	376.196	0.53323	-1.34E-03	-2.00E-03	7.33E-04	-1.96E-04	1.22E-04
IS2	479.513	0.67968	-8.35E-04	-3.00E-03	2.29E-03	-2.46E-04	1.21E-04
IS1	526.575	0.74639	-4.71E-04	-4.00E-03	3.64E-03	-2.32E-04	1.21E-04
MB13	263.894	0.52186	-1.73E-03	-5.59E-03	3.92E-03	-1.35E-04	7.82E-05
MB12	637.453	1.26059	-1.70E-03	-5.59E-03	3.88E-03	-5.17E-05	6.58E-05
MB11	370.487	0.73265	-1.80E-03	-5.59E-03	3.78E-03	-8.52E-05	9.32E-05
MB10	664.678	1.31442	-1.96E-03	-5.59E-03	3.65E-03	-1.13E-04	8.96E-05
MB9	491.599	0.97215	-2.17E-03	-5.59E-03	3.45E-03	-1.15E-04	8.86E-05
MB8	250.136	0.49465	-2.27E-03	-5.59E-03	3.28E-03	-4.51E-05	8.68E-05

Table 5.11: Reaction Forces TDS11

5.4.10 Loading condition "TAS11"

TAS11 is an 11T/TEU arrival condition at scantling draft (11T x 8984), displacement 151443.0 t, trim equal to -0.984m and draft 15.003m. On the figures below are the loads and shear force distribution (figure…), the global deflection (figure…) and the relative bearing offsets for both Euler-Bernoulli beam and Timoshenko beam assumption of hull girder (figure…).

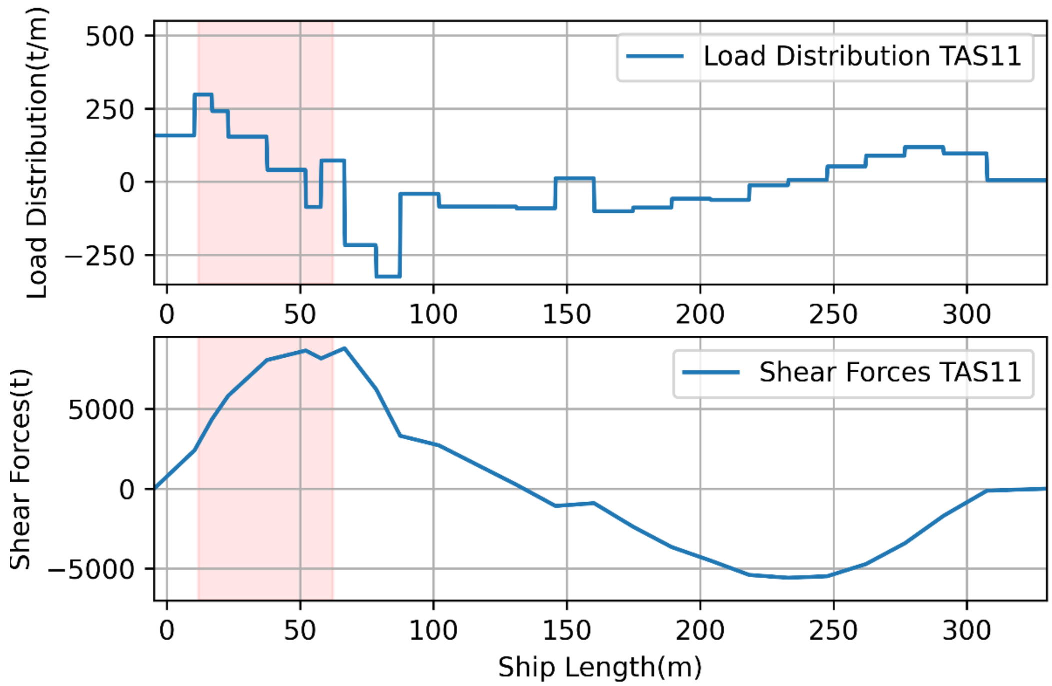

Figure 54: TAS11 load and shear force diagrams

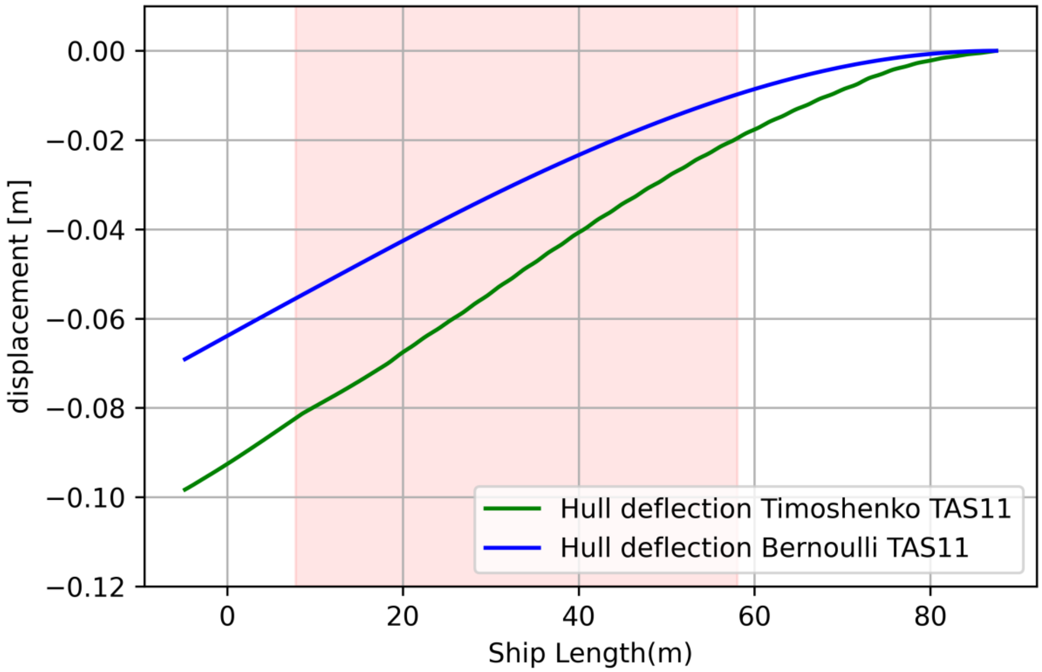

Figure 55: Hull Deflection TAS11

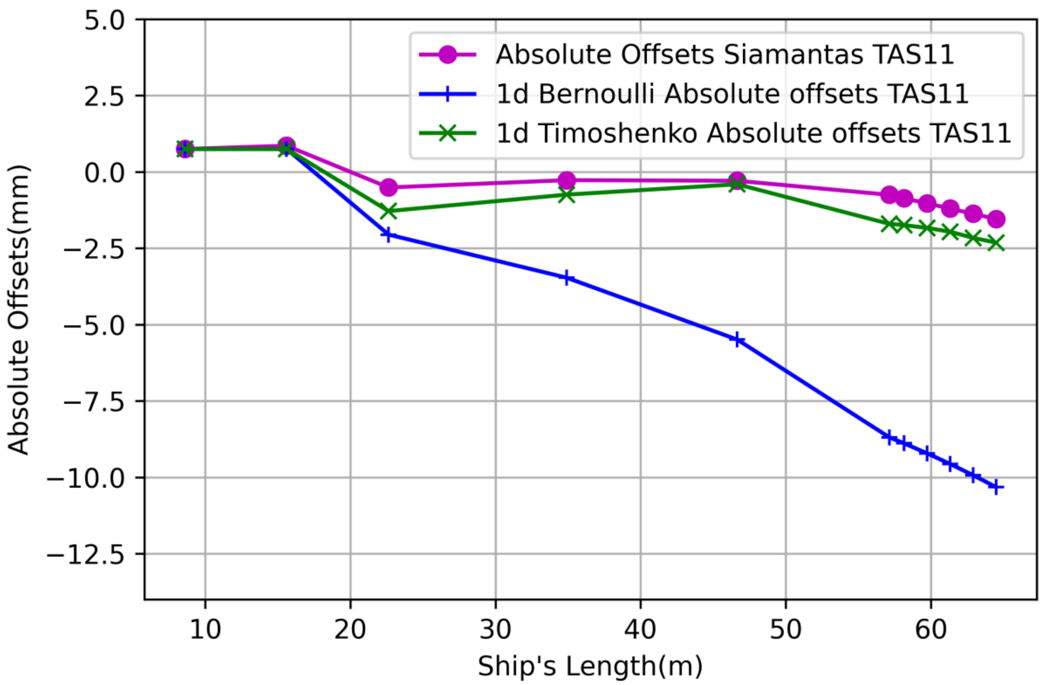

Figure 56: Absolute Offsets TAS11

Bearing	Reaction(kN)	Mean Pressure(Pa)	Total Offsets(m)	Initial Offsets(m)	Hull Deform. (m)	Support Elastic Deformation (m)	Minimum Film Thickness(m)
ASB	1628.5	0.75818	6.05E-04	7.50E-04	0.00E+00	-4.36E-04	2.91E-04
FSB	175.641	0.08161	9.24E-04	7.50E-04	0.00E+00	-5.75E-05	2.31E-04
IS3	375.419	0.53213	-1.36E-03	-2.00E-03	7.17E-04	-1.96E-04	1.22E-04
IS2	480.023	0.6804	-8.65E-04	-3.00E-03	2.26E-03	-2.46E-04	1.21E-04
IS1	525.863	0.74538	-5.11E-04	-4.00E-03	3.60E-03	-2.32E-04	1.21E-04
MB13	262.941	0.51998	-1.76E-03	-5.59E-03	3.89E-03	-1.35E-04	7.85E-05
MB12	648.191	1.28182	-1.73E-03	-5.59E-03	3.85E-03	-5.15E-05	6.59E-05
MB11	347.088	0.68638	-1.83E-03	-5.59E-03	3.75E-03	-8.57E-05	9.35E-05
MB10	692.288	1.36902	-1.98E-03	-5.59E-03	3.63E-03	-1.12E-04	9.01E-05
MB9	471.85	0.9331	-2.19E-03	-5.59E-03	3.43E-03	-1.16E-04	8.85E-05
MB8	256.343	0.50693	-2.28E-03	-5.59E-03	3.27E-03	-4.52E-05	8.68E-05

Table 5.12: Reaction Forces TAS11

5.4.11 Loading condition "TDS16"

TDS16 is a 16T/TEU departure condition at scantling draft (16T x 6474), displacement 153099.0t, trim equal to -0.493 m and draft 15.163 m. On the figures below are the loads and shear force distribution (figure…), the global deflection (figure…) and the relative bearing offsets for both Euler-Bernoulli beam and Timoshenko beam assumption of hull girder (figure…).

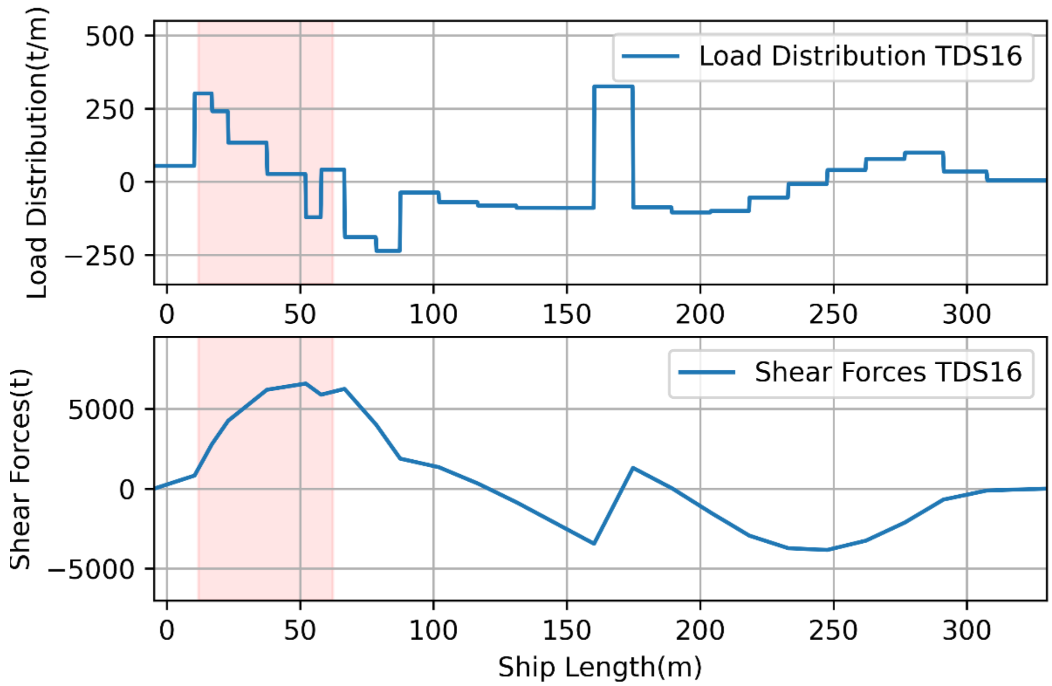

Figure 57: TDS16 load and shear force diagrams

The TAS16 condition deviates a lot compared to the other conditions. The deviation of the Shear Forces and Bending Moments at the engine bulkhead on the 3d model is **7.19%** and **8.24%** respectively. It is possible that the deviation of the two methods derive from the different loadings applied, since in the 1d finite element model the shear forces and bending moments are the exact same with the loading manual.

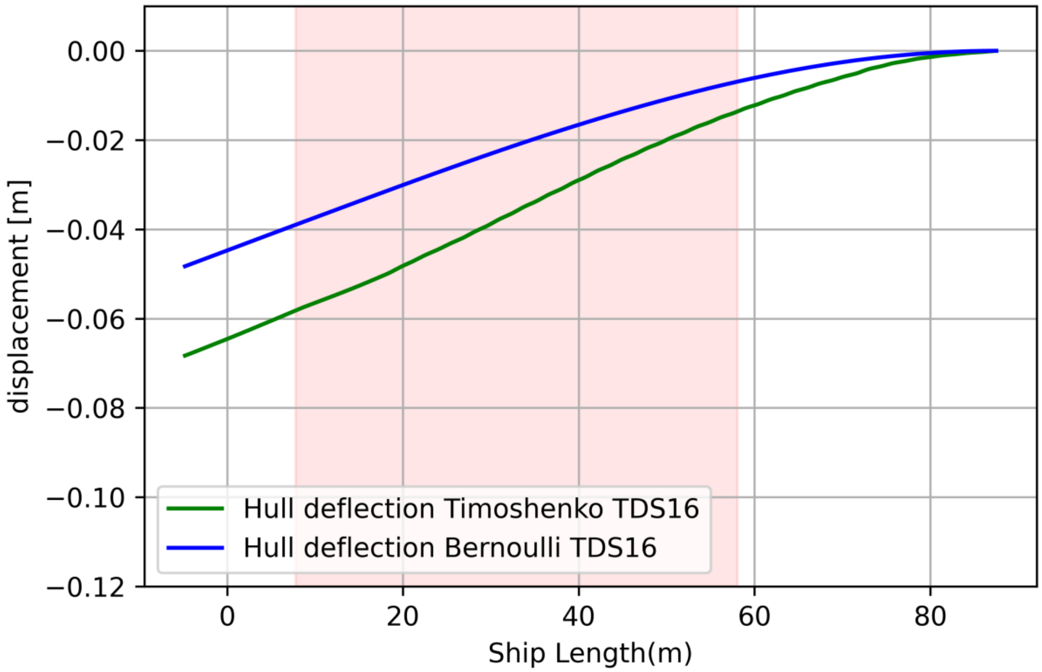

Figure 58: Hull Deflection TDS16

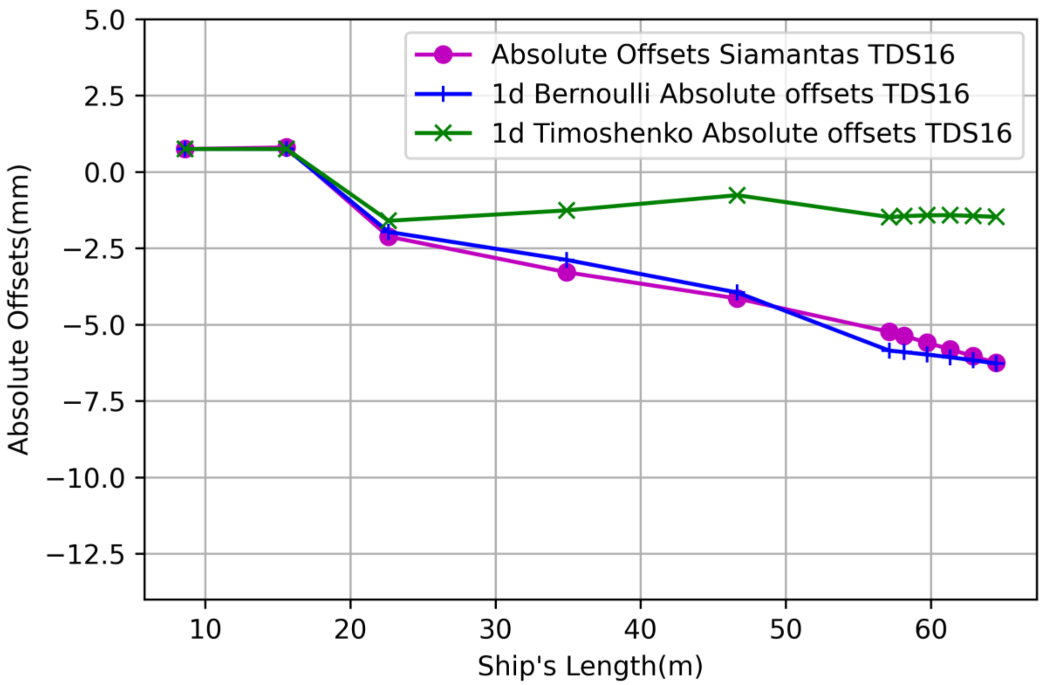

Figure 59: Absolute offsets TDS16

Bearing	Reaction(kN)	Mean Pressure(Pa)	Total Offsets(m)	Initial Offsets(m)	Hull Deform. (m)	Support Elastic Deformation (m)	Minimum Film Thickness(m)
ASB	1623.14	0.75568	6.11E-04	7.50E-04	0.00E+00	-4.28E-04	2.89E-04
FSB	185.564	0.08622	9.12E-04	7.50E-04	0.00E+00	-7.32E-05	2.35E-04
IS3	371.259	0.52624	-1.65E-03	-2.00E-03	4.00E-04	-1.82E-04	1.28E-04
IS2	480.798	0.6815	-1.38E-03	-3.00E-03	1.74E-03	-2.45E-04	1.22E-04
IS1	521.091	0.73861	-8.75E-04	-4.00E-03	3.24E-03	-2.36E-04	1.21E-04
MB13	340.454	0.67326	-1.53E-03	-5.59E-03	4.11E-03	-1.22E-04	7.67E-05
MB12	513.823	1.0161	-1.44E-03	-5.59E-03	4.14E-03	-6.64E-05	7.33E-05
MB11	467.008	0.92352	-1.41E-03	-5.59E-03	4.17E-03	-8.37E-05	9.64E-05
MB10	562.484	1.11233	-1.44E-03	-5.59E-03	4.17E-03	-1.11E-04	9.24E-05
MB9	573.659	1.13443	-1.47E-03	-5.59E-03	4.15E-03	-1.15E-04	8.94E-05
MB8	224.87	0.44469	-1.43E-03	-5.59E-03	4.12E-03	-4.56E-05	8.70E-05

Table 5.13: Reaction Forces TDS16

5.4.12 Loading condition "TAS16"

TAS16 is a 16T/TEU arrival condition at scantling draft (16T x 6474), displacement 146639.0t, trim equal to -0.937m and draft 14.654 m. On the figures below are the loads and shear force distribution (figure…), the global deflection (figure…) and the relative bearing offsets for both Euler-Bernoulli beam and Timoshenko beam assumption of hull girder (figure…).

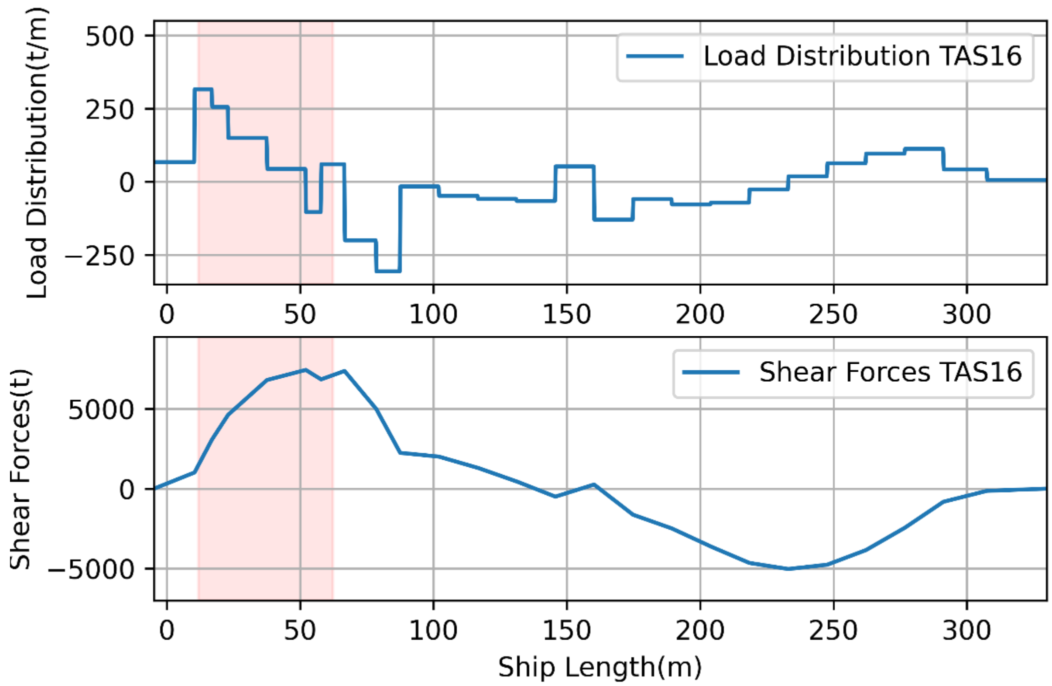

Figure 60: TAS16 load and shear force diagrams

The TAS16 condition deviates a lot compared to the other conditions. The deviation of the Shear Forces and Bending Moments at the engine bulkhead on the 3d model is **5.60%** and **6.65%** respectively. It is possible that the deviation of the two methods derive from the different loadings applied, since in the 1d finite element model the shear forces and bending moments are the exact same with the loading manual.

Figure 61: Hull Deflection TAS16

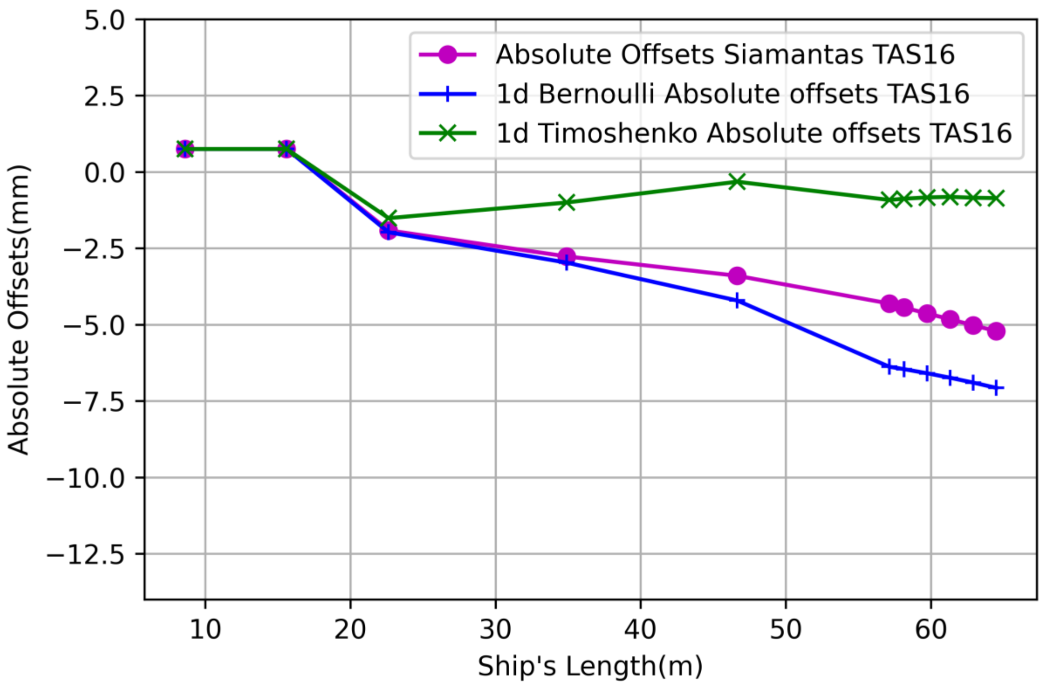

Figure 62: Absolute offsets TAS16

Bearing	Reaction(kN)	Mean Pressure(Pa)	Total Offsets(m)	Initial Offsets(m)	Hull Deform. (m)	Support Elastic Deformation (m)	Minimum Film Thickness(m)
ASB	1624.31	0.75623	6.13E-04	7.50E-04	0.00E+00	-4.29E-04	2.92E-04
FSB	184.016	0.0855	9.15E-04	7.50E-04	-9.99E-19	-7.01E-05	2.35E-04
IS3	371.2	0.52615	-1.57E-03	-2.00E-03	4.86E-04	-1.85E-04	1.26E-04
IS2	481.098	0.68192	-1.13E-03	-3.00E-03	2.00E-03	-2.46E-04	1.21E-04
IS1	520.823	0.73823	-4.34E-04	-4.00E-03	3.68E-03	-2.35E-04	1.21E-04
MB13	341.611	0.67555	-9.68E-04	-5.59E-03	4.67E-03	-1.25E-04	7.72E-05
MB12	524.865	1.03794	-8.71E-04	-5.59E-03	4.71E-03	-6.17E-05	7.12E-05
MB11	429.053	0.84847	-8.30E-04	-5.59E-03	4.75E-03	-8.45E-05	9.44E-05
MB10	622.167	1.23036	-8.40E-04	-5.59E-03	4.77E-03	-1.11E-04	9.12E-05
MB9	524.28	1.03678	-8.77E-04	-5.59E-03	4.74E-03	-1.16E-04	8.87E-05
MB8	240.724	0.47604	-8.18E-04	-5.59E-03	4.73E-03	-4.53E-05	8.70E-05

Table 5.14: Reaction Forces TAS16

5.4.13 Loading condition "MAX"

MAX is a homogenous at 15.2m draft (14T x 7390), displacement 153111.0t, trim equal to -0.009m and draft 15.2m. On the figures below are the loads and shear force distribution (figure…), the global deflection (figure…) and the relative bearing offsets for both Euler-Bernoulli beam and Timoshenko beam assumption of hull girder (figure…).

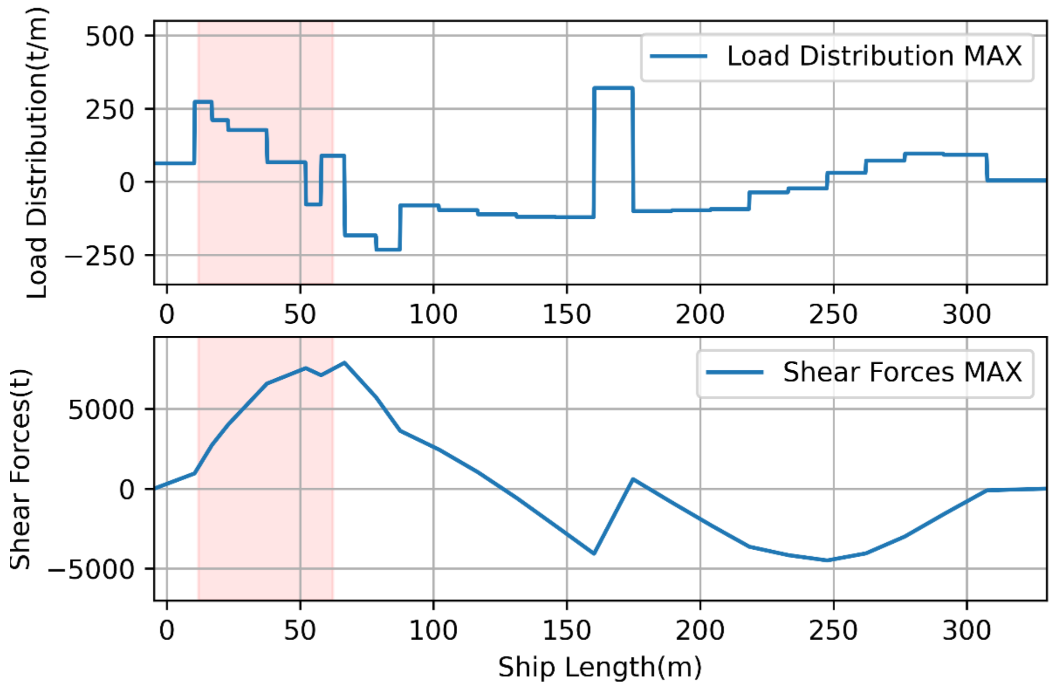

Figure 63: MAX load and shear force diagrams

The MAX condition deviates the most from all conditions from the one calculated by the 3d FEA model. The deviation of the Shear Forces and Bending Moments at the engine bulkhead on the 3d model is **6.69%** and **8.77%** respectively. It is possible that the deviation of the two methods derive from the different loadings applied, since in the 1d finite element model the shear forces and bending moments are the exact same with the loading manual. Another possible explanation is the small deviation in the calculated shear area. Small changes in the shear area may generate large differences of the deflection in the highly loaded conditions due to the high shear forces. A better investigation of the shear capacity of the vessel would lead to more proper results.

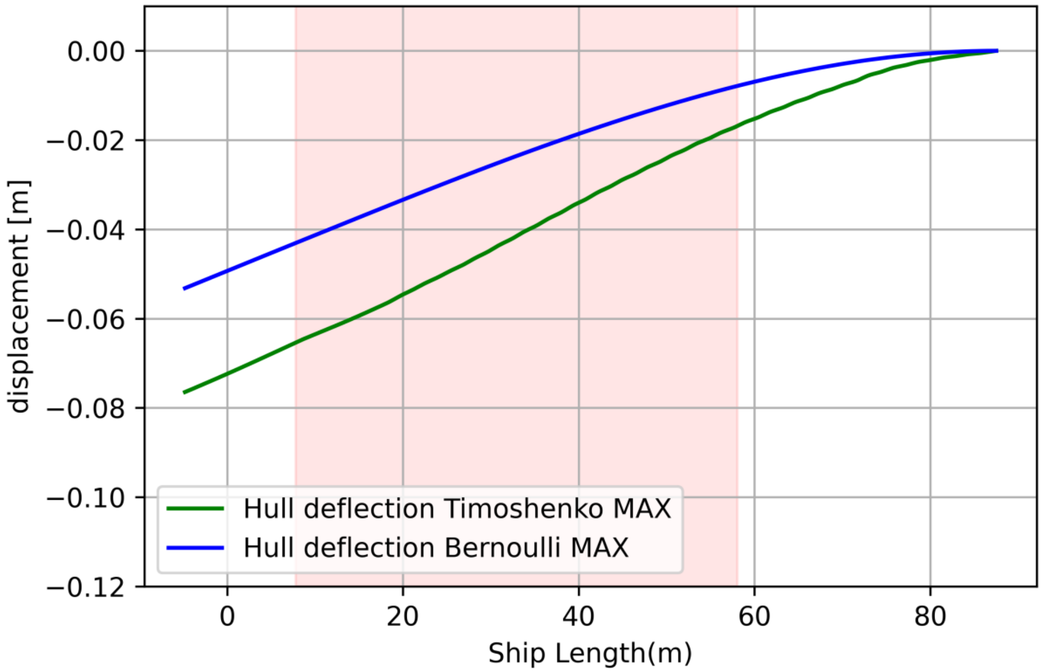

Figure 64: Hull Deflection MAX

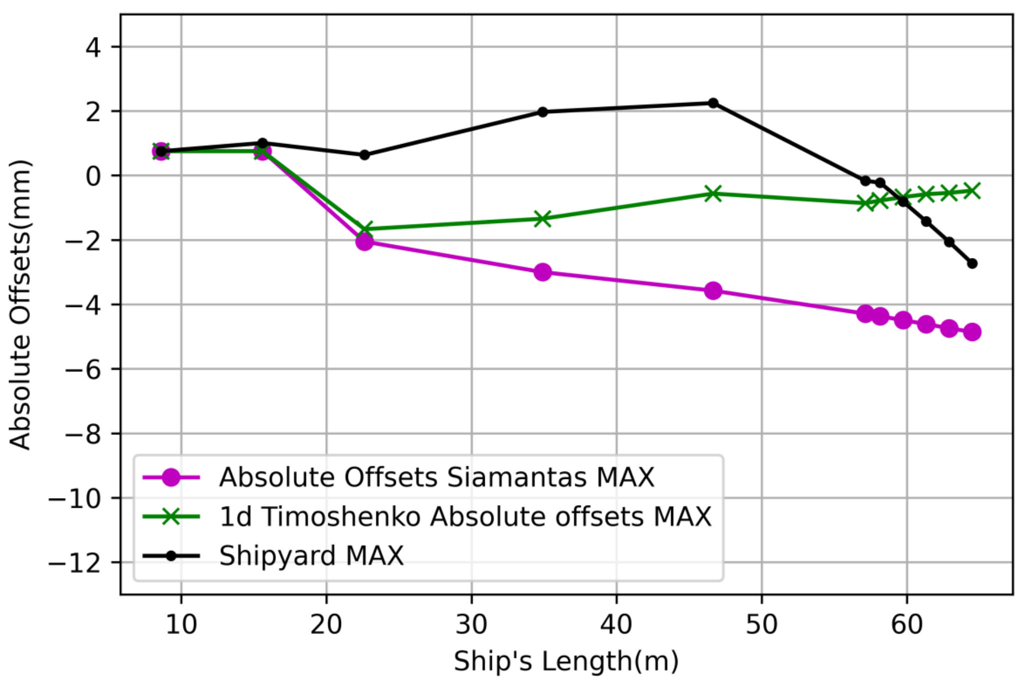

Figure 65: Absolute offsets MAX

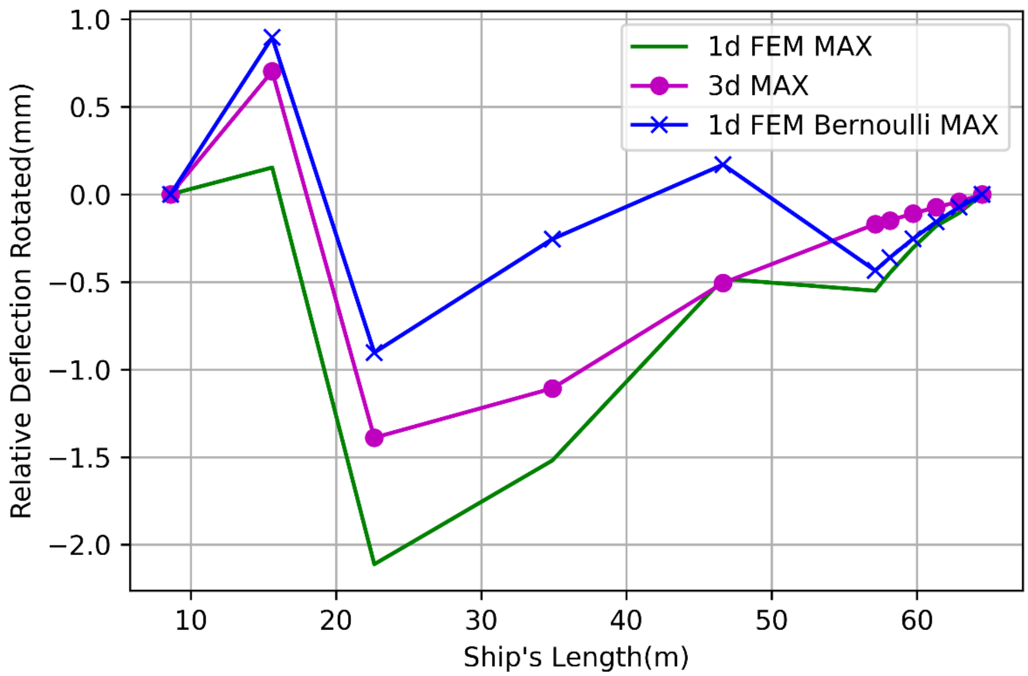

Figure 66: Rotated Reference Hull Deflections MAX

Even though the difference between the 3d and 1d Finite elements models seems to be quite big as we can notice it actually isn't. From the figure above the 1d Timoshenko FE model follows the same tendency with the 3d FE model with small differences which may be contributed in the different loading distribution of those two models or on the differences on the stiffness of 3d and 1d model. 3d model can achieve the exact stiffness of the vessel since every single part can be modeled and contribute to the stiffness. On contrary on the 1d model a small amount of frames is taken into so the exact stiffness cannot be achieved. An automation of the calculation would create faster and better results. The approximation of reference hull deflections is quite close to the 3d model and we notice that the biggest difference is in the fore stern tube bearing. A possible explanation is the rigid bodies applied in 3d FEM. Rigid bodies can be described as zero deformation and produce a flat zero line on the deflection diagram.

Bearing	Reaction(kN)	Mean Pressure(Pa)	Total Offsets(m)	Initial Offsets(m)	Hull Deform. (m)	Support Elastic Deformation (m)	Minimum Film Thickness(m)
ASB	1621.24	0.7548	6.11E-04	7.50E-04	0.00E+00	-4.28E-04	2.89E-04
FSB	189.284	0.08795	9.13E-04	7.50E-04	0.00E+00	-7.16E-05	2.35E-04
IS3	370.173	0.5247	-1.73E-03	-2.00E-03	3.31E-04	-1.83E-04	1.27E-04
IS2	479.445	0.67958	-1.46E-03	-3.00E-03	1.66E-03	-2.45E-04	1.21E-04
IS1	521.548	0.73926	-6.77E-04	-4.00E-03	3.44E-03	-2.38E-04	1.21E-04
MB13	325.562	0.64381	-9.06E-04	-5.59E-03	4.73E-03	-1.22E-04	7.56E-05
MB12	553.319	1.09421	-7.70E-04	-5.59E-03	4.81E-03	-5.90E-05	6.91E-05
MB11	402.159	0.79528	-6.68E-04	-5.59E-03	4.92E-03	-9.02E-05	9.19E-05
MB10	647.552	1.28056	-6.02E-04	-5.59E-03	5.01E-03	-1.11E-04	8.93E-05
MB9	507.343	1.00329	-5.68E-04	-5.59E-03	5.05E-03	-1.16E-04	8.81E-05
MB8	246.526	0.48751	-4.28E-04	-5.59E-03	5.12E-03	-4.52E-05	8.69E-05

Table 5.15: Bearing Reactions MAX

5.4.14 Reaction Forces

For the previous loading conditions the reaction forces were calculated in order to test the pressure applied on the bearings. For the total offsets we used the initial offsets calculated by the shipyard, the hull deflection we calculated in this thesis and the offsets due to hydrodynamic lubrications properties and elastic bearings' foundation. On the **figure 66** and table below the reaction forces calculated by the NTUA shaft alignment program are presented.

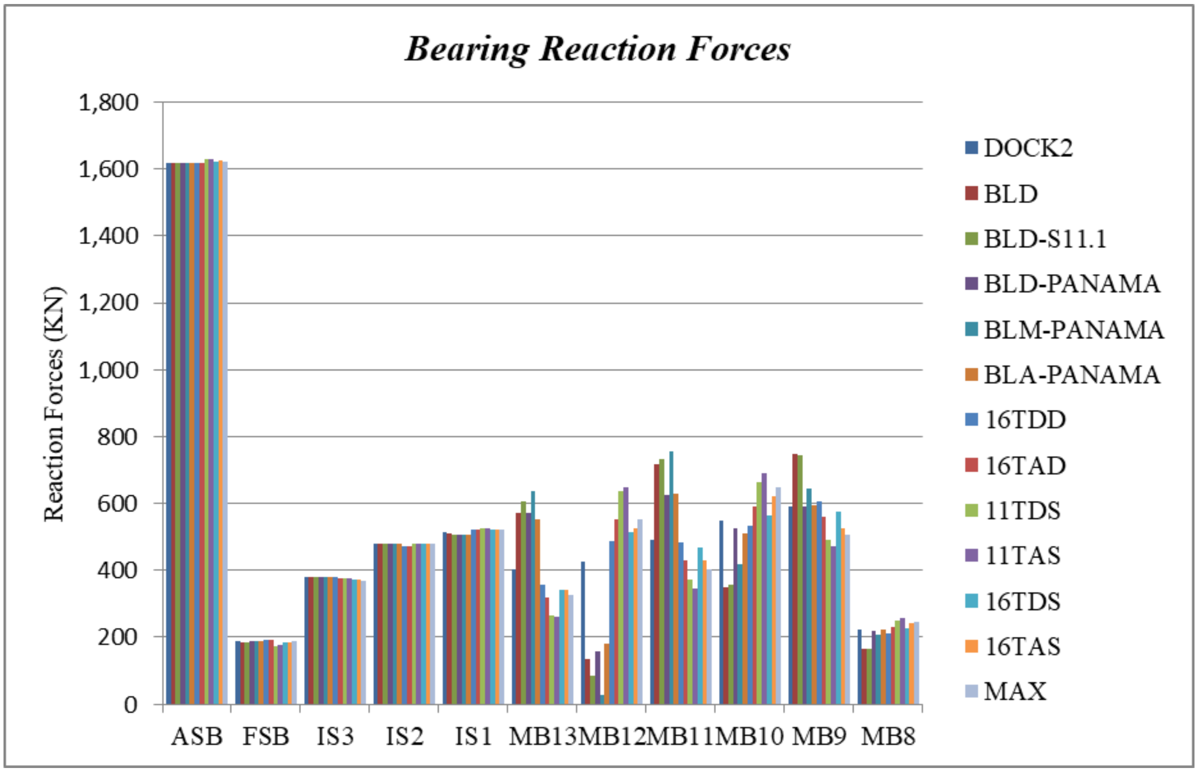

Figure 67: Reaction Forces for all the conditions

As we can see in **figure 66** the main engine bearing 12 (MB12) is not properly loaded. The alignment calculations are carried in order to achieve the things mentioned below.

- Bearing loads under all operating conditions are within the acceptable limits specified by the bearing manufacturer (Mean Pressure limits).
- Bearing reactions are always positive (i.e., supporting the shaft), except as determined acceptable in accordance with current ABS Rule requirements.
- Uniform load distribution at all bearings and conditions.

Another set of initial offsets would achieve better bearings' load distribution and would lead to better overall performance of the propulsion system and less wearing of the bearings.

Bearing	DOCK2	BLD	BLD-S11.1	BLD-PANAMA	BLM-PANAMA	BLA-PANAMA	16TDD	16TAD
ASB	1618	1619.1	1619.08	1618.94	1618.73	1618.63	1616.6	1617
FSB	188.92	186.02	186.021	186.519	187.128	187.305	191.9	192.7
IS3	378.18	380.27	380.149	379.87	379.159	379.303	379.14	377.6
IS2	478.53	479.5	479.977	479.821	480.773	480.2	471.86	471.9
IS1	515.56	509.02	507.455	508.261	506.306	508.336	521.16	523.1
MB13	402.19	571.97	607.145	572.732	635.239	553.785	358.67	320.1
MB12	427.69	136.58	85.6075	156.432	28.6708	180.71	487.47	551.4
MB11	493	717.72	732.367	624.955	756.312	628.786	482.79	429.9
MB10	549.11	348.91	356.678	527.287	418.804	511.7	533.49	592
MB9	590.54	749.09	742.793	590.212	645.18	593.356	607.87	558.3
MB8	222.44	165.98	166.881	219.123	207.855	222.039	213.22	230.5

Table 5.16: Reaction Forces for all Conditions

Bearing	11TDS	11TAS	16TDS	16TAS	MAX
ASB	1629.02	1628.5	1623.14	1624.31	1621.24
FSB	174.599	175.641	185.564	184.016	189.284
IS3	376.196	375.419	371.259	371.2	370.173
IS2	479.513	480.023	480.798	481.098	479.445
IS1	526.575	525.863	521.091	520.823	521.548
MB13	263.894	262.941	340.454	341.611	325.562
MB12	637.453	648.191	513.823	524.865	553.319
MB11	370.487	347.088	467.008	429.053	402.159
MB10	664.678	692.288	562.484	622.167	647.552
MB9	491.599	471.85	573.659	524.28	507.343
MB8	250.136	256.343	224.87	240.724	246.526

Table 5.17: Reaction Forces for all conditions (2)

5.5 Parameters Affecting Shaft Alignment Calculations

5.5.1 Voyage

While the vessel is on-going from departure port to arrival port, consumables such as fuels and lubricants reduce in volume. It is reasonable to say that the loading distribution (payload and buoyancy) will change and lead to different hull deflection. Figure … illustrates the difference of loads and hull deflection through a voyage.

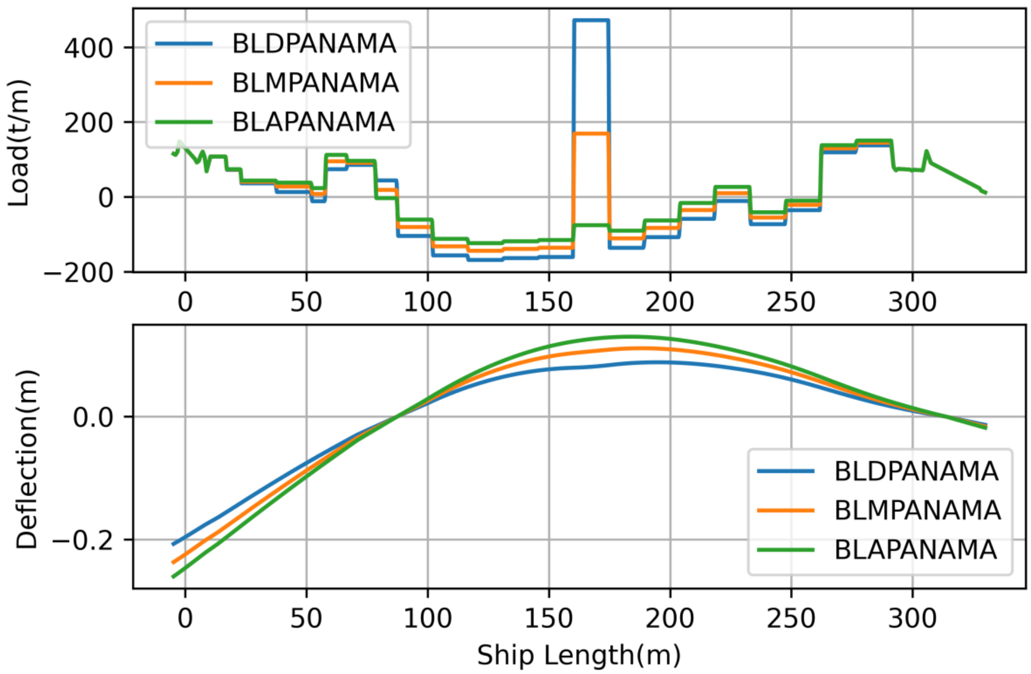

Figure 68: Load and Deflection change through Voyage

As we can notice above the change of the deflection is quite significant throughout a journey from one port to another. The total loss of displacement due to the consumables is 9832 tones, which corresponds to **12% loss of displacement** for departure condition. So throughout the journey the change in the bearings' offsets and the force applied on the bearings is quite extensive and need to be taken into consideration for every condition, ballast and laden.

The change of bearings' offsets is show on the table and graphically on the figure below:

Bearing	Position(m)	BLD-PANAMA(mm)	BLM-PANAMA(mm)	BLA-PANAMA(mm)
ASB	8.432	7.50E-01	7.50E-01	7.50E-01
FSB	15.182	7.50E-01	7.50E-01	7.50E-01
ISE3	25.096	-2.02E+00	-2.01E+00	-2.01E+00
IS2	35.361	-3.16E+00	-3.13E+00	-3.12E+00
IS1	46.654	-4.43E+00	-4.34E+00	-4.27E+00
MB13	57.135	-6.31E+00	-6.09E+00	-5.93E+00
MB12	58.145	-6.35E+00	-6.11E+00	-5.94E+00
MB11	59.735	-6.41E+00	-6.15E+00	-5.95E+00
MB10	61.325	-6.49E+00	-6.19E+00	-5.97E+00
MB9	62.915	-6.55E+00	-6.23E+00	-5.99E+00
MB8	64.505	-6.64E+00	-6.29E+00	-6.02E+00

Table 5.18: Ballast Panama Departure, Mid, Arrival Relative Bearings' Offsets

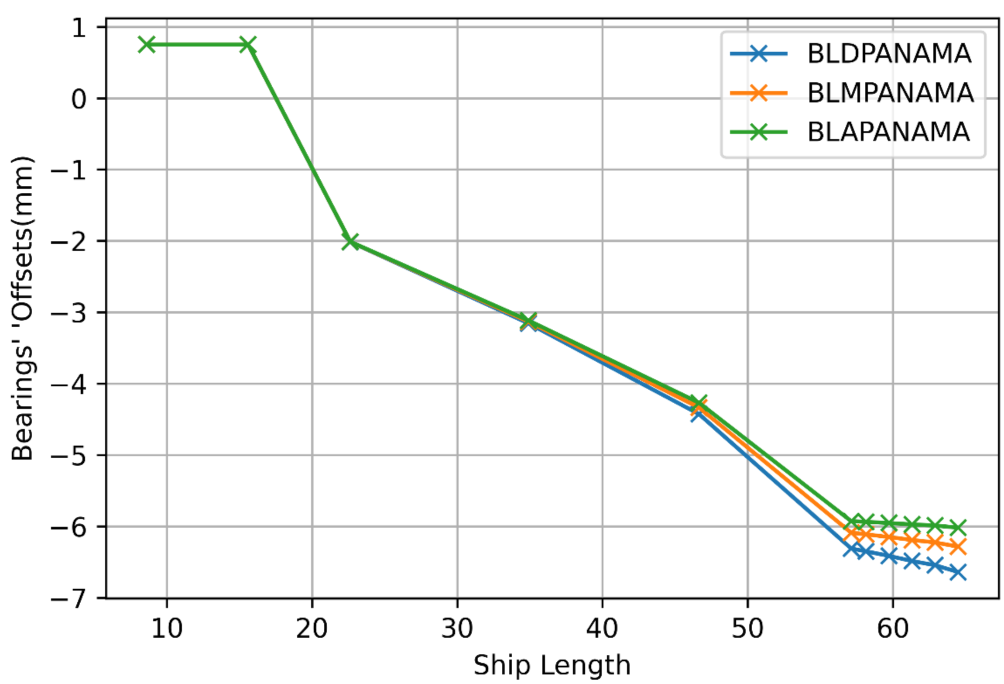

Figure 69: Bearing Offsets change through Voyage

5.5.2 Deckhouse

The time the shaft alignment process takes place is really important. All the blocks and parts (except from shaft) must be placed to achieve accurate reference line's initial offsets. If the shaft alignment plan has started and the deckhouse is not placed some calculations must be done to provide us the actual reference line.

The subtraction of the deckhouse from the hull will cause change in trim and draft of the vessel in the reference condition. To find this change, data from the loading manual is necessary. For the given condition DOCK1, trim and draft are known. With the use of Bonjean curves , trim and draft we can calculate the buoyancy distribution for the reference condition with the deckhouse weight. We add up the buoyancy to the load distribution, calculated by the derivative of Shear Forces, which produces the deadweight load. Afterward, the change of draft and trim from the subtraction of the deckhouse will derive from the use of TPC and MCT correspondingly.

$$Change\ in\ draught = \frac{w}{TPC}$$

$$Change\ in\ trim = -\frac{w * (LCG - Xposition)}{TPC}$$

w = weight load in tones (positive if adding weight or negative if subtracting)

LCG = longitudinal center of gravity for the vessel

Xposition = weight load longitudinal center of gravity

TPC = tonnes per centimeter

MCT = moment to change trim

In order to acquire the TPC and MCT one must go to the loading manual and for the given trim and draft, interpolate the data to find the values. The new buoyancy load can be obtained by using the new trim and draft value on the Bonjean curves. With known waterline area per frame, the buoyancy load is:

$$Buoyancy\ Load(x) = \gamma * A_{wl}(x) * coef_{force} * coef_{percentage}\ \left(\frac{N}{m}\right)$$

$$\int_0^L Buoyancy\ Load(x)dx = Displacement_i$$

γ = ρ*g

g = gravity acceleration ($9.80665 m/s^2$)

ρ = water density ($1.025\ t/m^3$)

Finally, extract the buoyancy load from the deadweight and we acquire the new distribution load for the reference condition. Then we feed the load distribution data in the Finite Differences Model.

5.5.3 Proper Modeling – Hatch Covers

In his 3d modeling, Stavros Siamantas modeled the hatch covers having the same stiffness k as the rest of the steel structure. According to studies, hatch covers are not welded with the hatches of the cargo holds, but the slide on and off when it is necessary to load and unload the containers. Moreover, they are pinned at certain points around the hatches, which do not allow the deformation of the hatch covers, so the stiffness contribution to the hull girder is small as well. On the figure below, it's the inertia difference if hatch covers are not included in the calculations.

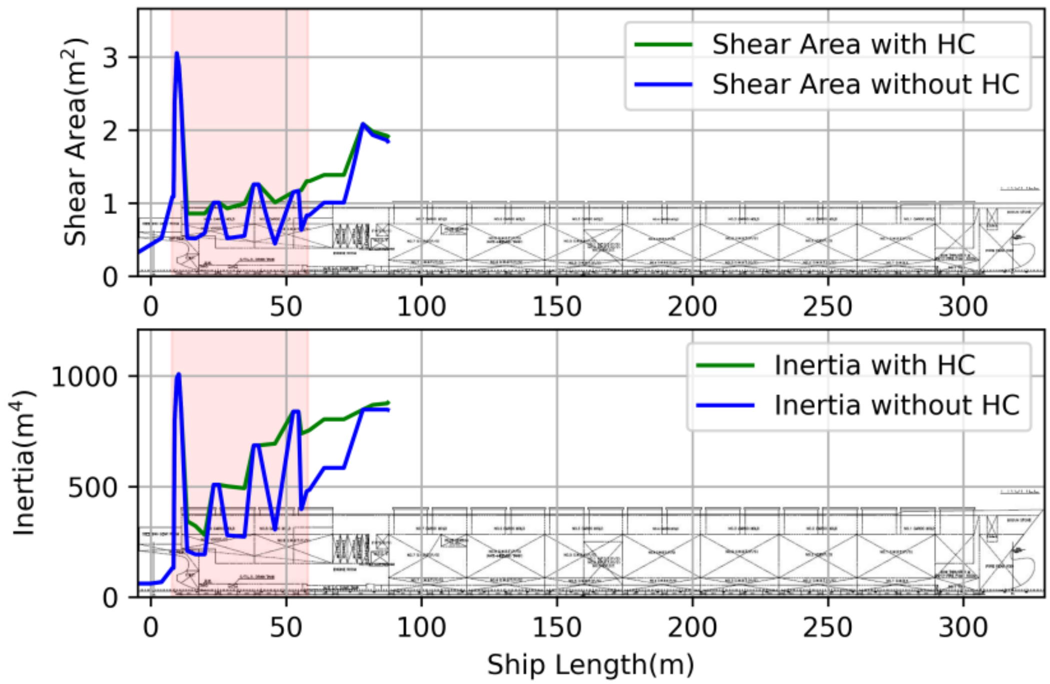

Figure 70: Effect of Hatch covers on Shear Area and Inertia

The absolute differences for a dock, ballast and laden condition is shown on the figures below. The change of second moment of area and shear area with the exclusion of hatch covers and deckhouse stiffness leads to great changes in the absolute vertical offsets of the shaft. As mentioned before, when the shear stiffness is noticeably higher than the shear force applied, the slope created by the shear is neglected and Timoshenko theory approaches Euler-Bernoulli beam theory.

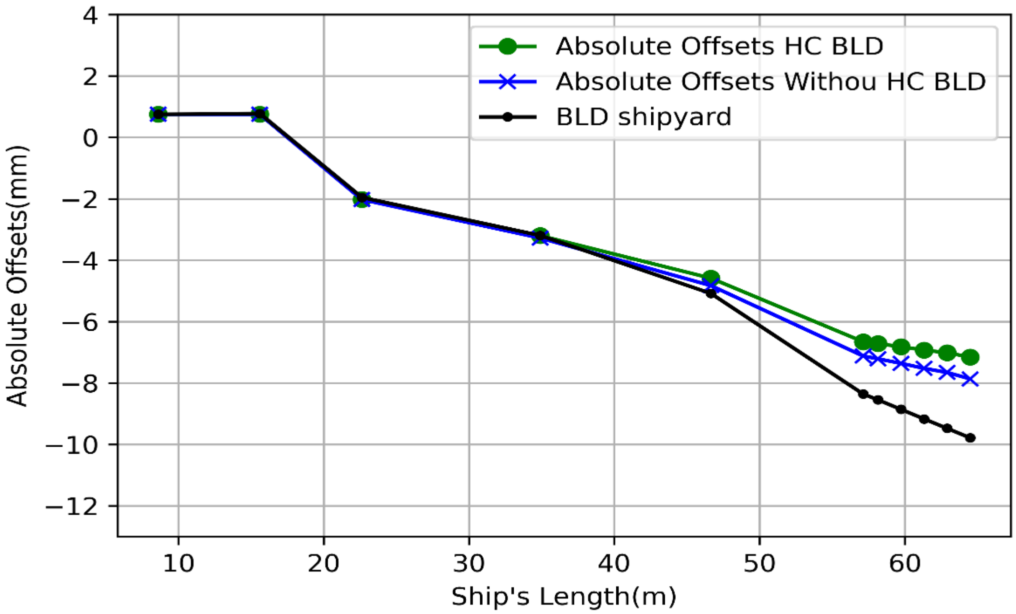

Figure 71: Effect of Hatch in Ballast condition bearing offsets

In figure 68 we can notice the small difference between the ballast condition with and without the effect of hatch covers. Since the ballast and dock1 conditions have relatively small deflections due to the little loading of the vessel, the differences are barely noticeable.

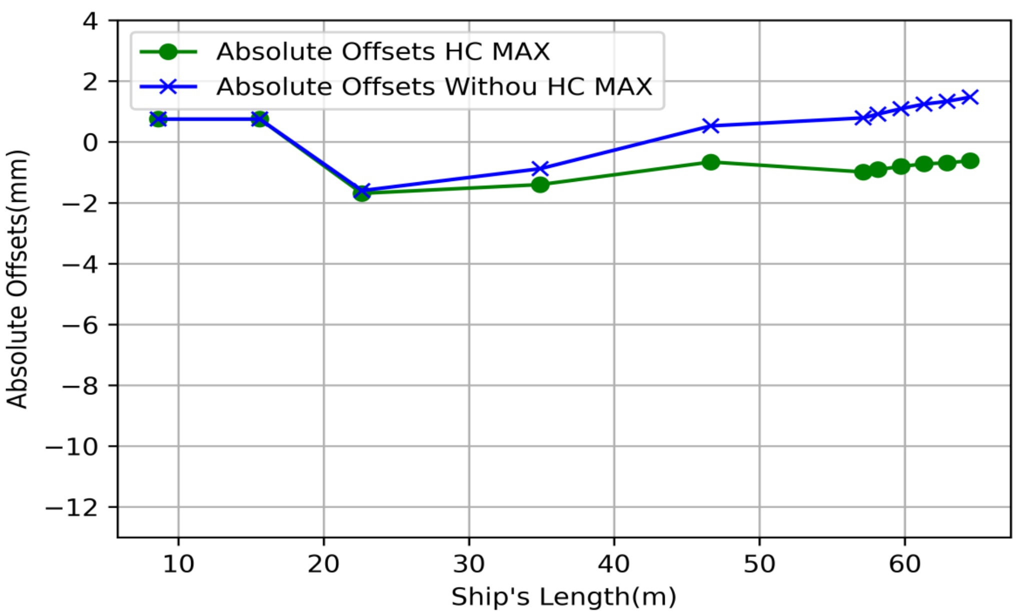

Figure 72: Effect of Hatch Covers in MAX condition

6. Conclusions – Future Work

6.1 Conclusions

In the present work, the shaft alignment of a typical 10,000 containership has been thoroughly investigated. A Graphical User Interface application was developed in this thesis to calculate the sectional properties, such as neutral axis, second moment of area and shear area, for several longitudinal transverse sections of the containership and automate the procedure of shaft alignment calculations. Several parts of the vessel must be taken into account in the calculations to properly assess the vertical bearings' offsets. The finite element method was used to calculate the deflections for each loading condition and DOCK1 was set as reference condition.

First, considering the afloat dock condition of the ship, a reference shaft alignment plan has been assumed, and a static equilibrium of the shaft has been calculated, yielding the reaction forces at the shaft bearings. Next, for thirteen (13) representative loading conditions of the vessel, corresponding to, ballast, design and scantling conditions hull deflections were calculated. The corresponding hull deflections have been computed, the offset of the bearings due to hull deflections have been determined. After the calculation of hull deflection offsets, we added the initial offsets and the oil film thickness and the offsets due to the stiffness of the bearing foundations to get the total offsets and generate the bearings' reaction forces.

The results demonstrate that in most conditions we can achieve a great early estimation of the hull deflections with the 1D beam Timoshenko theory. For most of the loading conditions, where the shear forces were quite similar the 1D model approached the 3D model. The accuracy of the 1D beam Timoshenko theory had a maximum deviation of 1.5mm. To the contrary, the 1D beam Bernoulli method showed a maximum deviation of up to 10mm. Thus, the Bernoulli method is considered insufficient for the specific vessel type.

The automation of the process and the minimum pre-processing by the user, improves significantly the amount of time required for the calculation of the hull deflections. The combination of low time and experience, but also the automation for the calculations of the sectional properties of each ship frame makes this method robust and an excellent tool to quickly assess the hull deflections and bearing offsets.

6.2 Future Work

The finite element method conducted in the present thesis creates a new path to extend our knowledge and comprehension of the various parameters affecting the shaft alignment calculations due to hull deflection. Future work is suggested below.

6.2.1 Neural Network for Image Processing

With digital image recognition and processing on each frame available of the ship, the calculation of the second moment of area would be much faster, more accurate and could produce a larger data of sections. This could lead to far greater results, since in our thesis we used 40 frames and we generated the results with the least possible frames. The development of an algorithm with the use of image processing neural networks would be a breakthrough and lead to better results.

6.2.2 Development of Inertia Calculator GUI application

The development of the GUI application created in this thesis for the calculation of sectional properties of transverse ship frames would be a great future work. By applying the shear stress distribution and torsional moment then we could not only get the deflections for the shaft alignment but also for every point of the vessel throughout its length. This could help not only in terms of deflection but also in strength assessment of the vessel and to define the vibration modes.

6.2.3 Sea swell

A probabilistic search on the waves and the sea, where the vessel travels, could lead to better overall assessment of the bearings' offsets. By conducting the dynamic analysis of the deflection of the vessel through time and different types of waves (wave length λ, significant wave height H, air speed etc.) one can achieve far better offsets that could decrease the power loss of the propulsion system.

6.2.4 1D investigation of different sizes and types of vessels

The investigation of different sizes and types of vessels would lead in a deeper understanding of the 1d method and how to properly use it to achieve more accurate results. The use of this method to different ships would generalize the process and maybe lead to calibration factors that would generate better results

6.2.5 Estimation of hull corrosion

An important future research task would be to calculate the corrosion of the vessel through time. Several parameters affect the corrosion of underwater plating, but also above the waterline, such as the sea where the ship travels (temperature, saltiness, significant waves at the area etc.), the vessel speed (Flow-accelerated corrosion), the type of coating etc. Plating corrosion leads to decrease of the sectional properties of the vessel, which cause change in the hull deflections. An early estimation of the hull deflections over time would help to assess the new reaction forces and the power loss caused by them. This could be a great asset for the ship-owners since they could program more precise the dry-dock of the vessel.

7. Literature – References

[1] Paik, J. K. (2003). Ultimate Limit State Design of Steel-Plated Structures. American Bureau of Shipping (2019). Guidance notes on Propulsion Shafting Alignment

[2] Chul-Oh Seo, Byongug Jeong , Jung-Ryul Kim , (2020). Determining the influence of ship hull deformations caused by draft change on shaft alignment application using FE analysis

[3] https://britishsteel.co.uk/media/40438/bulb-flats-brochure.pdf [3]

[4] Requirements concerning strength of ships, INTERNATIONAL ASSOCIATION OF CLASSIFICATION SOCIETIES (IACS)

[5] Ship structural analysis and design, by Owen F. Hughes and Jeom Kee Paik with Dominique Béghin, John B. Caldwell, Hans G. Payer and Thomas E. Schellin

[6] American Bureau of Shipping. (2019): Guidance notes on propulsion shafting alignment.

[7] Elastic Shaft Alignment of a Container Vessel, Stavros Siamantas

[8] Global hydroelastic analysis of ultra large container ships by improved beam structural model, Ivo Senjanovic, Nikola Vladimir

[9] Theory of Structures, Second Edition, by S.P. Timoshenko, D.H. Young

[10] Global Hull-Girder Response (Quasi-Static, Prismatic Beam Models), Petri Varsta, Heikki Remes, and Jani Romanoff

[11] Analysis of Tapered Timoshenko and Euler–Bernoulli Beams on an Elastic Foundation with Moving Loads, W. Abbas , Omar K. bakr

[12] The Effects of Shear Deformation in Rectangular and Wide Flange Sections, Hariharan Iyer

[13] Determining the influence of ship hull deformations caused by draught change on shaft alignment application using FE analysis Chul-Oh Seo, Byongug Jeong, Jung-Ryul Kim, Myeongho Song, Jung-Ho Noh, Jaeung Lee

[14] An advanced theory of thin-walled girders with application to ship vibrations, I. Senjanovic, S. Tomasevic, N. Vladimir

[15] Effects of Hull Deformation on the Static Shaft Alignment Characteristics of VLCCs: A Case Study, George Kourbetis et al

[16] Ελαστική Ευθυγράμμιση Αξονικού Συστήματος Πλοίου, Ορέστης Βλάχος

APPENDIX A

A/A	Name	Position	Length(m)	Diameter(m)
1	Shaft	0	0.57	0.695
2	Shaft	0.57	1.035	0.916
3	Propeller	1.605	0.925	0.965
4	Shaft	2.53	0.615	0.988
5	Bearing	3.145	1.087	0.988
6	ASB	4.232	1.087	0.988
7	Shaft	5.319	0.481	0.988
8	Shaft	5.8	0.1	0.957
9	Shaft	5.9	4.11	0.925
10	Shaft	10.01	0.1	0.958
11	Shaft	10.11	0.377	0.99
12	Bearing	10.487	0.495	0.99
13	FSB	10.982	0.495	0.99
14	Shaft	11.477	0.175	0.99
15	Shaft	11.652	0.558	0.99
16	Shaft	12.21	0.1	0.99
17	Shaft	12.31	1.23	0.898
18	Flange	13.54	0.17	1.66
19	Flange	13.71	0.17	1.66
20	Shaft	13.88	1.83	0.805
21	Shaft	15.71	4.33	0.805
22	Shaft	20.04	0.04	0.818
23	Shaft	20.08	0.391	0.83
24	Bearing	20.471	0.425	0.83
25	ISB3	20.896	0.425	0.83
26	Shaft	21.321	0.391	0.83
27	Shaft	21.712	0.04	0.818
28	Shaft	21.752	0.144	0.805
29	Shaft	21.896	4.444	0.805
30	Flange	26.34	0.17	1.66
31	Flange	26.51	0.17	1.66
32	Shaft	26.68	3.625	0.805
33	Shaft	30.305	0.04	0.818
34	Shaft	30.345	0.391	0.83
35	Bearing	30.736	0.425	0.83
36	ISB2	31.161	0.425	0.83
37	Shaft	31.586	0.391	0.83
38	Shaft	31.977	0.04	0.83
39	Shaft	32.017	0.144	0.805

40	Shaft	32.161	5.149	0.805
41	Shaft	37.31	1.83	0.805
42	Flange	39.14	0.17	1.66
43	Flange	39.31	0.17	1.66
44	Shaft	39.48	2.118	0.805
45	Shaft	41.598	0.04	0.818
46	Shaft	41.638	0.391	0.83
47	Bearing	42.029	0.425	0.83
48	ISB1	42.454	0.425	0.83
49	Shaft	42.879	0.391	0.83
50	Shaft	43.27	0.04	0.818
51	Shaft	43.31	0.144	0.805
52	Shaft	43.454	4.856	0.805
53	Shaft	48.31	3.63	0.805
54	Flange	51.94	0.17	1.83
55	Engine	52.11	0.14	1.83
56	Flywheel	52.25	0.1	2.19
57	Bearing	52.35	0.585	1.18
58	MB13	52.935	0.325	1.18
59	Shaft	53.26	0.09	2.29
60	Shaft	53.35	0.18	1.93
61	Shaft	53.53	0.09	2.29
62	Bearing	53.62	0.325	1.18
63	MB12	53.945	0.42	0.602
64	Shaft	54.365	0.375	0.602
65	Shaft	54.74	0.375	0.602
66	Bearing	55.115	0.42	0.602
67	MB11	55.535	0.42	0.602
68	Shaft	55.955	0.375	0.602
69	Shaft	56.33	0.375	0.602
70	Bearing	56.705	0.42	0.602
71	MB10	57.125	0.42	0.602
72	Shaft	57.545	0.375	0.602
73	Shaft	57.92	0.375	0.602
74	Bearing	58.295	0.42	0.602
75	MB9	58.715	0.42	0.602
76	Shaft	59.135	0.375	0.602
77	Shaft	59.51	0.375	0.602
78	Bearing	59.885	0.42	0.602
79	MB8	60.305	0.42	0.602

APPENDIX B

This appendix was made to help understand the calculations of shear area. The calculations were made for the simple section shown on figure below.

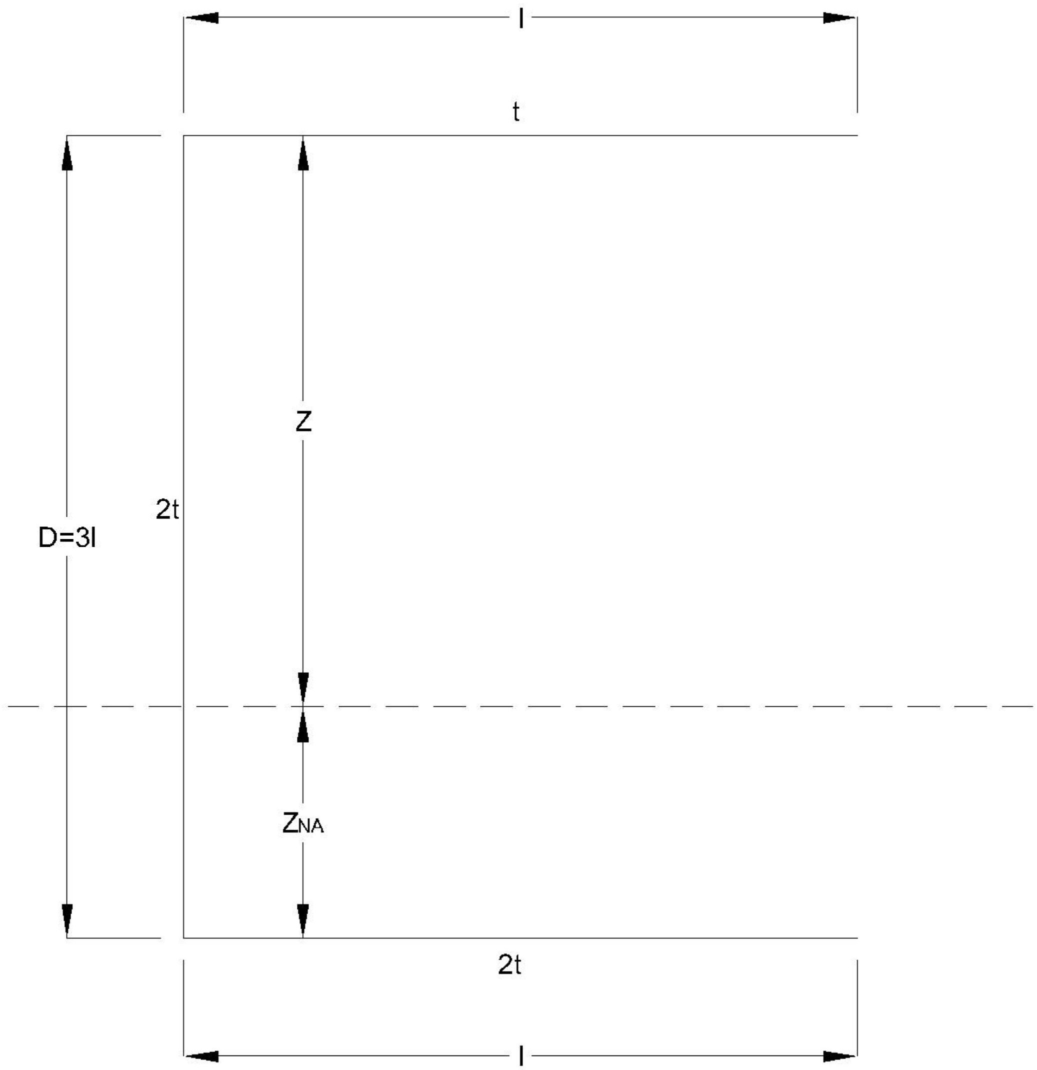

Figure 73: Shear Area Calculation

$$z_{NA} = \frac{3tl^2 + 9tl^2}{9tl} = \frac{4}{3}l$$

$$I_y = 2 * \left([9tl^2 + 6tl * 2.25l^2] - 9tl\left(\frac{4}{3}l\right)^2 \right) = 13tl^3$$

$$A_{sz} = \frac{{I_y}^2}{\int_{z0}^{zu} \frac{Q^2(z)}{t(z)} dz} = \frac{{I_y}^2}{\sum \int_{z0}^{zu} \frac{t_i}{2} [(D - z_{NA})^2 - z^2]^2 dz}$$

Where z_u and z_o are the start and end of each plating element, D: Depth of vessel, z_{NA}: Neutral axis vertical position. The calculations must start from negative to positive. When starting from positive put an absolute in the value calculated per element. We divide the plating elements in parts of the same thickness. The horizontal plates can be neglected from the calculations of shear area, as they don't contribute much compared with a vertical plate.

$$\sum \int_{z_i}^{z_{i+1}} \frac{t_i}{2} [(D - z_{NA})^2 - z^2]^2 dz = \sum \frac{t_i}{2} \left[(D - z_{NA})^4 z - \frac{2z^3}{3}(D - z_{NA})^2 - \frac{z^5}{5} \right]_{z_i}^{z_{i+1}}$$

$$A_{sz} = \frac{(13tl^3)^2}{2 * \int_{3l - z_{NA}}^{-z_{NA}} \frac{t_i}{2} [(D - z_{NA})^2 - z^2]^2 dz}$$

$$A_{sz} = \frac{(13tl^3)^2}{\frac{2t}{2}\left[\left(\frac{5}{3}l\right)^4 * (-3l) - \frac{2}{3}(-z_{NA})^3 * \left(\frac{5}{3}l\right)^2 + \frac{2}{3}(3l - z_{NA})^3 * \left(\frac{5}{3}l\right)^2 + \left(\frac{-z_{NA}}{5}\right)^5 - \left(\frac{3l - z_{NA}}{5}\right)^5 \right]}$$

$A_{sz} = \frac{169tl}{44,38}$, assuming t = 0.1m and l=7m then $A_{sz} = \frac{169tl}{44,76} = 2.643m^2 = k * A \rightarrow k = 0.2433$

This means that 24.33% of the total sectional area contributes to the shear stiffness. In an actual vessel, many of the plates are not horizontal or vertical so the angle of the plate must be taken into consideration.

In order to assess the denominator for elements with an angle, a simple approach is to transform the thickness in consider with the angle.

$$t_{transf} = \frac{t}{sin\theta}$$

For very small angles (close to horizontal) the denominator of the element can be considered zero.

APPENDIX C

LOAD: DOCK1 : NORMAL DOCKING

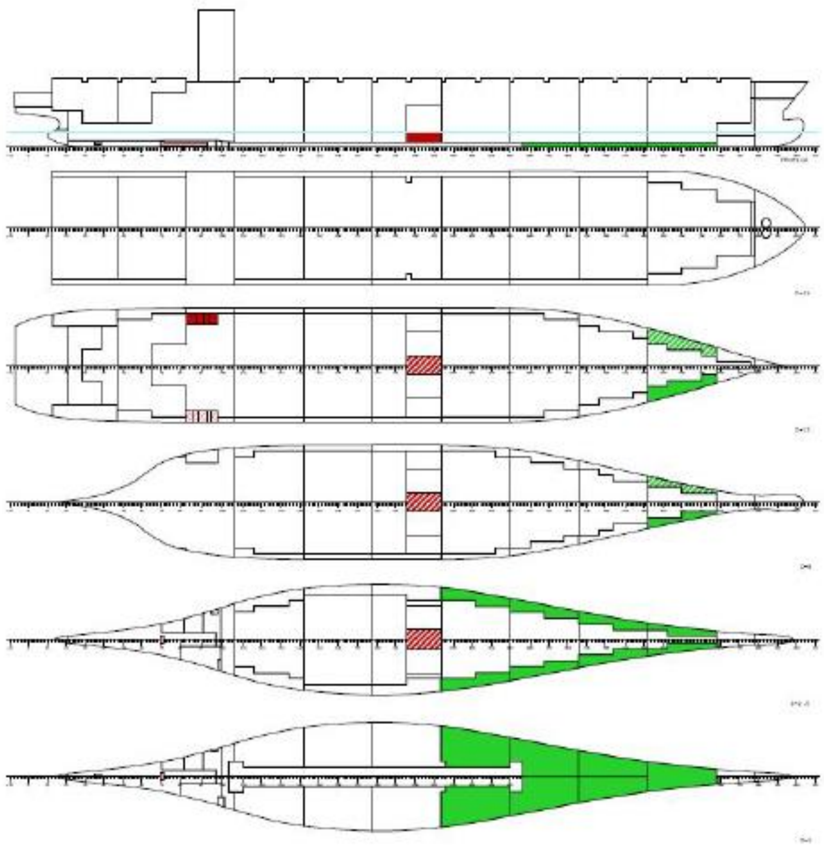

XFRAM		BEND	REL	BMMX	BMMN	RELSHREL		SHMX	SHMN	TORS	REL	TMMX	TMMN
m	#	tm	%	tm	tm	t	%	t	t	tm	%	tm	tm
10.40	13	14993	33.3	45028	-19086	1749	43.0	4065	-801	942	4.2	22432	-22432
16.91	21	28666	32.1	89337	-39357	2465	42.1	5861	-1652	935	4.2	22432	-22432
23.00	29	45218	32.7	138272	-58310	2957	40.9	7229	-2448	921	4.1	22432	-22432
37.55	47	95261	34.0	280510	-103841	3853	40.3	9569	-4350	891	4.0	22432	-22432
52.10	65	155175	35.2	440575	-150045	4291	38.2	11231	-6063	866	3.9	22432	-22432
57.85	72	180463	35.7	504815	-168356	4565	39.8	11464	-6494	891	4.0	22432	-22432
66.65	83	226495	37.8	599292	-196327	5838	50.2	11623	-6848	729	3.3	22432	-22432
78.50	96	308116	43.2	713937	-234032	8260	73.8	11191	-6962	9426	42.0	22432	-22432
87.50	106	387365	48.9	791423	-262669	9264	83.6	11075	-6962	11318	50.5	22432	-22432
102.0	124	512522	58.4	878094	-308632	7708	72.7	10606	-6887	11316	50.4	22432	-22432
116.6	142	609234	66.6	915087	-353413	5522	66.5	8298	-6550	11286	50.3	22432	-22432
131.1	160	671863	70.7	950587	-396375	3050	49.0	6223	-6223	11254	50.2	22432	-22432
145.7	178	697370	73.4	950587	-396375	441	7.1	6223	-8086	11218	50.0	22432	-22432
160.2	196	684698	72.5	945001	-396375	-2177	26.1	6223	-8354	11179	49.8	22432	-22432
174.8	214	637840	69.8	914398	-396333	-4234	50.4	6223	-8397	11136	49.6	22432	-22432
189.3	232	569371	65.4	871062	-395751	-5174	60.9	6237	-8498	11113	49.5	22432	-22432
203.9	250	488677	60.5	808296	-394958	-5918	65.0	6548	-9102	11110	49.5	22432	-22432
218.4	268	398845	56.9	700417	-362651	-6329	63.3	7012	-10005	11109	49.5	22432	-22432
233.0	286	306612	54.7	560467	-310689	-6342	60.8	7230	-10429	11107	49.5	22432	-22432
247.6	304	216057	51.5	419892	-258730	-6098	62.4	7230	-9766	11107	49.5	22432	-22432
262.1	322	130925	44.7	292602	-206773	-5597	64.6	7230	-8664	11106	49.5	22432	-22432
276.7	340	63854	33.0	193763	-154818	-3601	55.1	6618	-6532	4534	20.2	22432	-22432
291.2	358	27166	23.5	115648	-99620	-1564	39.1	4327	-3999	-57	0.3	22432	-22432
307.5	378	6994	15.5	45089	-45553	-785	44.9	1901	-1749	-35	0.2	22432	-22432

LOAD: DOCK2 : DOCKING WITH 12000t CARGO

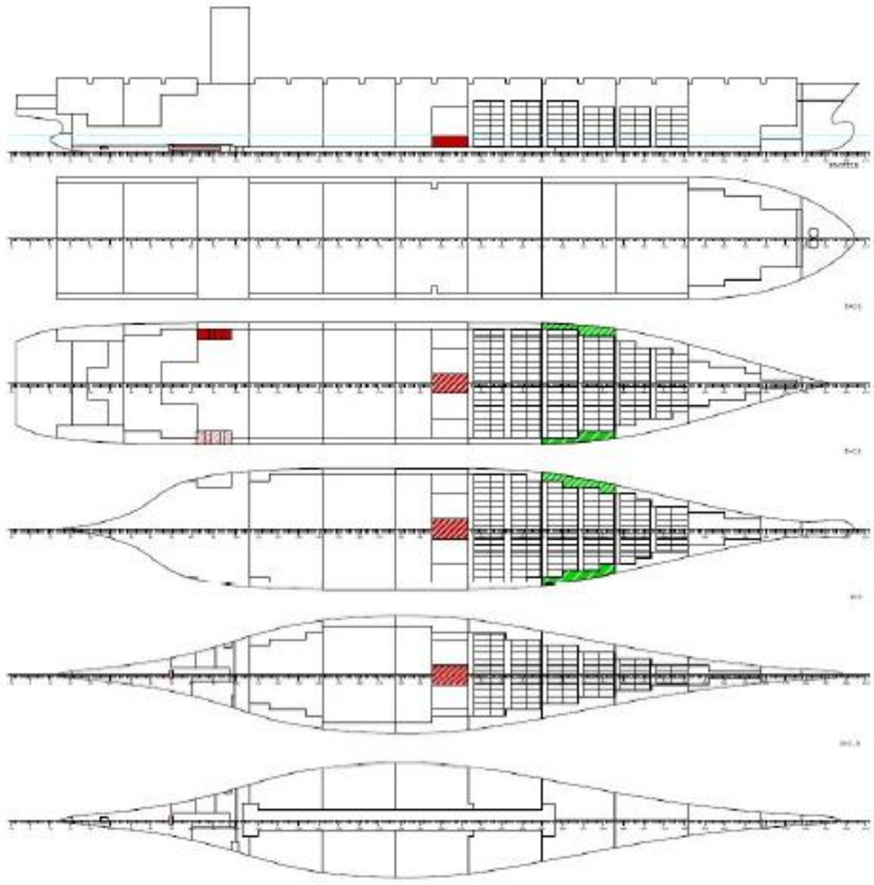

XFRAM		BEND	REL	BMMX	BMMN	RELSHREL		SHMX	SHMN	TORS	REL	TMMX	TMMN
m	#	tm	%	tm	tm	t	%	t	t	tm	%	tm	tm
10.40	13	14978	33.3	45028	-19086	1749	43.0	4065	-801	902	4.0	22432	-22432
16.91	21	28635	32.1	89337	-39357	2461	42.0	5861	-1652	879	3.9	22432	-22432
23.00	29	45136	32.6	138272	-58310	2945	40.7	7229	-2448	850	3.8	22432	-22432
37.55	47	94748	33.8	280510	-103841	3801	39.7	9569	-4350	784	3.5	22432	-22432
52.10	65	153321	34.8	440575	-150045	4150	37.0	11231	-6063	722	3.2	22432	-22432
57.85	72	177638	35.2	504815	-168356	4368	38.1	11464	-6494	733	3.3	22432	-22432
66.65	83	221434	36.9	599292	-196327	5523	47.5	11623	-6848	550	2.5	22432	-22432
78.50	96	298152	41.8	713937	-234032	7743	69.2	11191	-6962	9217	41.1	22432	-22432
87.50	106	371977	47.0	791423	-262669	8575	77.4	11075	-6962	11087	49.4	22432	-22432
102.0	124	484962	55.2	878094	-308632	6723	63.4	10606	-6887	11049	49.3	22432	-22432
116.6	142	565096	61.8	915087	-353413	4228	51.0	8298	-6550	10983	49.0	22432	-22432
131.1	160	606627	63.8	950587	-396375	1444	23.2	6223	-6223	10914	48.7	22432	-22432
145.7	178	606490	63.8	950587	-396375	-1477	18.3	6223	-8086	10842	48.3	22432	-22432
160.2	196	563643	59.6	945001	-396375	-4406	52.7	6223	-8354	10767	48.0	22432	-22432
174.8	214	482104	52.7	914398	-396333	-6771	80.6	6223	-8397	10688	47.6	22432	-22432
189.3	232	382030	43.9	871062	-395751	-6592	77.6	6237	-8498	10628	47.4	22432	-22432
203.9	250	286083	35.1	808296	-391958	-6201	68.1	6548	-9102	10590	47.2	22432	-22432
218.4	268	205208	29.3	700417	-362651	-4561	45.6	7012	-10005	5339	23.8	22432	-22432
233.0	286	147736	26.4	560467	-310689	-3022	29.0	7230	-10429	188	0.8	22432	-22432
247.6	304	106512	25.4	419892	-258730	-2418	24.8	7230	-9766	151	0.7	22432	-22432
262.1	322	74966	25.6	292602	-206773	-1737	20.0	7230	-8664	115	0.5	22432	-22432
276.7	340	49175	25.4	193763	-154818	-1752	26.8	6618	-6532	79	0.4	22432	-22432
291.2	358	25494	22.0	115648	-99620	-1460	36.5	4327	-3999	43	0.2	22432	-22432
307.5	378	6533	14.5	45089	-45553	-735	42.0	1901	-1749	25	0.1	22432	-22432

LOAD: BLD : BALLAST DEP.

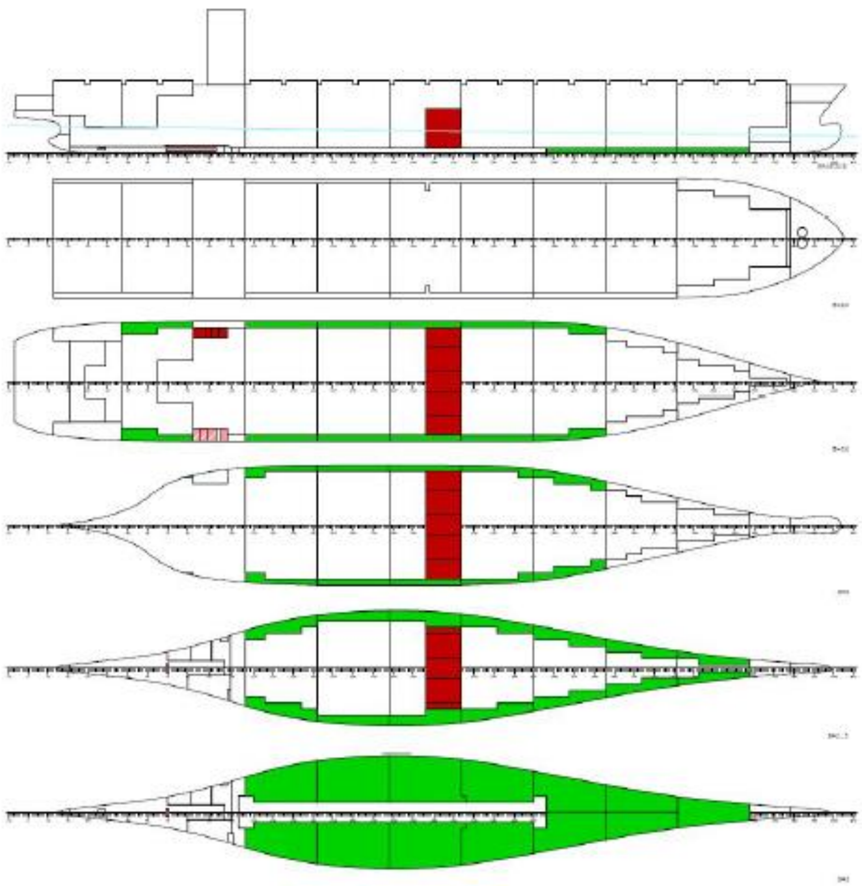

XFRAM m	#	BEND tm	REL %	BMMX tm	BMMN tm	RELSH t	SHREL %	SHMX t	SHMN t	TORS tm	REL %	TMMX tm	TMMN tm
10.40	13	15270	49.3	30997	-238	1746	43.5	4019	-528	855	3.8	22432	-22432
16.91	21	29022	48.2	60230	-490	2444	43.4	5633	-1088	812	3.6	22432	-22432
23.00	29	45397	47.6	95457	-725	2870	42.1	6813	-1613	765	3.4	22432	-22432
37.55	47	91663	44.5	206184	-1502	3277	37.9	8656	-2866	656	2.9	22432	-22432
52.10	65	140401	41.8	335725	-3008	3173	32.4	9786	-3919	550	2.5	22432	-22432
57.85	72	158071	40.7	387938	-3639	2985	30.5	9786	-4077	543	2.4	22432	-22432
66.65	83	186948	40.3	463885	-4605	3468	36.0	9646	-4077	334	1.5	22432	-22432
78.50	96	231534	41.9	552831	-5906	4291	47.2	9092	-4077	1553	6.9	22432	-22432
87.50	106	270758	44.4	610295	-6894	4575	51.0	8970	-4077	1491	6.6	22432	-22432
102.0	124	327422	49.4	662589	-8142	2944	34.6	8499	-4077	1410	6.3	22432	-22432
116.6	142	354752	53.5	662589	-8155	629	10.2	6167	-4077	1300	5.8	22432	-22432
131.1	160	346676	52.3	662589	-8155	-1760	43.2	4077	-4077	1188	5.3	22432	-22432
145.7	178	304872	46.0	662589	-8155	-4006	66.4	4077	-6038	1072	4.8	22432	-22432
160.2	196	231423	35.2	656706	-8155	-6109	96.7	4077	-6320	953	4.2	22432	-22432
174.8	214	195264	31.3	624486	-8111	1102	27.0	4077	-6365	831	3.7	22432	-22432
189.3	232	199800	34.5	578875	-7499	-472	7.3	4077	-6465	728	3.2	22432	-22432
203.9	250	184586	36.0	512809	-6664	-1571	22.6	4077	-6962	646	2.9	22432	-22432
218.4	268	158552	37.2	426647	-5809	-1899	24.6	4077	-7705	564	2.5	22432	-22432
233.0	286	133235	41.1	323839	-4975	-1527	19.0	4077	-8053	483	2.2	22432	-22432
247.6	304	106867	48.5	220372	-4144	-2088	28.4	4077	-7355	403	1.8	22432	-22432
262.1	322	75944	58.0	130890	-3315	-2159	34.9	4077	-6195	323	1.4	22432	-22432
276.7	340	46135	64.7	71356	-2488	-1897	45.2	3732	-4199	243	1.1	22432	-22432
291.2	358	22796	62.1	36697	-1950	-1327	53.2	2480	-2493	164	0.7	22432	-22432
307.5	370	5590	59.6	9370	1062	604	63.0	1072	1072	96	0.4	22432	22432

LOAD: BLD-S11.1 : BALLAST DEP.(URS11.1)

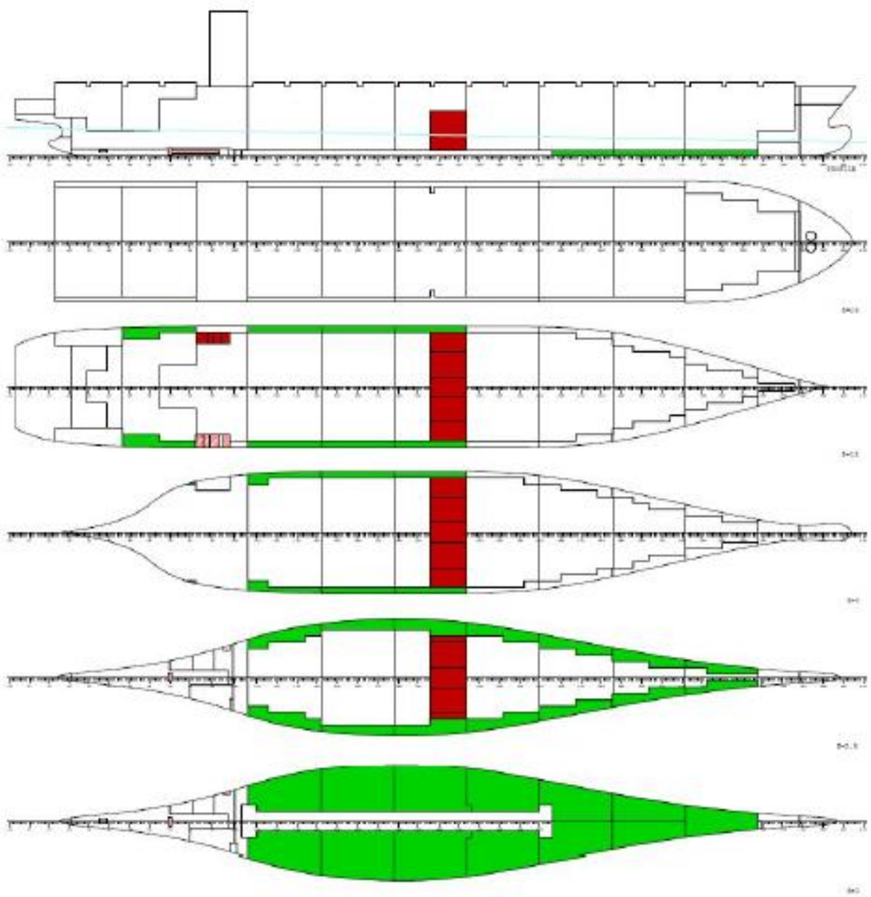

XFRAM		BEND	REL	BMMX	BMMN	RELSHREL		SHMX	SHMN	TORS	REL	TMMX	TMMN
m	#	tm	%	tm	tm	t	%	t	t	tm	%	tm	tm
10.40	13	15397	49.7	30997	-238	1746	43.4	4019	-528	855	3.8	22432	-22432
16.91	21	29199	48.5	60230	-490	2443	43.4	5633	-1088	812	3.6	22432	-22432
23.00	29	45606	47.8	95457	-725	2865	42.1	6813	-1613	765	3.4	22432	-22432
37.55	47	91715	44.5	206184	-1502	3235	37.4	8656	-2866	656	2.9	22432	-22432
52.10	65	139572	41.6	335725	-3008	3081	31.5	9786	-3919	550	2.5	22432	-22432
57.85	72	156731	40.4	387938	-3639	2884	29.5	9786	-4077	543	2.4	22432	-22432
66.65	83	184774	39.8	463885	-4605	3366	34.9	9646	-4077	334	1.5	22432	-22432
78.50	96	228402	41.3	552831	-5906	4220	46.4	9092	-4077	1554	6.9	22432	-22432
87.50	106	267266	43.8	610295	-6894	4552	50.7	8970	-4077	1491	6.6	22432	-22432
102.0	124	324550	49.0	662589	-8142	3045	35.8	8499	-4077	1410	6.3	22432	-22432
116.6	142	354718	53.5	662589	-8155	911	14.8	6167	-4077	1300	5.8	22432	-22432
131.1	160	352517	53.2	662589	-8155	-1241	30.4	4077	-4077	1188	5.3	22432	-22432
145.7	178	320438	48.4	662589	-8155	-3196	52.9	4077	-6038	1072	4.8	22432	-22432
160.2	196	261377	39.8	656706	-8155	-4950	78.3	4077	-6320	953	4.2	22432	-22432
174.8	214	245133	39.3	624486	-8111	2665	65.4	4077	-6365	831	3.7	22432	-22432
189.3	232	268029	46.3	578875	-7499	447	11.0	4077	-6465	728	3.2	22432	-22432
203.9	250	261437	51.0	512809	-6664	-1369	19.7	4077	-6962	646	2.9	22432	-22432
218.4	268	231939	54.4	426647	-5809	-2600	33.7	4077	-7705	564	2.5	22432	-22432
233.0	286	189916	58.6	323839	-4975	-3188	39.6	4077	-8053	483	2.2	22432	-22432
247.6	304	142798	64.8	220372	-4144	-3306	45.0	4077	-7355	403	1.8	22432	-22432
262.1	322	97097	74.2	130890	-3315	-3002	48.5	4077	-6195	323	1.4	22432	-22432
276.7	340	57421	80.5	71356	-2488	-2441	58.1	3732	-4199	243	1.1	22432	-22432
291.2	358	27955	76.2	36697	-1950	-1655	66.4	2480	-2493	164	0.7	22432	-22432
307.5	378	6955	74.2	9378	-1862	-848	79.1	1072	-1072	96	0.4	22432	-22432

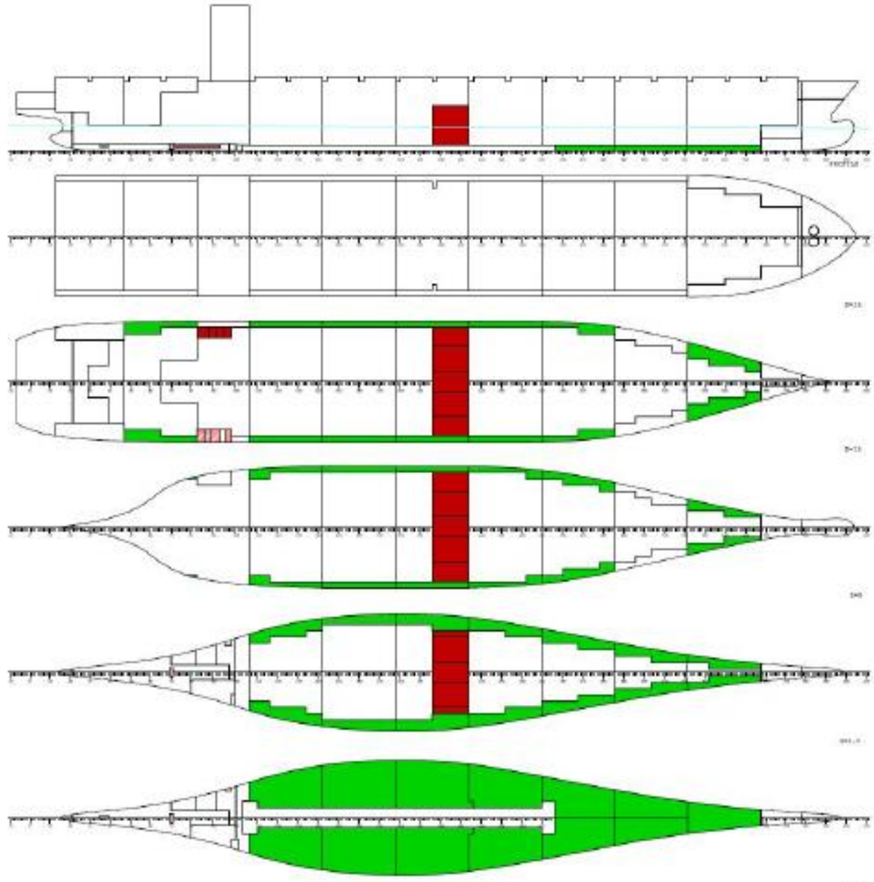

XFRAM		BEND	REL	BMMX	BMMN	RELSHREL		SHMX	SHMN	TORS	REL	TMMX	TMMN
m	#	tm	%	tm	tm	t	%	t	t	tm	%	tm	tm
10.40	13	15060	48.6	30997	-238	1747	43.5	4019	-528	855	3.8	22432	-22432
16.91	21	28729	47.7	60230	-490	2447	43.4	5633	-1088	812	3.6	22432	-22432
23.00	29	45069	47.2	95457	-725	2885	42.4	6813	-1613	765	3.4	22432	-22432
37.55	47	91987	44.6	206184	-1502	3409	39.4	8656	-2866	656	2.9	22432	-22432
52.10	65	144480	43.0	335725	-3008	3596	36.7	9786	-3919	550	2.5	22432	-22432
57.85	72	164850	42.5	387938	-3639	3528	36.0	9786	-4077	543	2.4	22432	-22432
66.65	83	199128	42.9	463885	-4605	4178	43.3	9646	-4077	334	1.5	22432	-22432
78.50	96	253137	45.8	552831	-5906	5191	57.1	9092	-4077	1553	6.9	22432	-22432
87.50	106	300856	49.3	610295	-6894	5585	62.3	8970	-4077	1491	6.6	22432	-22432
102.0	124	372945	56.3	662589	-8142	4067	47.9	8499	-4077	1410	6.3	22432	-22432
116.6	142	416720	62.9	662589	-8155	1780	28.9	6167	-4077	1300	5.8	22432	-22432
131.1	160	424859	64.1	662589	-8155	-668	16.4	4077	-4077	1188	5.3	22432	-22432
145.7	178	397785	60.0	662589	-8155	-3060	50.7	4077	-6038	1072	4.8	22432	-22432
160.2	196	336325	51.2	656706	-8155	-5394	85.3	4077	-6320	953	4.2	22432	-22432
174.8	214	308077	49.3	624486	-8111	1500	36.8	4077	-6365	831	3.7	22432	-22432
189.3	232	315373	54.5	578875	-7499	-477	7.4	4077	-6465	728	3.2	22432	-22432
203.9	250	296504	57.8	512809	-6664	-2051	29.5	4077	-6962	646	2.9	22432	-22432
218.4	268	259494	60.8	426647	-5809	-2905	37.7	4077	-7705	564	2.5	22432	-22432
233.0	286	215448	66.5	323839	-4975	-3067	38.1	4077	-8053	483	2.2	22432	-22432
247.6	304	162735	73.8	220372	-4144	-4135	56.2	4077	-7355	403	1.8	22432	-22432
262.1	322	98496	75.3	130890	-3315	-4653	75.1	4077	-6195	323	1.4	22432	-22432
276.7	340	43041	60.3	71356	-2488	-2916	69.4	3732	-4199	243	1.1	22432	-22432
291.2	358	16258	44.3	36697	-1950	-920	36.9	2480	-2493	164	0.7	22432	-22432
307.5	378	3767	40.2	9378	-1862	-473	44.1	1072	-1072	96	0.4	22432	-22432

LOAD: BLM-PANAMA : BALLAST AFT. MID.-PANAMA

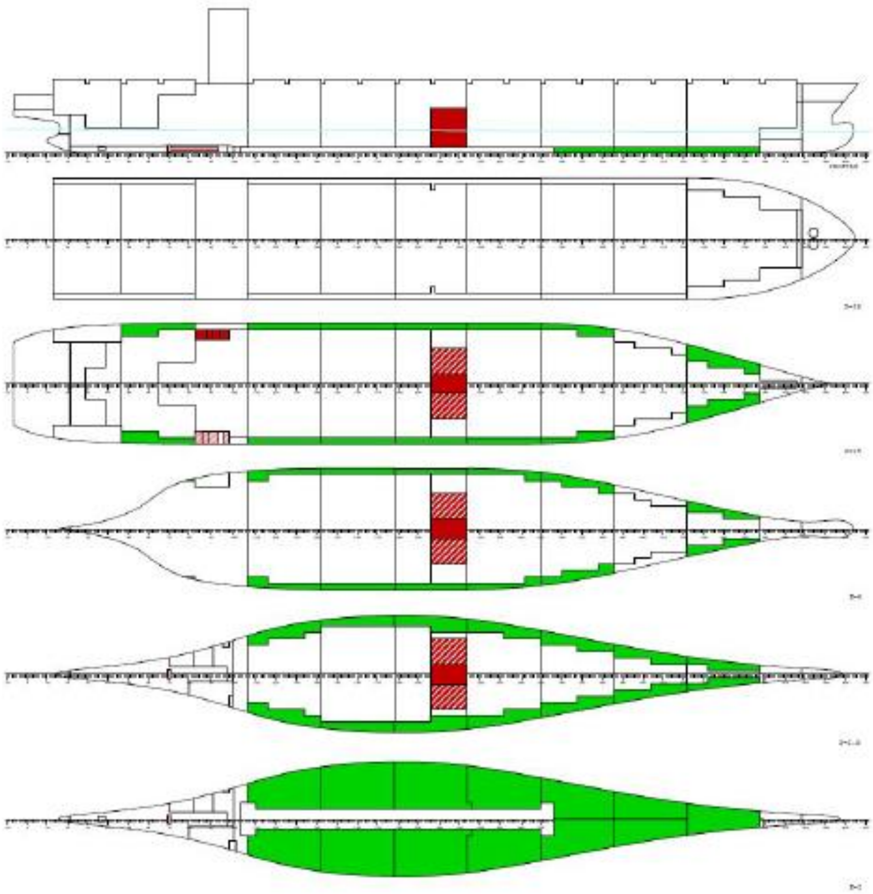

XFRAM		BEND	REL	BMMX	BMMN	RELSHREL		SHMX	SHMN	TORS	REL	TMMX	TMMN
m	#	tm	%	tm	tm	t	%	t	t	tm	%	tm	tm
10.40	13	15068	48.6	30997	-238	1747	43.5	4019	-528	610	2.7	22432	-22432
16.91	21	28743	47.7	60230	-490	2449	43.5	5633	-1088	466	2.1	22432	-22432
23.00	29	45112	47.3	95457	-725	2894	42.5	6813	-1613	326	1.5	22432	-22432
37.55	47	92493	44.9	206184	-1502	3479	40.2	8656	-2866	-8	0.0	22432	-22432
52.10	65	147372	43.9	335725	-3008	3878	39.6	9786	-3919	-337	1.5	22432	-22432
57.85	72	169687	43.7	387938	-3639	3922	40.1	9786	-4077	-433	1.9	22432	-22432
66.65	83	208239	44.9	463885	-4605	4758	49.3	9646	-4077	-778	3.5	22432	-22432
78.50	96	269401	48.7	552831	-5906	5836	64.2	9092	-4077	4472	19.9	22432	-22432
87.50	106	322479	52.8	610295	-6894	6002	66.9	8970	-4077	5250	23.4	22432	-22432
102.0	124	403151	60.8	662589	-8142	4831	56.8	8499	-4077	4944	22.0	22432	-22432
116.6	142	460611	69.5	662589	-8155	2897	47.0	6167	-4077	4611	20.6	22432	-22432
131.1	160	487599	73.6	662589	-8155	806	19.8	4077	-4077	4274	19.1	22432	-22432
145.7	178	484580	73.1	662589	-8155	-1227	20.3	4077	-6038	3934	17.5	22432	-22432
160.2	196	452419	68.9	656706	-8155	-3200	50.6	4077	-6320	3591	16.0	22432	-22432
174.8	214	423884	67.9	624486	-8111	-732	11.5	4077	-6365	3245	14.5	22432	-22432
189.3	232	401369	69.3	578875	-7499	-2343	36.2	4077	-6465	2918	13.0	22432	-22432
203.9	250	357977	69.8	512809	-6664	-3558	51.1	4077	-6962	2611	11.6	22432	-22432
218.4	268	301555	70.7	426647	-5809	-4071	52.8	4077	-7705	2306	10.3	22432	-22432
233.0	286	242809	75.0	323839	-4975	-3929	48.8	4077	-8053	2001	8.9	22432	-22432
247.6	304	179505	81.5	220372	-4144	-4738	64.4	4077	-7355	1696	7.6	22432	-22432
262.1	322	108065	82.6	130890	-3315	-5049	81.5	4077	-6195	1392	6.2	22432	-22432
276.7	340	48038	67.3	71356	-2488	-3157	75.2	3732	-4199	1088	4.8	22432	-22432
291.2	358	18562	50.6	36697	-1950	-1057	42.4	2480	-2493	785	3.5	22432	-22432
307.5	378	4454	47.5	9378	-1862	-541	50.4	1072	-1072	465	2.1	22432	-22432

LOAD: BLA-PANAMA : BALLAST ARR.-PANAMA

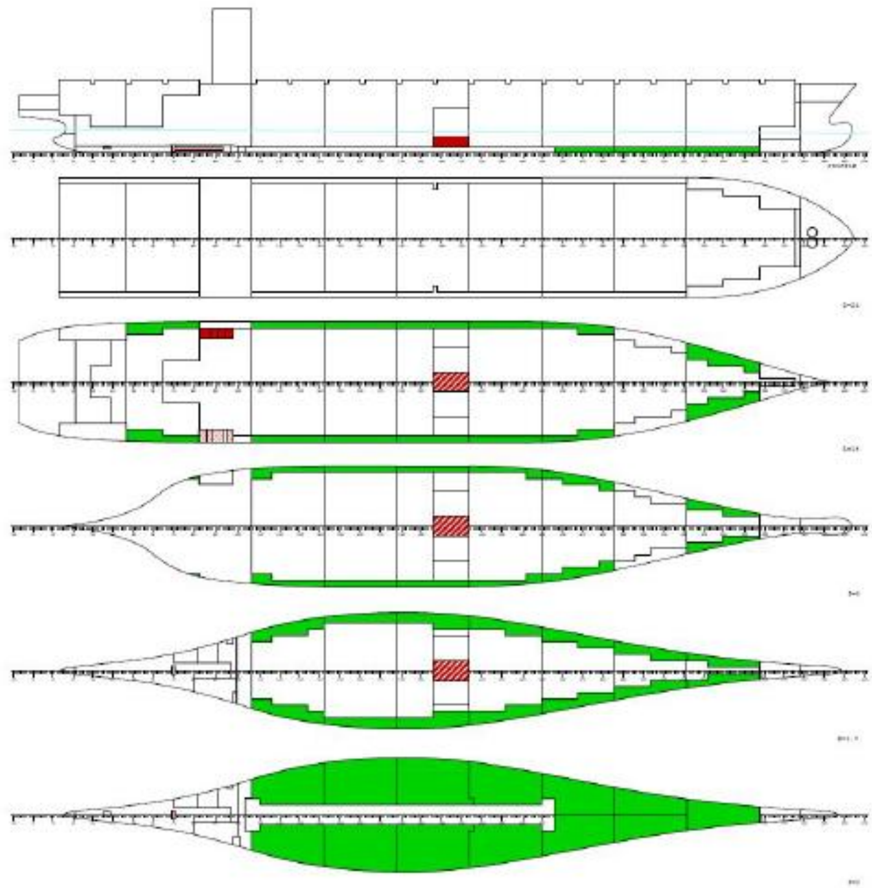

XFRAM		BEND	REL	BMMX	BMMN	RELSHREL		SHMX	SHMN	TORS	REL	TMMX	TMMN
m	#	tm	%	tm	tm	t	%	t	t	tm	%	tm	tm
10.40	13	15076	48.6	30997	-238	1748	43.5	4019	-528	415	1.9	22432	-22432
16.91	21	28755	47.7	60230	-490	2450	43.5	5633	-1088	192	0.9	22432	-22432
23.00	29	45146	47.3	95457	-725	2900	42.6	6813	-1613	-23	0.1	22432	-22432
37.55	47	92888	45.1	206184	-1502	3532	40.8	8656	-2866	-535	2.4	22432	-22432
52.10	65	149499	44.5	335725	-3008	4085	41.7	9786	-3919	-1043	4.6	22432	-22432
57.85	72	173262	44.7	387938	-3639	4219	43.1	9786	-4077	-1208	5.4	22432	-22432
66.65	83	215085	46.4	463885	-4605	5206	54.0	9646	-4077	-1661	7.4	22432	-22432
78.50	96	281816	51.0	552831	-5906	6345	69.8	9092	-4077	6644	29.6	22432	-22432
87.50	106	339256	55.6	610295	-6894	6313	70.4	8970	-4077	8237	36.7	22432	-22432
102.0	124	426546	64.4	662589	-8142	5430	63.9	8499	-4077	7753	34.6	22432	-22432
116.6	142	494858	74.7	662589	-8155	3789	61.4	6167	-4077	7242	32.3	22432	-22432
131.1	160	536982	81.0	662589	-8155	1993	48.9	4077	-4077	6727	30.0	22432	-22432
145.7	178	553402	83.5	662589	-8155	257	6.3	4077	-6038	6209	27.7	22432	-22432
160.2	196	545005	83.0	656706	-8155	-1418	22.4	4077	-6320	5688	25.4	22432	-22432
174.8	214	516369	82.7	624486	-8111	-2526	39.7	4077	-6365	5164	23.0	22432	-22432
189.3	232	469941	81.2	578875	-7499	-3838	59.4	4077	-6465	4658	20.8	22432	-22432
203.9	250	406950	79.4	512809	-6664	-4760	68.4	4077	-6962	4174	18.6	22432	-22432
218.4	268	335064	78.5	426647	-5809	-4999	64.9	4077	-7705	3690	16.4	22432	-22432
233.0	286	264632	81.7	323839	-4975	-4613	57.3	4077	-8053	3207	14.3	22432	-22432
247.6	304	192915	87.5	220372	-4144	-5217	70.9	4077	-7355	2724	12.1	22432	-22432
262.1	322	115749	88.4	130890	-3315	-5365	86.6	4077	-6195	2241	10.0	22432	-22432
276.7	340	52070	73.0	71356	-2488	-3351	79.8	3732	-4199	1759	7.8	22432	-22432
291.2	358	20426	55.7	36697	-1950	-1168	46.8	2480	-2493	1278	5.7	22432	-22432
307.5	378	5004	53.4	9378	-1862	-596	55.6	1072	-1072	758	3.4	22432	-22432

LOAD: 16TDD : 16T/TEU DEP. AT DESIGN DRAFT

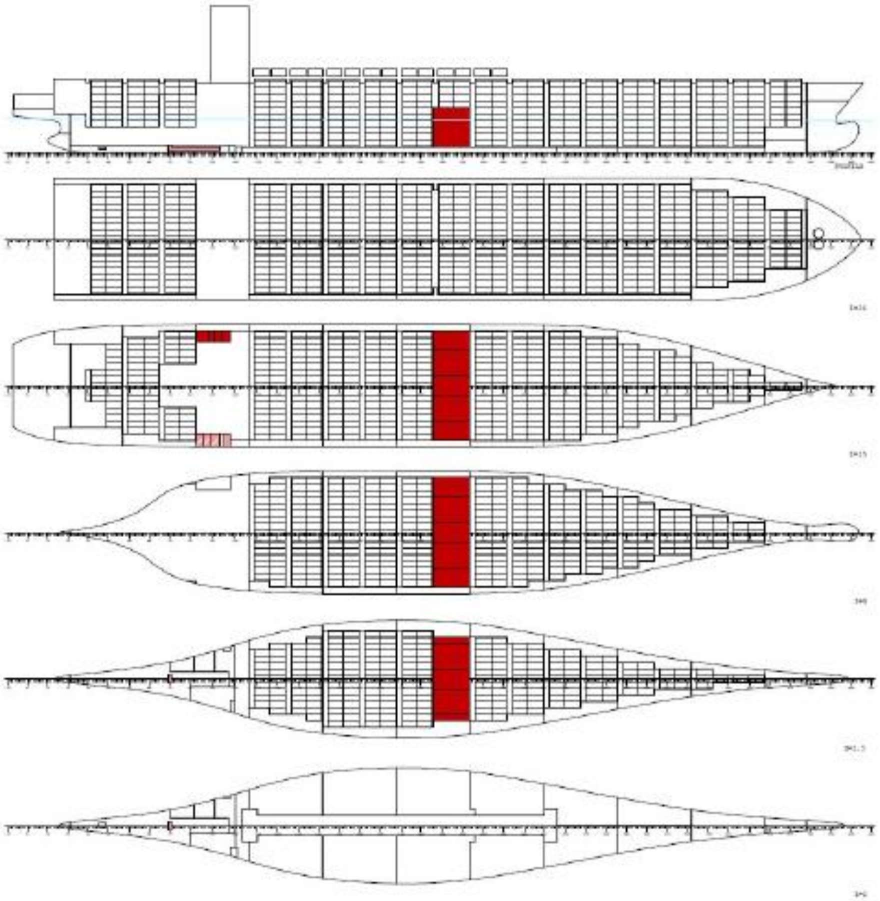

XFRAM		BEND	REL	BMMX	BMMN	RELSHREL		SHMX	SHMN	TORS	REL	TMMX	TMMN
m	#	tm	%	tm	tm	t	%	t	t	tm	%	tm	tm
10.40	13	15023	48.5	30997	-238	1730	43.0	4019	-528	886	4.0	22432	-22432
16.91	21	28266	46.9	60230	-490	2306	40.9	5633	-1088	857	3.8	22432	-22432
23.00	29	42977	45.0	95457	-725	2460	36.1	6813	-1613	822	3.7	22432	-22432
37.55	47	93406	45.3	206184	-1502	4622	53.4	8656	-2866	742	3.3	22432	-22432
52.10	65	164204	48.9	335725	-3008	5282	54.0	9786	-3919	665	3.0	22432	-22432
57.85	72	192176	49.5	387938	-3639	4762	48.7	9786	-4077	670	3.0	22432	-22432
66.65	83	236881	51.1	463885	-4605	5253	54.5	9646	-4077	478	2.1	22432	-22432
78.50	96	291713	52.8	552831	-5906	4244	46.7	9092	-4077	1720	7.7	22432	-22432
87.50	106	323888	53.1	610295	-6894	3073	34.3	8970	-4077	1677	7.5	22432	-22432
102.0	124	359008	54.2	662589	-8142	2290	26.9	8499	-4077	1625	7.2	22432	-22432
116.6	142	377799	57.0	662589	-8155	1005	16.3	6167	-4077	1544	6.9	22432	-22432
131.1	160	376631	56.8	662589	-8155	-432	10.6	4077	-4077	1461	6.5	22432	-22432
145.7	178	353542	53.4	662589	-8155	-1984	32.9	4077	-6038	1374	6.1	22432	-22432
160.2	196	307820	46.9	656706	-8155	-3522	55.7	4077	-6320	1284	5.7	22432	-22432
174.8	214	286722	45.9	624486	-8111	993	24.4	4077	-6365	1192	5.3	22432	-22432
189.3	232	286627	49.5	578875	-7499	-237	3.7	4077	-6465	465	2.1	22432	-22432
203.9	250	266866	52.0	512809	-6664	-1751	25.1	4077	-6962	391	1.7	22432	-22432
218.4	268	228118	53.5	426647	-5809	-2836	36.8	4077	-7705	338	1.5	22432	-22432
233.0	286	178083	55.0	323839	-4975	-3341	41.5	4077	-8053	286	1.3	22432	-22432
247.6	304	124919	56.7	220372	-4144	-3319	45.1	4077	-7355	235	1.0	22432	-22432
262.1	322	76009	58.1	130890	-3315	-2826	45.6	4077	-6195	184	0.8	22432	-22432
276.7	340	37559	52.6	71356	-2488	-2034	48.4	3732	-4199	133	0.6	22432	-22432
291.2	358	12506	34.1	36697	-1950	-1081	43.4	2480	-2493	83	0.4	22432	-22432
307.5	378	778	8.3	9378	-1862	-177	16.5	1072	-1072	48	0.2	22432	-22432

LOAD: 16TAD : 16T/TEU ARR. AT DESIGN DRAFT

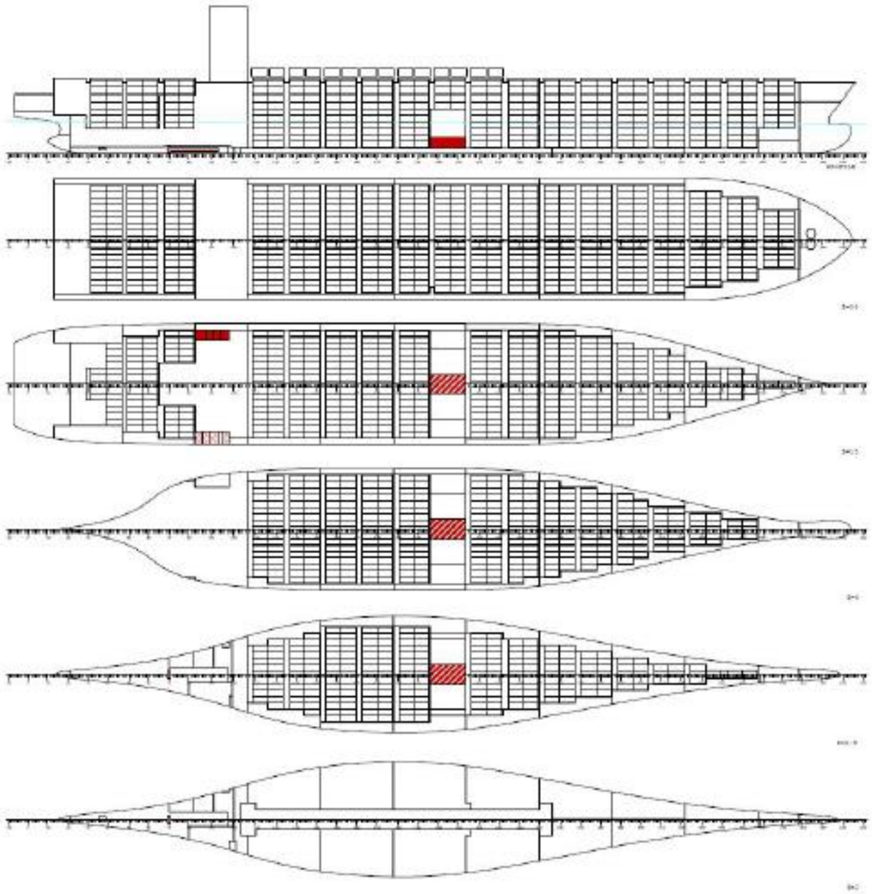

XFRAM		BEND	REL	BMMX	BMMN	RELSHREL		SHMX	SHMN	TORS	REL	TMMX	TMMN
m	#	tm	%	tm	tm	t	%	t	t	tm	%	tm	tm
10.40	13	15147	48.9	30997	-238	1745	43.4	4019	-528	447	2.0	22432	-22432
16.91	21	28797	47.8	60230	-490	2413	42.8	5633	-1088	237	1.1	22432	-22432
23.00	29	44567	46.7	95457	-725	2692	39.5	6813	-1613	34	0.2	22432	-22432
37.55	47	101008	49.0	206184	-1502	5216	60.3	8656	-2866	-449	2.0	22432	-22432
52.10	65	183507	54.7	335725	-3008	6290	64.3	9786	-3919	-928	4.1	22432	-22432
57.85	72	217813	56.1	387938	-3639	5944	60.7	9786	-4077	-1082	4.8	22432	-22432
66.65	83	274158	59.1	463885	-4605	6708	69.5	9646	-4077	-1517	6.8	22432	-22432
78.50	96	346265	62.6	552831	-5906	5725	63.0	9092	-4077	6811	30.4	22432	-22432
87.50	106	390803	64.0	610295	-6894	4049	45.1	8970	-4077	8423	37.6	22432	-22432
102.0	124	443864	67.0	662589	-8142	3771	44.4	8499	-4077	7968	35.5	22432	-22432
116.6	142	488104	73.7	662589	-8155	3013	48.9	6167	-4077	7486	33.4	22432	-22432
131.1	160	520186	78.5	662589	-8155	2122	52.1	4077	-4077	7000	31.2	22432	-22432
145.7	178	538447	81.3	662589	-8155	1136	27.9	4077	-6038	6511	29.0	22432	-22432
160.2	196	542471	82.6	656706	-8155	186	4.6	4077	-6320	6019	26.8	22432	-22432
174.8	214	516752	82.7	624486	-8111	-3357	52.7	4077	-6365	5524	24.6	22432	-22432
189.3	232	457997	79.1	578875	-7499	-3959	61.2	4077	-6465	4395	19.6	22432	-22432
203.9	250	388843	75.8	512809	-6664	-4829	69.4	4077	-6962	3919	17.5	22432	-22432
218.4	268	310114	72.7	426647	-5809	-5268	68.4	4077	-7705	3464	15.4	22432	-22432
233.0	286	229333	70.8	323839	-4975	-5155	64.0	4077	-8053	3010	13.4	22432	-22432
247.6	304	154014	69.9	220372	-4144	-4576	62.2	4077	-7355	2556	11.4	22432	-22432
262.1	322	90416	69.1	130890	-3315	-3617	58.4	4077	-6195	2103	9.4	22432	-22432
276.7	340	43307	60.7	71356	-2488	-2464	58.7	3732	-4199	1650	7.4	22432	-22432
291.2	358	14040	38.3	36697	-1950	-1262	50.6	2480	-2493	1197	5.3	22432	-22432
307.5	378	844	9.0	9378	-1862	-211	19.7	1072	-1072	711	3.2	22432	-22432

LOAD: 11TDS :   11T/TEU DEP. AT SCANTLING DRAFT

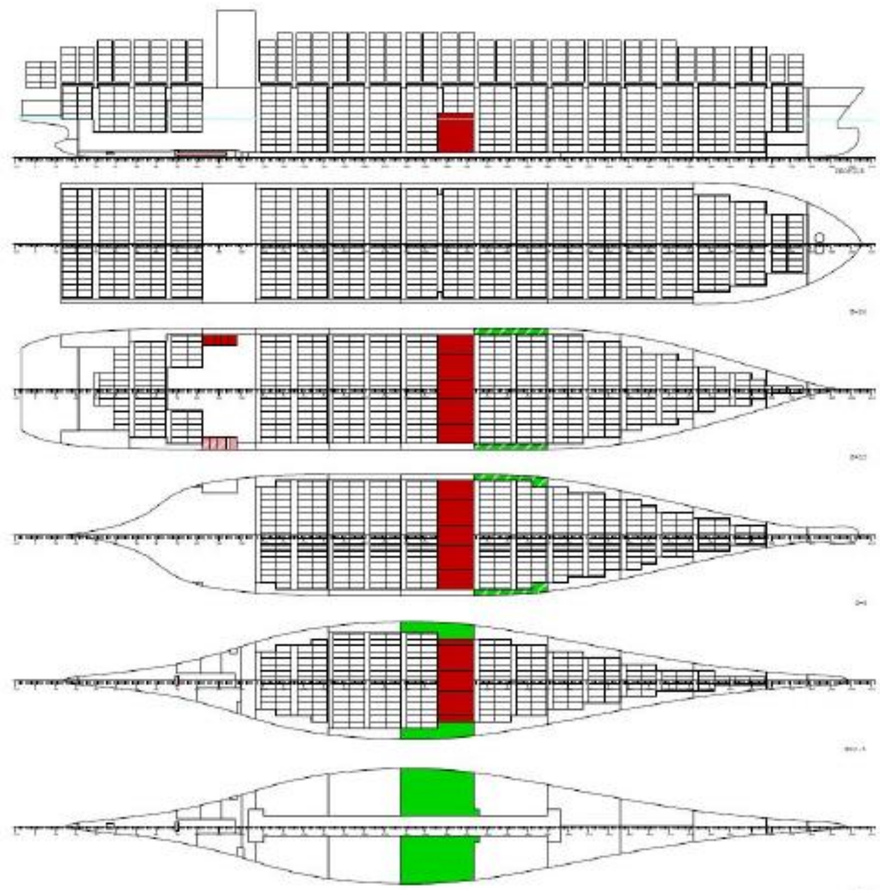

XFRAM		BEND	REL	BMMX	BMMN	RELSHREL		SHMX	SHMN	TORS	REL	TMMX	TMMN
m	#	tm	%	tm	tm	t	%	t	t	tm	%	tm	tm
10.40	13	22056	71.2	30997	-238	2448	60.9	4019	-528	965	4.3	22432	-22432
16.91	21	44794	74.4	60230	-490	4402	78.2	5633	-1088	967	4.3	22432	-22432
23.00	29	76333	80.0	95457	-725	5883	86.3	6813	-1613	962	4.3	22432	-22432
37.55	47	176614	85.7	206184	-1502	8140	94.0	8656	-2866	954	4.3	22432	-22432
52.10	65	297518	88.6	335725	-3008	8738	89.3	9786	-3919	949	4.2	22432	-22432
57.85	72	345123	89.0	387938	-3639	8240	84.2	9786	-4077	982	4.4	22432	-22432
66.65	83	420689	90.7	463885	-4605	8869	91.9	9646	-4077	834	3.7	22432	-22432
78.50	96	511468	92.5	552831	-5906	6643	73.1	9092	-4077	2134	9.5	22432	-22432
87.50	106	560976	91.9	610295	-6894	4513	50.3	8970	-4077	2136	9.5	22432	-22432
102.0	124	608199	91.8	662589	-8142	2562	30.1	8499	-4077	3341	14.9	22432	-22432
116.6	142	623980	94.2	662589	-8155	337	5.5	6167	-4077	4325	19.3	22432	-22432
131.1	160	606339	91.5	662589	-8155	-2029	49.8	4077	-4077	4313	19.2	22432	-22432
145.7	178	553223	83.5	662589	-8155	-4516	74.8	4077	-6038	4298	19.2	22432	-22432
160.2	196	474618	72.3	656706	-8155	-5518	87.3	4077	-6320	4280	19.1	22432	-22432
174.8	214	434585	69.6	624486	-8111	492	12.1	4077	-6365	4259	19.0	22432	-22432
189.3	232	424146	73.3	578875	-7499	-1166	18.0	4077	-6465	1998	8.9	22432	-22432
203.9	250	392095	76.5	512809	-6664	-2410	34.6	4077	-6962	-238	1.1	22432	-22432
218.4	268	339115	79.5	426647	-5809	-4076	52.9	4077	-7705	-219	1.0	22432	-22432
233.0	286	267468	82.6	323839	-4975	-4982	61.9	4077	-8053	-199	0.9	22432	-22432
247.6	304	188881	85.7	220372	-4144	-5049	68.6	4077	-7355	-179	0.8	22432	-22432
262.1	322	115413	88.2	130890	-3315	-4438	71.6	4077	-6195	-158	0.7	22432	-22432
276.7	340	55156	77.3	71356	-2488	-3260	77.6	3732	-4199	-137	0.6	22432	-22432
291.2	358	16036	43.7	36697	-1950	-1631	65.4	2480	-2493	-115	0.5	22432	-22432
307.5	378	366	3.9	9378	-1862	-113	10.5	1072	-1072	-70	0.3	22432	-22432

LOAD: 11TAS :   11T/TEU ARR. AT SCANTLING DRAFT

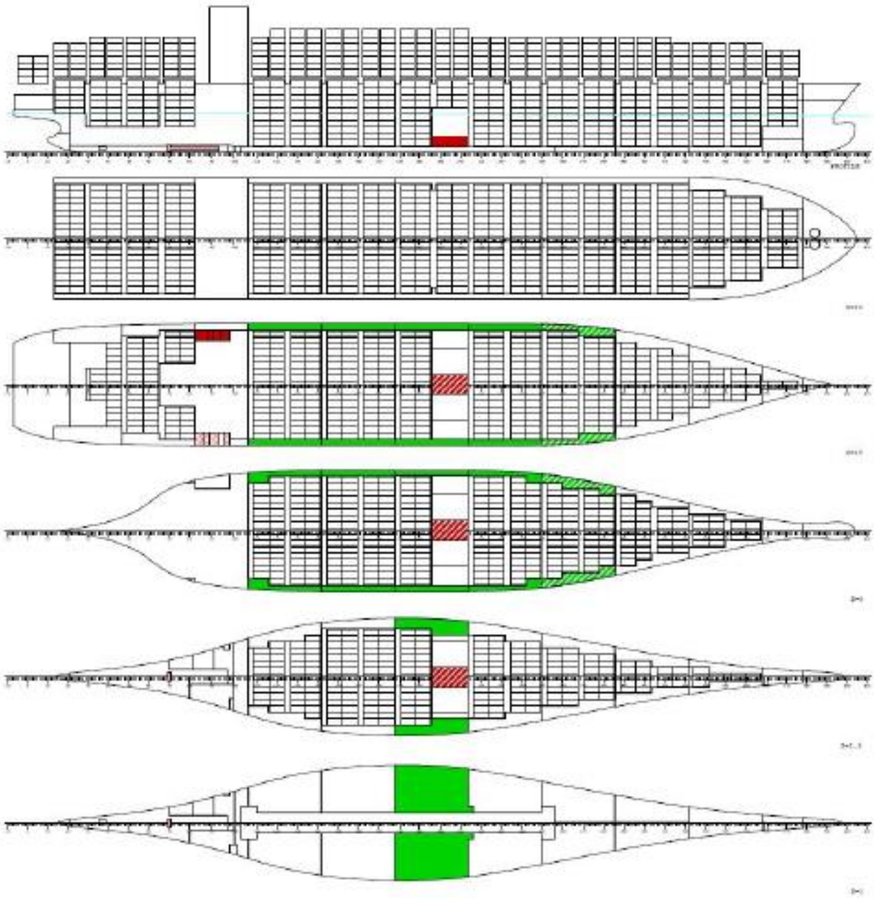

XFRAM		BEND	REL	BMMX	BMMN	RELSHREL		SHMX	SHMN	TORS	REL	TMMX	TMMN
m	#	tm	%	tm	tm	t	%	t	t	tm	%	tm	tm
10.40	13	21836	70.4	30997	-238	2405	59.8	4019	-528	856	3.8	22432	-22432
16.91	21	44303	73.6	60230	-490	4345	77.1	5633	-1088	813	3.6	22432	-22432
23.00	29	75511	79.1	95457	-725	5815	85.4	6813	-1613	767	3.4	22432	-22432
37.55	47	174785	84.8	206184	-1502	8055	93.1	8656	-2866	659	2.9	22432	-22432
52.10	65	294538	87.7	335725	-3008	8650	88.4	9786	-3919	554	2.5	22432	-22432
57.85	72	341693	88.1	387938	-3639	8155	83.3	9786	-4077	548	2.4	22432	-22432
66.65	83	416620	89.8	463885	-4605	8793	91.2	9646	-4077	339	1.5	22432	-22432
78.50	96	504405	91.2	552831	-5906	6229	68.5	9092	-4077	8972	40.0	22432	-22432
87.50	106	547978	89.8	610295	-6894	3313	36.9	8970	-4077	10815	48.2	22432	-22432
102.0	124	588181	88.8	662589	-8142	2716	32.0	8499	-4077	11922	53.1	22432	-22432
116.6	142	614239	92.7	662589	-8155	1478	24.0	6167	-4077	12805	57.1	22432	-22432
131.1	160	621530	93.8	662589	-8155	247	6.1	4077	-4077	12694	56.6	22432	-22432
145.7	178	610066	92.1	662589	-8155	-1080	17.9	4077	-6038	12579	56.1	22432	-22432
160.2	196	590116	89.9	656706	-8155	-906	14.3	4077	-6320	12461	55.6	22432	-22432
174.8	214	562867	90.1	624486	-8111	-2378	37.4	4077	-6365	12341	55.0	22432	-22432
189.3	232	513544	88.7	578875	-7499	-3655	56.5	4077	-6465	12238	54.6	22432	-22432
203.9	250	448269	87.4	512809	-6664	-4502	64.7	4077	-6962	12157	54.2	22432	-22432
218.4	268	370408	86.8	426647	-5809	-5401	70.1	4077	-7705	5747	25.6	22432	-22432
233.0	286	284754	87.9	323839	-4975	-5576	69.2	4077	-8053	476	2.1	22432	-22432
247.6	304	198834	90.2	220372	-4144	-5481	74.5	4077	-7355	397	1.8	22432	-22432
262.1	322	120301	91.9	130890	-3315	-4722	76.2	4077	-6195	317	1.4	22432	-22432
276.7	340	56963	79.8	71356	-2488	-3421	81.5	3732	-4199	239	1.1	22432	-22432
291.2	358	16335	44.5	36697	-1950	-1700	68.2	2480	-2493	161	0.7	22432	-22432
307.5	378	212	2.3	9378	-1862	-124	11.6	1072	-1072	95	0.4	22432	-22432

LOAD: 16TDS : 16T/TEU DEP. AT SCANTLING DRAFT

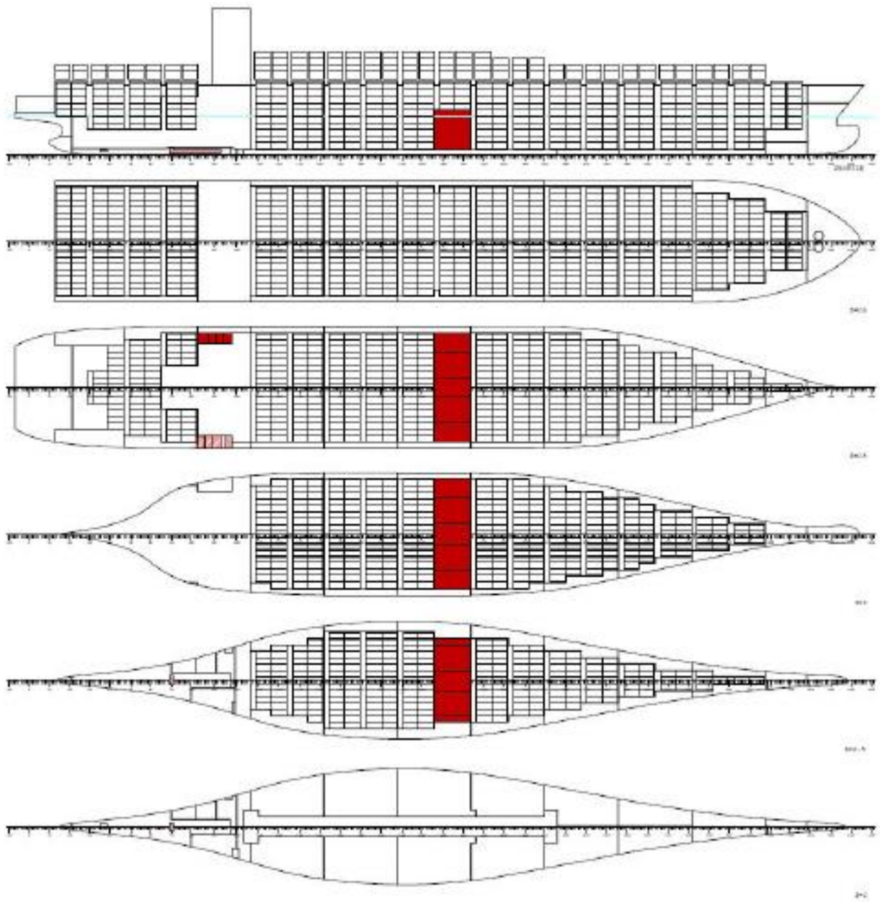

XFRAM		BEND	REL	BMMX	BMMN	RELSHREL		SHMX	SHMN	TORS	REL	TMMX	TMMN
m	#	tm	%	tm	tm	t	%	t	t	tm	%	tm	tm
10.40	13	8886	28.7	30997	-238	821	20.4	4019	-528	911	4.1	22432	-22432
16.91	21	20881	34.7	60230	-490	2785	49.4	5633	-1088	891	4.0	22432	-22432
23.00	29	42604	44.6	95457	-725	4252	62.4	6813	-1613	866	3.9	22432	-22432
37.55	47	116751	56.6	206184	-1502	6196	71.6	8656	-2866	807	3.6	22432	-22432
52.10	65	207645	61.8	335725	-3008	6582	67.3	9786	-3919	753	3.4	22432	-22432
57.85	72	242309	62.5	387938	-3639	5885	60.1	9786	-4077	767	3.4	22432	-22432
66.65	83	296204	63.9	463885	-4605	6250	64.8	9646	-4077	588	2.6	22432	-22432
78.50	96	355714	64.3	552831	-5906	4009	44.1	9092	-4077	1849	8.2	22432	-22432
87.50	106	381516	62.5	610295	-6894	1884	21.0	8970	-4077	1819	8.1	22432	-22432
102.0	124	399611	60.3	662589	-8142	1346	15.8	8499	-4077	1789	8.0	22432	-22432
116.6	142	405310	61.2	662589	-8155	328	5.3	6167	-4077	1731	7.7	22432	-22432
131.1	160	394870	59.6	662589	-8155	-850	20.9	4077	-4077	1669	7.4	22432	-22432
145.7	178	366217	55.3	662589	-8155	-2152	35.6	4077	-6038	1605	7.2	22432	-22432
160.2	196	318526	48.5	656706	-8155	-3447	54.5	4077	-6320	1538	6.9	22432	-22432
174.8	214	298932	47.9	624486	-8111	1304	32.0	4077	-6365	1467	6.5	22432	-22432
189.3	232	302943	52.3	578875	-7499	38	0.9	4077	-6465	1415	6.3	22432	-22432
203.9	250	286688	55.9	512809	-6664	-1493	21.4	4077	-6962	233	1.0	22432	-22432
218.4	268	248170	58.2	426647	-5809	-2938	38.1	4077	-7705	166	0.7	22432	-22432
233.0	286	193597	59.8	323839	-4975	-3726	46.3	4077	-8053	136	0.6	22432	-22432
247.6	304	132788	60.3	220372	-4144	-3836	52.2	4077	-7355	107	0.5	22432	-22432
262.1	322	75845	57.9	130890	-3315	-3255	52.5	4077	-6195	78	0.3	22432	-22432
276.7	340	32466	45.5	71356	-2488	-2120	50.5	3732	-4199	49	0.2	22432	-22432
291.2	358	8618	23.5	36697	-1950	-681	27.3	2480	-2493	22	0.1	22432	-22432
307.5	378	429	4.6	9378	-1862	-112	10.4	1072	-1072	12	0.1	22432	-22432

LOAD: 16TAS : 16T/TEU ARR. AT SCANTLING DRAFT

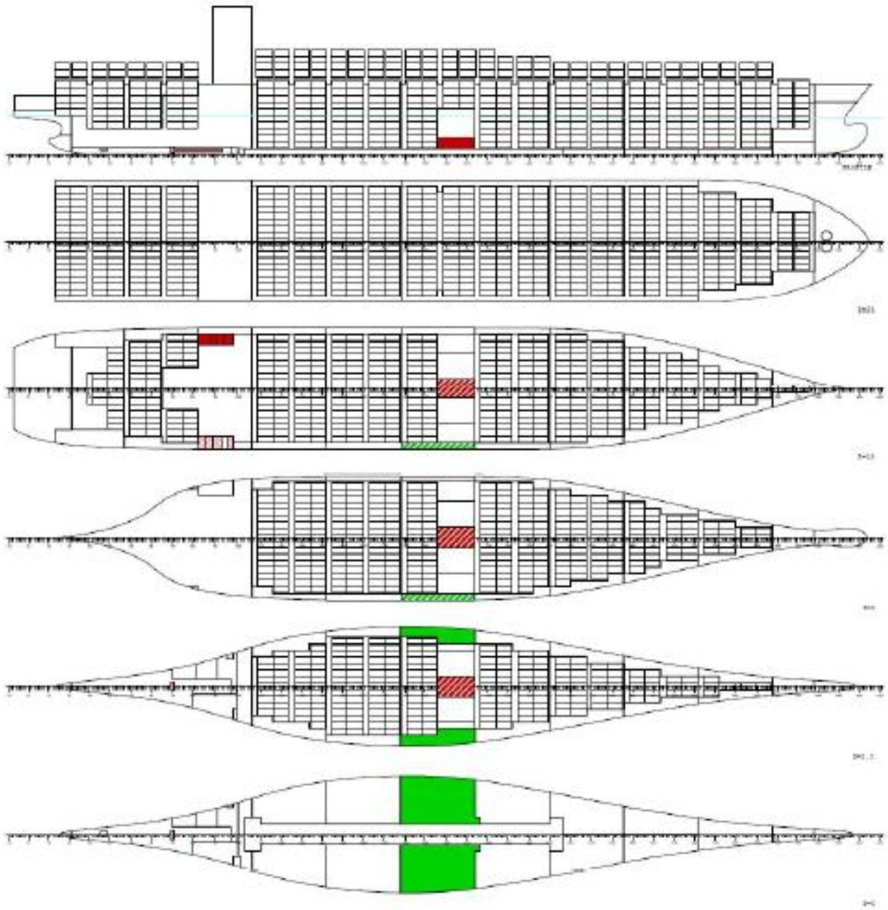

XFRAM m	#	BEND tm	REL %	BMMX tm	BMMN tm	RELSH t	REL %	SHMX t	SHMN t	TORS tm	REL %	TMMX tm	TMMN tm
10.40	13	10471	33.8	30997	-238	1015	25.3	4019	-528	933	4.2	22432	-22432
16.91	21	24070	40.0	60230	-490	3071	54.5	5633	-1088	922	4.1	22432	-22432
23.00	29	47845	50.1	95457	-725	4627	67.9	6813	-1613	905	4.0	22432	-22432
37.55	47	129212	62.7	206184	-1502	6802	78.6	8656	-2866	867	3.9	22432	-22432
52.10	65	230812	68.8	335725	-3008	7437	76.0	9786	-3919	833	3.7	22432	-22432
57.85	72	270730	69.8	387938	-3639	6843	69.9	9786	-4077	855	3.8	22432	-22432
66.65	83	333818	72.0	463885	-4605	7370	76.4	9646	-4077	689	3.1	22432	-22432
78.50	96	405720	73.4	552831	-5906	5000	55.0	9092	-4077	9379	41.8	22432	-22432
87.50	106	438915	71.9	610295	-6894	2245	25.0	8970	-4077	11266	50.2	22432	-22432
102.0	124	464538	70.1	662589	-8142	2009	23.6	8499	-4077	11256	50.2	22432	-22432
116.6	142	482256	72.8	662589	-8155	1307	21.2	6167	-4077	11219	50.0	22432	-22432
131.1	160	488538	73.7	662589	-8155	459	11.3	4077	-4077	11178	49.8	22432	-22432
145.7	178	481522	72.7	662589	-8155	-498	8.2	4077	-6038	11134	49.6	22432	-22432
160.2	196	472955	72.0	656706	-8155	260	6.4	4077	-6320	6135	27.3	22432	-22432
174.8	214	459274	73.5	624486	-8111	-1629	25.6	4077	-6365	1248	5.6	22432	-22432
189.3	232	423815	73.2	578875	-7499	-2484	38.4	4077	-6465	1216	5.4	22432	-22432
203.9	250	373872	72.9	512809	-6664	-3613	51.9	4077	-6962	55	0.2	22432	-22432
218.4	268	307598	72.1	426647	-5809	-4647	60.3	4077	-7705	8	0.0	22432	-22432
233.0	286	231231	71.4	323839	-4975	-5029	62.4	4077	-8053	-2	0.0	22432	-22432
247.6	304	154363	70.0	220372	-4144	-4760	64.7	4077	-7355	-11	0.0	22432	-22432
262.1	322	86548	66.1	130890	-3315	-3848	62.1	4077	-6195	-19	0.1	22432	-22432
276.7	340	36649	51.4	71356	-2488	-2448	58.3	3732	-4199	-27	0.1	22432	-22432
291.2	358	9609	26.2	36697	-1950	-818	32.8	2480	-2493	-35	0.2	22432	-22432
307.5	378	371	4.0	9378	-1862	-134	12.5	1072	-1072	-22	0.1	22432	-22432

LOAD: MAX : HOMOGENEOUS 14T TEU AT 15.2m DRAFT

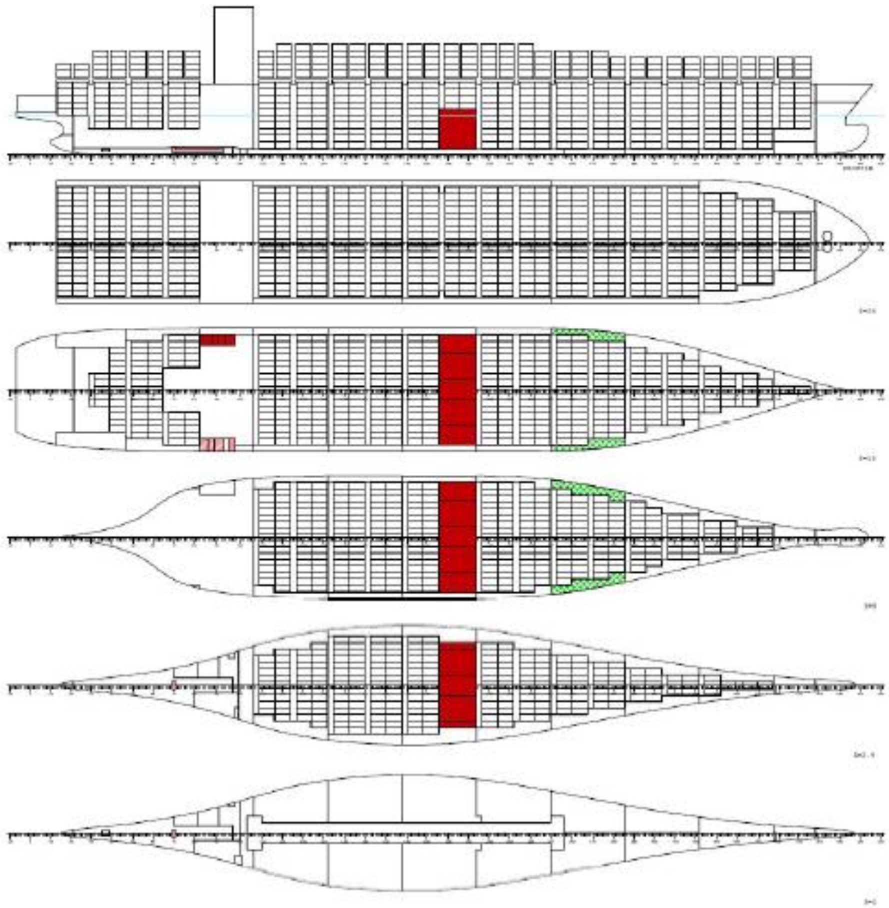

XFRAM m	#	BEND tm	REL %	BMMX tm	BMMN tm	RELSHREL t	%	SHMX t	SHMN t	TORS tm	REL %	TMMX tm	TMMN tm
10.40	13	9832	31.7	30997	-238	954	23.7	4019	-528	915	4.1	22432	-22432
16.91	21	22020	36.6	60230	-490	2730	48.5	5633	-1088	896	4.0	22432	-22432
23.00	29	42791	44.8	95457	-725	4012	58.9	6813	-1613	873	3.9	22432	-22432
37.55	47	117529	57.0	206184	-1502	6580	76.0	8656	-2866	818	3.6	22432	-22432
52.10	65	217918	64.9	335725	-3008	7549	77.1	9786	-3919	768	3.4	22432	-22432
57.85	72	258711	66.7	387938	-3639	7104	72.6	9786	-4077	783	3.5	22432	-22432
66.65	83	324947	70.0	463885	-4605	7885	81.7	9646	-4077	606	2.7	22432	-22432
78.50	96	404248	73.1	552831	-5906	5715	62.9	9092	-4077	1870	8.3	22432	-22432
87.50	106	445494	73.0	610295	-6894	3625	40.4	8970	-4077	1843	8.2	22432	-22432
102.0	124	484032	73.1	662589	-8142	2455	28.9	8499	-4077	1816	8.1	22432	-22432
116.6	142	503369	76.0	662589	-8155	1039	16.8	6167	-4077	1762	7.9	22432	-22432
131.1	160	500530	75.5	662589	-8155	-570	14.0	4077	-4077	1704	7.6	22432	-22432
145.7	178	473101	71.4	662589	-8155	-2318	38.4	4077	-6038	1643	7.3	22432	-22432
160.2	196	420028	64.0	656706	-8155	-4074	64.5	4077	-6320	1579	7.0	22432	-22432
174.8	214	390720	62.6	624486	-8111	599	14.7	4077	-6365	1512	6.7	22432	-22432
189.3	232	382194	66.0	578875	-7499	-854	13.2	4077	-6465	1464	6.5	22432	-22432
203.9	250	353710	69.0	512809	-6664	-2280	32.8	4077	-6962	1437	6.4	22432	-22432
218.4	268	305605	71.6	426647	-5809	-3433	44.6	4077	-7705	1856	8.3	22432	-22432
233.0	286	245086	75.7	323839	-4975	-4160	51.7	4077	-8053	2191	9.8	22432	-22432
247.6	304	176395	80.0	220372	-4144	-4491	61.1	4077	-7355	2165	9.7	22432	-22432
262.1	322	108859	83.2	130890	-3315	-4052	65.4	4077	-6195	2140	9.5	22432	-22432
276.7	340	53317	74.7	71356	-2488	-2997	71.4	3732	-4199	1713	7.6	22432	-22432
291.2	358	16223	44.2	36697	-1950	-1605	64.4	2480	-2493	857	3.8	22432	-22432
307.5	378	583	6.2	9378	-1862	-103	9.6	1072	-1072	6	0.0	22432	-22432